UNIVERSITÀ
DEGLI STUDI
DI PADOVA

Administrative office: University of Padova

Department of *Comparative Biomedicine and Food Science*

DOCTORAL SCHOOL IN: VETERINARY SCIENCE

SERIES XXVII

Morphological and Biochemical Characterization of Bovine Congenital Pseudomyotonia

Coordinator of the School: Ch.mo Prof. Gianfranco Gabai
Supervisor: Ch.mo Prof. Francesco Mascarello
Co-supervisor: Dr. Roberta Sacchetto

PhD student : Dr. Tiziano Dorotea

INDEX:

SUMMARY

The Ca^{2+}-ATPase of sarco(endo)plasmic reticulum (SERCA) is a protein of about 110 kDa member of the P-type ATPases family. SERCA pumps utilize the energy derived from the hydrolysis of a molecule of ATP to transport two Ca^{2+} ions across the Sarcoplasmic Reticulum (SR) membrane to decrease the Ca^{2+} concentration in the cytosol. SERCA isoform 1a (SERCA1a) is the mainly expressed isoform in adult fast-twitch muscle fibre and it is both structurally and functionally the best characterized member of the P-type ion translocating ATPases.

An inherited muscle disorder defined as Bovine Congenital Pseudomyotonia (PMT) has been recently described in two important Italian cattle breeds Chianina and Romagnola (RMG) and, as a single case, in a Dutch improved Red&White (VRB) crossbred calf in the Netherlands. Clinically the disorder is characterized by an exercise-induced muscle contraction not associated to electromyogram alterations. Basing on the clinical signs, the explanation proposed for the delayed relaxation of muscle was a prolonged elevation in Ca^{2+} ion cytoplasmic concentration. Because the structure primary involved in the re-uptake of the Ca^{2+} ion into the SR after muscle-contraction is the ATPase pump, the more likely aetiological hypothesis was an involvement of SERCA1a protein. Indeed, DNA sequencing of affected animals provided evidence of mutations in ATP2A1 gene coding for SERCA1. So far, different point mutations have been described in the different breeds that displayed the disease.

Bovine PMT has been well characterized at both genetic and biochemical levels in Chianina breed. The main objective of this project is to complete the characterization of the disease by mean of analysing from a morphological, histochemical and biochemical point of view the other PMT-cases diagnosed in RMG and VRB breeds. The final aims are to increase the knowledge on morphological and biochemical effects of the disease on muscle tissue, to evaluate phenotypic variability of the disease and to identify possible adaptive/compensatory mechanisms that could drive the future research to develop new therapeutic approaches. The interest on bovine PMT arises from its similarities with a rare human inherited muscular dysfunction named Brody disease. Indeed, PMT-affected Chianina cattle has been accepted as an interesting and useful non-conventional animal model for the study of this human pathological condition.

The histopathological examinations on *semimembranosus* muscle biopsies from RMG and VRB affected animals did not show severe signs of muscle damage. Some pale degenerated fibres, filled or surrounded by macrophages, were identified within the tissue, although they were always accompanied by regenerative phenomena (small size fibres neonatal MHC-positive). Histochemical protocols (COX-SDH and PAS staining) did not reveal metabolic alterations or changes in glycogen distribution.

Immunohistochemical investigations on SERCA1 expression showed that pathological cases had a decrease in immunoreactivity for SERCA1 antibody suggesting a lower presence of the protein. The latter finding was confirmed by biochemical analysis on microsomal fractions enriched in content of SR membranes. Immunoblotting proved that only SERCA1 protein had a reduction in quantity whereas nor junctional (RyR) nor non-junctional (SL and GP53) markers of SR showed any variance. The quantitative decrease was also associated with a lower activity of the protein demonstrated by Ca^{2+}ATPase activity assay. Real Time RT-PCR assays demonstrated that mRNA for SERCA1 was normally expressed suggesting that the protein reduction was due to post-transcriptional events.

Interestingly, the sections of the affected VRB subject showed an increased and more homogeneous stain for COX and SDH suggesting an augmentation in mitochondria content. This finding was reinforced by immunohistochemical and immunoblot surveys using an antibody against a protein of the mitochondrial outer membrane (Tom20). Moreover, microsomal fractions from VRB animal showed an increase in plasma membrane Ca^{2+}ATPase (PMCA) when compare with controls.

Finally in RMG and VRB affected subjects some fibres were immunoreactive for SERCA1 and phospholamban (PLB, regulator protein of SERCA2) or SERCA isoforms 1 and 2 suggesting an alteration in the classic mutually exclusive protein expression pattern (either SERCA1 or SERCA2 and PLB).

The results of this research describe Bovine Congenital Pseudomyotonia in RGM and VRB as a muscular disease characterized by mild histopathological alterations and a sole decrease in SERCA1 content and activity, in full agreement with the studies on Chianina. All the analyses performed on VRB and RGM animals allow to obtain a complete picture of the PMT in these breeds and afford to define a general histopathological and biochemical case of PMT. In addition, for the first time

compensatory mechanisms were demonstrated providing histochemical and biochemical evidences to support mitochondria and PMCA involvement in the Ca^{2+} homeostasis during the pathological condition caused by PMT mutation. Finally, the first evidence of co-expression of SERCA1, SERCA2 and PLB in affected animals, was an intriguing collateral finding that suggests a great potential plasticity of cattle muscle resembling the human muscle once again.

A side project was developed in collaboration with the group of Prof. R. Smith and Dr. J. Dudhia of the Clinical Sciences and Services Department of the Royal Veterinary College (London). Two different pilot studies were carry out on extracellular matrix response to tendon injury in equine. The first had as object of study the cartilage oligomeric matrix protein (COMP) recently proposed as useful biomarker of tendinopathy. The aim of this project was to assess the level of fragmentation (index of alteration but also re-modelling) of COMP in healthy tendon tissue collected in sites well-known to be more frequently involved in lesions (predisposed to injury). The tendons analysed were the superficial digital flexor (SDFT) and the deep digital flexor (DDFT). Immunoblotting and densitometric analysis of total protein extracts showed an higher COMP fragmentation level in healthy predisposed sites when compare with non-predisposed sites. Moreover, for the first time the different patterns of COMP expression in SDFT and DDFT of young and old subjects were described. The second pilot study analysed the morphological aspect of tendon tissue affected by tear-type lesion. The objective was to evaluate the influence of the lesion on the tissue adjacent, far and remote to the injury site. The tendon was extremely altered close to the lesion while the other areas showed high cellularity and vascularity but normal matrix organization. Masson trichrome staining distinguished damaged tissue (blue) from healthy (red) running to become an intriguing tool for histological investigation. Immunohistochemistry showed an increased reactivity for COMP antibody in the areas more proximal to the tear reinforcing the studies that support a fundamental role of this protein in the matrix re-modelling. Increasing the knowledge of COMP distribution in SDFT and DDFT, and providing information of tendon response to tear lesion, these two pilot studies create a useful platform for future researches with possible clinical and therapeutic implication.

RIASSUNTO

La Ca^{2+}-ATPasi del reticolo sarco(endo)plasmatico (SERCA) è una proteina di circa 110 kDa membro della famiglia delle P-type ATPasi. Le SERCA utilizzano l'energia ricavata dall'idrolisi di una molecola di ATP per trasportare due ioni Ca^{2+} attraverso la membrana del reticolo sarcoplasmatico (SR) e diminuire così la concentrazione di Ca^{2+} nel citosol. La SERCA1a è l'isoforma espressa prevalentemente dalle fibre muscolari fast nell'adulto ed è strutturalmente e funzionalmente la meglio caratterizzata tra tutte le ATPasi.

Un disturbo muscolare ereditario definito come Pseudomiotonia Congenita Bovina (PMT) è stato recentemente descritto in due importanti razze bovine da carne italiane Chianina e Romagnola (RMG) e, come caso isolato, in un incrocio olandese (Dutch improved Red&White -VRB-). La malattia è caratterizzata clinicamente da una contrazione muscolare indotta da esercizio ma non associata ad alterazioni elettromiografiche. La causa attribuita al ritardato rilassamento muscolare è stata una prolungata permanenza del Ca^{2+} nel citoplasma. Poiché la struttura primariamente coinvolta nel re-uptake del Ca^{2+} all'interno del SR dopo la contrazione muscolare è la pompa ATPasi, è stato proposto un coinvolgimento della proteine SERCA1a. Il sequenziamento del DNA di animali affetti ha dimostrato la presenza di mutazioni nel gene ATP2A1 che codifica appunto la SERCA1. Ad oggi diverse mutazioni puntiformi sono state descritte nelle varie razze che manifestano la malattia. La PMT è stato caratterizzata a livello genetico e biochimico nella razza Chianina.

L'obiettivo principale di questo progetto è quello di completare la caratterizzazione della malattia attraverso l'analisi morfologica, istochimica e biochimica dei casi di PMT descritti nelle razze RMG e VRB. Scopo ultimo è quello di aumentare le conoscenze sugli effetti morfologici e biochimici della malattia sul tessuto muscolare, valutare la variabilità fenotipica della malattia e individuare eventuali meccanismi di adattamento o compensatori che potrebbero suggerire nuovi approcci terapeutici alle ricerche future. L'interesse per la PMT deriva dalla sua stretta somiglianza con una rara disfunzione muscolare ereditaria dell'uomo chiamata malattia di Brody. Il bovino di razza Chianina affetto da PMT è stato di fatto accettato come un interessante e utile modello animale non convenzionale per lo studio di questa condizione patologica umana.

L'esame istopatologico delle biopsie muscolari ottenute dai soggetti RMG e VRB non hanno mostrato alterazioni particolarmente severe. Sono state individuate alcune fibre in degenerazione sempre accompagnate da fenomeni di rigenerazione (piccole fibre positive per la MHC neonatale). I protocolli istochimici (COX-SDH e PAS) non hanno evidenziato alterazioni metaboliche o cambiamenti nella distribuzione del glicogeno. Le indagini immunoistochimiche sull'espressione SERCA1 hanno mostrato una diminuita immunoreattività nei casi patologici suggerendo una minore presenza della proteina. Le analisi biochimiche effettuate sulle frazioni microsomiali hanno confermato la sola riduzione in contenuto di SERCA1, mentre né il RyR (marker del SR giunzionale) né SL e GP53 (marker del SR non-giunzionale) hanno mostrato alcuna variazione. Saggi di attività per la Ca^{2+} -ATPasi hanno associato una minore attività della proteina alla diminuzione quantitativa della stessa, mentre la Real Time RT-PCR ha dimostrato che l'mRNA della SERCA1 è espresso normalmente suggerendo che la riduzione della proteina avviene post-trascrizione.

Un'interessante osservazione è stata che le sezioni del soggetto VRB mostravano una maggiore e più omogenea colorazione per COX e SDH suggerendo un aumento in contenuto di mitocondri. Quest'ultimo risultato è stato rafforzato da indagini di immunoistochimica e immunoblot utilizzando un anticorpo contro una proteina della membrana mitocondriale esterna (Tom20). Inoltre, frazioni microsomiali ottenute dal soggetto VRB hanno mostrato un aumento in contenuto della Ca^{2+}-ATPasi della membrana plasmatica (PMCA).

Infine, alcune fibre dei soggetti analizzati in questo studio hanno mostrato immunoreattività per SERCA1 e fosfolambano (PLB, proteina regolatrice della SERCA2) o per entrambe le isoforme 1 e 2 suggerendo un'alterazione nel classico pattern di espressione esclusivo delle tre proteine.

I risultati di questa ricerca descrivono la Pseudomyotonia Congenita Bovina nei soggetti RGM e VRB come una malattia muscolare caratterizzata da alterazioni istopatologiche lievi e una diminuzione del contenuto e dell'attività della SERCA1, sovrapponibile al quadro descritto nella Chianina. Le analisi effettuate su VRB e RGM hanno permesso di ottenere un'immagine dettagliata della PMT in queste razze e, insieme ai dati sulla Chianina, ha permesso di definire un quadro istopatologico e biochimico generale della PMT. Inoltre, per la prima volta sono stati dimostrati

meccanismi compensatori fornendo prove istochimiche e biochimiche a sostegno di un coinvolgimento dei mitocondri e della PMCA nell'omeostasi del Ca^{2+} in situazioni patologiche come la PMT. Infine, il ritrovamento di fibre che co-esprimevano SERCA1, SERCA2 e PLB è stato un risultato collaterale interessante che suggerisce una elevata plasticità del muscolo bovino che lo avvicina ancora una volta al muscolo umano.

Un progetto parallelo è stato sviluppato in collaborazione con il gruppo del Prof. R. Smith e del Dr. J. Dudhia del Clinical Sciences and Services Department of the Royal Veterinary College (London). Due diversi studi pilota sono stati effettuati per valutare la risposta della matrice extracellulare alla lesione tendinea nel cavallo. Il primo ha avuto come oggetto di studio la cartilage oligomeric matrix protein (COMP), recentemente proposta come biomarker di tendinopatia. Lo scopo di questo progetto è stato quello di valutare il livello di frammentazione (indice di alterazione, ma anche rimodellamento) di COMP nel tessuto tendineo sano raccolti in siti noti per essere più frequentemente coinvolti nelle lesioni (predisposti a lesione). I tendini analizzati sono stati il flessore digitale superficiale (SDFT) e il flessore digitale profondo (DDFT). L'immunoblot e l'analisi densitometrica di estratti totali di proteine hanno mostrato un più alto livello di frammentazione della COMP in siti sani ma predisposti a lesione quando confrontati con i siti non predisposti. Inoltre, per la prima volta sono stati descritti i diversi pattern di espressione della COMP in SDFT e DDFT di soggetti giovani e vecchi. Il secondo studio pilota ha analizzato l'aspetto morfologico del tessuto tendineo affetto da lacerazione (tear-type lesion). L'obiettivo è stato quello di valutare l'influenza della lesione sul tessuto adiacente, lontano e remoto al sito della lesione. Il tendine era estremamente alterato vicino alla lesione mentre nelle altre aree rimanevano un'alta cellularità e vascolarizzazione ma l'organizzazione della matrice migliorava notevolmente. La tricromica di Masson distingueva il tessuto danneggiato (blu) da quello sano (rosso) proponendosi come un interessante strumento nelle indagini istologiche. L'immunoistochimica ha mostrato un aumento della marcatura per COMP nelle aree più vicine allo strappo rafforzando gli studi che propongono questa proteina come fondamentale nel rimodellamento della matrice. Aumentando le conoscenze sulla distribuzione della COMP in SDFT e DDFT, e fornendo dati sulla risposta tissutale del tendine lacerato, questi due studi pilota hanno creato una piattaforma utile per le future ricerche con possibili implicazioni cliniche e terapeutiche.

LIST OF ABBREVIATIONS:

Ala = alanine
Arg = arginine
CMD1 = Congenital Muscular Dystonia type 1
Coll1 = collagene type I
Coll3 = collagene type III
COMP = cartilage oligomeric matrix protein
COMP100 = 100kDa fragment of COMP
COX = cytocrome oxidase
CS = calsequestrin
Cys = cysteine
DDFT = deep digital flexor tendon
ECM = extracellular matrix
ERAD = endoplasmic reticulum associated protein degradation
GAGs = glycosaminoglycans
GDF8 = Growth Differentiation Factor 8
Glu = glutamic acid
Gly = glycine
GP53 = 53kDa glycoprotein
H&E = hematoxylin and eosin
His = histidine
IHC = immune-histochemistry
Ile = isoleucine
Leu = leucine
Lys = lysine
m-ATPase = myofibrillar ATPase
MCP = metacarpophalangeal joint
MCU = mitochondrial Ca^{2+} uniporter
Met = methionine
MHC = myosin heavy chain
MidM = midmetacarpal region
MLC = myosin light chain
MMPs = mettalloproteinases
MP = myofibrillar pellet microsomal fraction
OD = optical density
PAS = periodic acid-Schiff
PGs = proteoglycans
PLB = phospholamban
PMCA = plasma membrane Ca^{2+}-ATPase
PMT = Congenital Pseudomyotonia
PS = proteic surnatant microsomal fraction
RMG = Romagnola cattle breed
RyR = ryanodin receptor
SDFT = superficial digital flexor tendon
SDH = succinic dehydrogenases
Ser = serine
SERCA1 = sarco(endo)plasmic reticulum Ca^{2+}-ATPase isoform 1
SERCA2 = sarco(endo)plasmic reticulum Ca^{2+}-ATPase isoform 2
SL = sarcalumenin
SLN = sarcolipin
SR = sarcoplasmic reticulum
Thr = threonine
TM = total membrane microsomal fraction
UPD = unfolded protein disease
UPS = ubiquitin-proteosome disease
Val = valine
VRB = Verbeterd Roodbont or Dutch improved Red&White cattle breed

Main project

Morphological and biochemical characterization of Bovine Congenital Pseudomyotonia

1.INTRODUCTION

1.1.Muscle anatomy and physiology

Skeletal muscle tissue is the largest organ in the animals, representing up to 50% of body mass in some athletic species such as the dog and the horse (Gunn, 1989).

Each muscle is composed of hundreds to hundreds of thousands of individual, elongated, multinucleated cells named fibres. Each fibre is constituted of many parallel myofibrils which consist of a repetitive series of an identical banded unit called sarcomere (Figure 1).

A sarcomere is formed by overlapping arrays of thick filaments and thin filaments (constituted of the contractile proteins myosin and actin, respectively), which represent the contractile machinery (Brooks, 2003; Schiaffino and Reggiani, 2011).

In mammals, the number of fibres in a muscle is determined at birth and it is barely modified during the life except in case of injury or disease. Whereas, the number of myofibrils and fibre diameter (CSA: cross-sectional area of muscle fibre) can radically change depending on external factors. For example, training exercise can induce hypertrophy while immobilization, inactivity, disease, or old age may lead to atrophy that means decrease in number of myofibres and volume of fibres (Brooks, 2003).

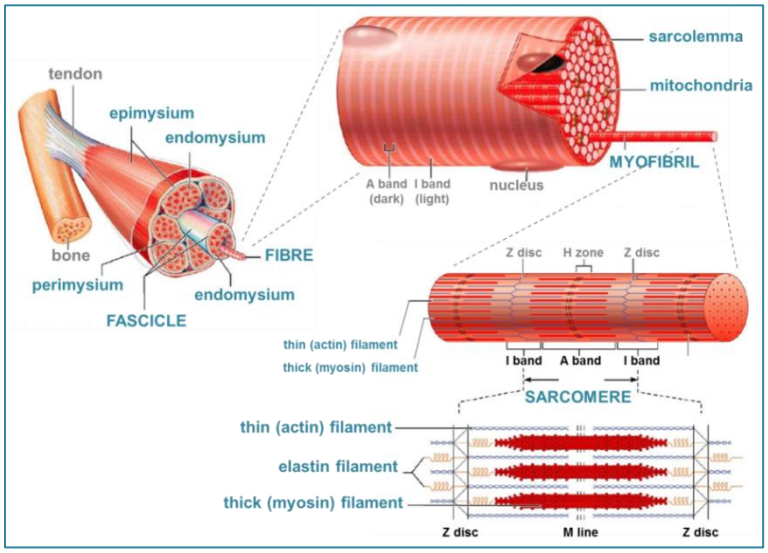

Figure 1. Muscle structural organization. Modified from Benjamin Cummings Interactive Physiology Anatomy Review: Skeletal Muscle Tissue (2006).

Muscle myosin

Myosin is an hexamer consisting of two heavy chains (MHC) and two pairs of light chains (MLC). The two heavy chains have the COOH-terminal ends that form a coiled spiral of two α-helices creating the body of the thick filaments. The other end of the heavy chains projects outward from the thick filament forming the cross-bridge portion of the molecule that connect the light chains with a non-covalently bound (Brooks, 2003). The heavy chains are organized into three structurally and functionally different domains. The globular head domain (catalytic domain) contains both actin-binding site and ATP-binding site and is responsible for generating force, this is the most conserved region among the various myosins. The long α-helical neck domain lies adjacent to the head domain and extends toward the tail of the molecule. It appears to be stabilized by its interaction with the MLCs (essential or alkali MLC and regulatory or phosphorylatable MLC) that regulate the activity of the head domain. Between the head and neck domains a "converter domain" is described. The tail domain is the third and longer domain. It contains the binding sites that determine the specific activities of a particular myosin (Vale, 2000; Rüegg et al., 2002). The myosin tails create a packed filament through a process of self-assembly. The final product is the thick filament decorated with hundreds of myosin heads responsible for force generation and filaments sliding movement (Schiaffino and Reggiani, 2011).

Heavy and Light myosin chains are present in multiple isoforms with a fibre type-specific expression. For this reason MHC isoforms has been used as marker for the classification of fibre types.

In brief, mammalian genomes contain 11 sarcomeric myosin heavy chain genes coding each one for a different MHC isoform (Berg et al., 2001). The isoforms expressed in cardiac muscle are MHC-α and MHC-β/slow or MHC-1 and they are coded by MYH6 and MYH7. Three isoforms are coded by MYH2, MYH1, and MYH4 in adult skeletal muscle fibres and they are named MHC-2A, MHC-2X, and MHC-2B. Two more isoforms are expressed in embryonic and neonatal muscles (developmental isoforms): MHC-emb and MHC-neo, coded by MYH3 and MYH8. MHC-EO isoform is expressed exclusively in extraocular muscles (gene MYH13). Three additional MHC isoforms named MHC-slow tonic, MHC-15 and MHC-M (genes MYH7b, MYH15, and MYH16,

respectively) are expressed exclusively in some head and neck muscles (Schiaffino and Reggiani, 2011).

Actin filaments

Actin filaments constitute the thin filaments of sarcomere. They are helical polymers which have 13 actin molecules arranged on six left-handed turns. The actin monomer consists of two similar domains each of which contains a 5-stranded β-sheet and associated α-helices. One of the domains carries a sub-domain involved in actin-actin interactions while the other is involved in the formation of the nucleotide-binding pocket. Moreover, the thin filaments contain the regulatory proteins tropomyosin and troponin that are involved in the interaction between myosin and actin (Geeves and Holmes, 1999). The thin filament basic components are very similar in all muscle fibres. Actin is the main structural component of the thin filaments which form the trail along which myosin motors work. Two isoforms of actin can be expressed in mammalian skeletal muscle fibres: α-skeletal and α-cardiac isoforms, which differ by only four amino acids and are encoded by two different genes (Schiaffino and Reggiani, 2011).

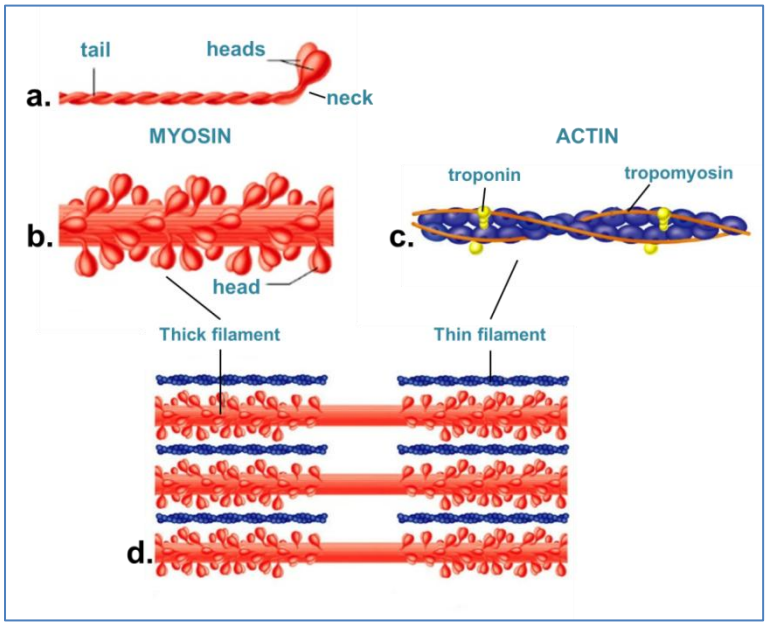

Figure 2. Myosin-actin interaction. (a) Myosin molecule, (b) portion of a thick filament constituted by several myosin molecules, (c) portion of a thin filament constituted by actin molecule and its regulator proteins (troponin and tropomyosin), (d) organization of thick and thin filaments within a sarcomere. Modified from Benjamin Cummings Interactive Physiology Anatomy Review: Skeletal Muscle Tissue (2006).

The cross-bridge working stroke is produced by the angular swinging movement of the neck domain about a pivot point located in the converter domain. The neck domain appears to act as a lever arm that "amplifies" small, subnanometer movements associated with the closing and opening of the active site, ultimately producing a displacement at the end of the neck domain (Vale, 2000). With the catalytic domain rigidly attached to actin, the swinging lever arm drives the displacement of the thin filament relative to the thick filament to generate shortening of muscle fibres (Brooks, 2003). Once the working stroke is completed, an attached myosin head ejects its ATP hydrolysis products, binds another ATP molecule, and detaches from the actin site. The bound ATP molecule then is split and the head returns to its original orientation. The head can repeat this cycle by attaching to a different actin monomer further along the thin filament (Julian et al., 1978).

The rapidity of muscle fibre shortening depends on how rapidly the thick and thin filaments can slide past one another and this velocity of shortening is determined by ATPase activity. Myosin heavy-chain (MHC) isoform determines the enzyme activity (Brooks, 2003).
Thus, the speed of shortening is determined by MHC isoform whereas the fatigue resistance depends on the fibre metabolism.

The combination of different fibres in the same muscle confers the typical flexibility which allows the organ to be used for various tasks demanding different intensity activity levels (e.g. in maintaining posture is required a low-intensity but continuous activity, whereas in jumping is requested a strong maximal contraction). Moreover, the structural and functional properties of the fibres (fibre phenotype) are influenced by hormonal and neural stimuli which can determine and shift the fibre type profile. This property is defined muscle plasticity or malleability (Schiaffino and Reggiani, 2011).

1.2.*Types of fibres*

The traditional classification of fibre types based on myosin composition and metabolic profile has been integrated during the last 50 years due to the increased knowledge on muscle fibre diversity in terms of cell structure and function, from surface membrane

properties to calcium homeostasis. Schiaffino (2010) published a work that summarizes the evolution of the classification of fibre types since the first half of the 19th century till the current notion of muscle fibre types. In the paper he identifies three phases in the evolution of this notion (Schiaffino, 2010; Schiaffino and Reggiani, 2011).

Phase I: two major types of skeletal muscles and corresponding fibre types are described as: i) slow red muscles, composed of fibres rich in myoglobin and mitochondria, characterized by an oxidative metabolism and involved in continuous, tonic activity; ii) fast white muscles, composed of fibres poor in myoglobin and mitochondria, relying more on glycolytic metabolism and involved in phasic activity (Needham, 1926).

Phase II: analysis of motor units (Close, 1967), enzyme histochemistry with succinate dehydrogenase (SDH), myoglobin staining and electron microscopy (Schiaffino et al., 1970) led to the view that skeletal muscles contain three major fibre types: the slow or type 1 fibres, the fast highly oxidative or type 2A fibres and the fast weakly oxidative or type 2B fibres. The introduction of novel histochemical staining procedures for the demonstration of ATPase activity creates the meeting point between the mechanical and the biochemical approach for fibre classification. Indeed, this procedure connects the actin-activated ATPase activity of myosin and the speed of muscle shortening (Barany, 1967; Guth and Samaha, 1969; Brooke and Kaiser, 1970). These findings were integrated with studies on the physiological properties of the single fibres. Peter et al. (1972) found that both 2A and 2B fibres have high levels of glycolytic enzymes in spite of different oxidative enzyme content. The classification was then modified in slow oxidative (type 1), fast-twitch oxidative glycolytic (2A), and fast-twitch glycolytic fibres (2B) (Peter et al., 1972).

Phase III: the discovery of a third fast fibre type with myosin heavy chain (MHC) composition different from 2A and 2B fibres leads to a further modification of the fibre types classification. Independent studies identified a type 2X or 2D MHC band distinct from the other MHC bands (Termin et al., 1989) and the novel fibre expressing this

MHC was called 2X (LaFramboise et al., 1990; De Nardi et al., 1993; Schiaffino and Reggiani, 2011).
Type 2X fibres have twitch properties similar to 2A and 2B fibres. Their resistance to fatigue and their maximal velocity of shortening are intermediate between 2A and 2B (Bottinelli et al., 1991; Bottinelli, Betto, et al., 1994; Schiaffino and Reggiani, 2011).

In addition to these findings, immunohistochemical and in situ hybridization analyses of muscle sections (Gorza, 1990; De Nardi et al., 1993) together with biochemical and physiological studies of single fibres (Bottinelli, Canepari, et al., 1994) demonstrated the existence of a spectrum of fibre types with pure or hybrid MHC composition.
Even if not obligatory, a pattern of MHC gene expression has been described as it follows: 1 ↔ 1/2A ↔ 2A ↔ 2A/2X ↔ 2X ↔ 2X/2B ↔ 2B. Moreover, single fibre studies reported that fibres with apparently pure MYH composition may vary in terms of metabolic enzyme complement (Pette et al., 1999) suggesting a further degree of complexity in the fibre heterogeneity.
The four major fibre types discussed above (type 1, 2A, 2X, 2B) are variously distributed in body muscles of mammals, including limb, trunk, and head muscles (Schiaffino and Reggiani, 2011). In addition, several studies demonstrated species-specific MHC type expression. In particular, in humans, monkey, dog, sheep and llama only three fibre types and three MHC isoforms (slow, 2A and 2X) have been identified in skeletal muscles whereas 2B fibre type seems to be specific only for mouse, rabbit, rat and marsupials (Reggiani and Mascarello, 2004). Although in pig and bovine skeletal muscles, pure 2B fibres have been found only in specialised muscles such as extraocular muscles whereas hybrid fibres (2A/X and 2X/B) have been recognised in pig trunk and limb muscles (Maccatrozzo et al., 2004; Toniolo et al., 2004). In addition, an hybrid fibre type (2C) characterized by the co-expression of slow and α-cardiac MHC was identified in bovine *masseter* muscle (Maccatrozzo et al., 2004).

1.3.*Calcium homeostasis and structures involved*

All muscles use Ca^{2+} ion as their main regulatory and signalling molecule. Indeed, the main functions of all muscle types have Ca^{2+} ion as second messenger (Gissel, 2005).

At resting state, the concentration of free Ca^{2+} inside the muscle fibres ($[Ca^{2+}]_c$) is maintained at ~50 nM (Berchtold et al., 2000) whereas the concentration of Ca^{2+} in the extracellular fluid ($[Ca^{2+}]_o$) is around 1 mM. This enormous difference creates a strong chemical gradient for Ca^{2+} across the sarcolemma that overcomes the low permeability of the membrane and generates a continuous passive diffusion of the ion into the muscle fibre (Hidalgo et al., 1986). In addition, during a contraction-relaxation cycle there is an active flux of Ca^{2+} ions from and to the Sarcoplasmic Reticulum (SR) that causes relatively large changes in $[Ca^{2+}]_c$ (up to 100-fold) although short in time and local in distribution (Gissel, 2005).

To preserve the physiological functionalities, the muscle fibre must maintain and reinstate the $[Ca^{2+}]_c$ at low levels and therefore it must actively remove from the cytosol the Ca^{2+} ions entered passively or actively (Michalak et al., 1984; Hidalgo et al., 1986; Carafoli, 1987). The skeletal muscle cell has several ways of clearing Ca^{2+} from the cytoplasm. The most important are the Ca^{2+}-ATPases in the sarcoplasmic reticulum (SR) and in the sarcolemmal/T-tubular membranes, a secondary system of Ca^{2+} transport is the Na^{+}-Ca^{2+} exchanger and the mitochondrial Ca^{2+} uniporter (MCU).

(1) The Sarco(endo)plasmic Ca^{2+}-ATPase (SERCA) is responsible for the re-uptake of Ca^{2+} into the SR. It is characterized by a high affinity for Ca^{2+} (K_m[1]<0.5 µM) on the cytoplasmic side and a high capacity to transport the ions inside the SR [Salviati, 1984].

(2) The plasma membrane or sarcolemmal/T-tubular Ca^{2+}-ATPases (PMCA) are active especially at resting state and export Ca^{2+} ions from the muscle cell cytosol to the extracellular fluids to regulate the $[Ca^{2+}]_c$. They have high-affinity for Ca^{2+} (K_m=0.5 µM) but a low-capacity of transporting ions (12-30 nmol/mg fibre protein/min in rabbit white muscle) (Michalak et al., 1984; Hidalgo et al., 1986; Monteith and Roufogalis, 1995).

(3) The Na^{+}-Ca^{2+} exchanger plays a major role in Ca^{2+} regulation in cardiac muscle, whereas in skeletal muscle the capacity and quantitative importance of this transport

[1] The Michaelis-Menden constant (K_m) is the substrate concentration at which the reaction rate is at half-maximum, and is an inverse measure of the substrate's affinity for the enzyme: as a small K_m indicates high affinity, meaning that the rate will approach V_{max} more quickly.

system is more controversial. It seems that Na^+-Ca^{2+} exchanger activity in skeletal muscle is low during normal resting state but increases when $[Ca^{2+}]_c$ exceeds 80 nM (Balnave and Allen, 1998). These observations suggest an important role of the Na^+-Ca^{2+} exchanger during fatiguing stimulation (Balnave and Allen, 1998) and in the long-term regulation of Ca^{2+} concentration in the cytosol (Deval et al., 2002; Gissel, 2005).
(4) The mitochondrial Ca^{2+} uniporter (MCU) of the inner membrane is the main structure primarily involved in mitochondrial Ca^{2+} uptake. It has a low Ca^{2+} affinity (K_m between 10 and 100 µM) and consequently it seems involved especially when $[Ca^{2+}]_c$ is extremely high (Gunter and Pfeiffer, 1990; Baughman et al., 2011; De Stefani et al., 2011).

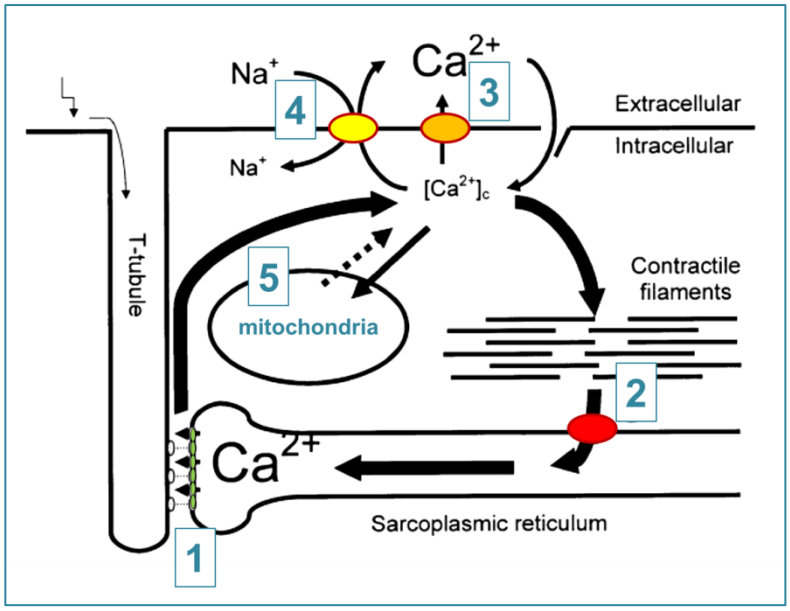

Figure 3. Structures involved in Ca^{2+} homeostasis. (1) ryanodine receptor Ca^{2+} release channels (RyRs); (2) Sarco(endo)plasmic Ca^{2+}-ATPase (SERCA); (3) plasma membrane or sarcolemmal/T-tubular Ca^{2+}-ATPases (PMCA); (4) Na^+-Ca^{2+} exchanger; (5) mitochondrial Ca^{2+} uniporter (MCU). Modified from Gissel, 2005.

Considering the above, there are three different compartments where the Ca^{2+} free in the cytosol can be moved. The PMCA and the Na^+-Ca^{2+}exchanger pump the ions out of the muscle fibre in the extracellular fluid compartment. The SERCA uptakes the Ca^{2+} ions into the SR that is the most important storing compartment. The last compartment is constituted by the mitochondrial matrix where the ions are transported through the mitochondrial Ca^{2+} uniporter (MCU) of the inner membrane.

The Sarcoplasmic Reticulum

The sarcoplasmic reticulum (SR) is an intracellular membranous network found in muscle fibres (Figure 4). The release and re-uptake of Ca^{2+} ions by the SR essentially direct the entire process of contraction and relaxation of skeletal muscle, whereas the other structures seem to have a secondary role. Ca^{2+} ions can be released extremely rapidly into the cytosol of the fibre through the ryanodine receptor Ca^{2+} release channels (RyRs) that are primarily concentrated in the SR terminal cisternae (Franzini-Armstrong and Protasi, 1997). The Ca^{2+} ions are subsequently sequestered back into the SR by the activity of Sarco(endo)plasmic reticulum Ca^{2+}-ATPase (SERCA) (Periasamy and Kalyanasundaram, 2007). There are different fibre type-specific isoforms of SERCA which influence the properties of the SR and consequently the dynamics of muscle contraction-relaxation cycle (Lyttons et al., 1992; Wu and Lytton, 1993; Talmadge et al., 2002; Murphy et al., 2009; Lamboley et al., 2013; Lamboley et al., 2014).

The SR network can be divided in two parts called junctional and non-junctional SR different in structure and proteomic profile. The junctional portion consists of bulbous enlargements of the SR named "terminal cisternae" that are the part of the SR connected with the transverse tubules (T-tubules). A T-tubule is an invagination of the sarcolemma normally perpendicular to the fibre length and it locates at the junction between the A and I bands of the sarcomere. A single T-tubule, together with the adjacent pair of terminal cisternae, forms an arrangement called "triad" that is the key structure for the excitation-contraction (E-C) coupling. There are two triads per sarcomere (Peachey, 1965).

The junctional SR contains primarily the ryanodine sensitive Ca^{2+} channels or ryanodine receptor (RyR) involved in E-C coupling (Meissner, 1994; Franzini-Armstrong, 1996) together with associated proteins such as triadin, junctin and calsequestrin (CS) (Brandt et al., 1993; Guo et al., 1996). The tetrameric form of RyR is called "feet" and it interacts with the dihydropyridine receptors (DHPRs) of the T-tubules. RyR, DHPR and their associated proteins form an ordered array that assures the mechanical stability of the contacts between the sarcolemma and the SR and facilitates the spatial and temporal coordination of the events (Meissner, 1994; Meissner and Lu, 1995; Franzini-Armstrong, 1996; Protasi et al., 1996; Protasi et al., 1998). The non-junctional portion of SR consists of longitudinal tubules and cisternae, it corresponds to

the part of the sarcoplasmic network between two triads. The non-junctional SR contains the Ca^{2+}-ATPases, most of the luminal protein components of SR, the enzymes of phospholipid and sterol biosynthesis, cytochromes and various transporters (Figure 4). The cisternae near the junctional SR contain also CS (Franzini-Armstrong and Jorgensen, 1994).

The SR is the major storage compartment of the muscle fibre and its large buffer capacity is due to the presence of the high capacity and low affinity Ca^{2+}-binding protein calsequestrin (CS) which is able to bind 40-50 moles of Ca^{2+}/mol (MacLennan and Wong, 1971; Berchtold et al., 2000; Beard et al., 2004; Murphy et al., 2009). Thus, the Ca^{2+} concentration within the SR is maintained high at resting state (11 and 21 mM for slow-twitch and fast-twitch fibres, respectively), in contrast with a low Ca^{2+} concentration in the cytosol (1 mM). Differences in SR properties have been described between slow- and fast-twitch fibres. At resting, it has been shown that the SR of slow-twitch fibres is saturated with Ca^{2+}, whereas in fast-twitch fibres the SR is saturated for one-third suggesting a larger buffer capacity of the SR of the second fibre type (Fryer and Stephenson, 1996; Gissel, 2005).

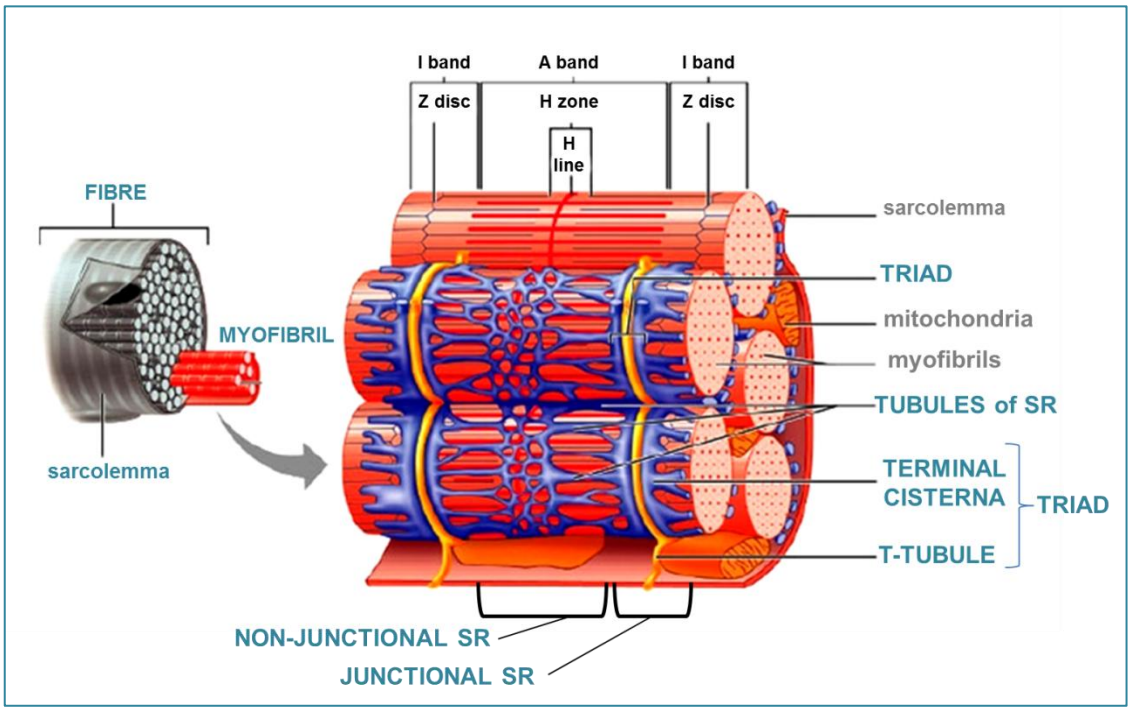

Figure 4. Sarcoplasmic Reticulum. Junctional and non-junctional portions are indicated. Modified from Benjamin Cummings Interactive Physiology Anatomy Review: Skeletal Muscle Tissue (2006).

The Mitochondria

Since 1960s, it has been proposed that the mitochondria are capable of up-taking and storing Ca^{2+} (De Luca and Engstrom, 1961). William *et al.* demonstrated that under physiological conditions, the Ca^{2+} influx into mitochondria per litre of cytosol is small and thus the $[Ca^{2+}]_c$ is not altered. Nevertheless, the study also demonstrated that under extreme conditions (e.g. significant lack of Ca^{2+} extrusion pathways), very large fluxes can occur and mitochondrial Ca^{2+} uptake is more likely to influence cytosolic Ca^{2+} concentration, especially during rapid and large changes in $[Ca^{2+}]_c$ (Williams et al., 2013).

Mitochondria possess an elaborated system for facilitating the transport of Ca^{2+} across their inner membrane. The low affinity mitochondrial Ca^{2+} uniporter (MCU) of the inner membrane and the mitochondrial Na^+/Ca^{2+} exchanger (mNCX) are considered the main structures primarily involved in mitochondrial Ca^{2+} uptake and extrusion, respectively (Gunter and Pfeiffer, 1990; Palty et al., 2010; Baughman et al., 2011; De Stefani et al., 2011; Scorzeto et al., 2013). Scorzeto *et al.* indicated that mitochondrial Ca^{2+}-uptake and release are fast enough to allow the rapid adjustment of metabolic activity to increased demand (during exercise). In their experiment, by using a CS-null muscle they observed an increase in mitochondria number and in the resting free $[Ca^{2+}]$ inside the mitochondria (Scorzeto et al., 2013). These alterations together with the increase in mitochondrial volume noted by Paolini *et al.* (Paolini et al., 2011) represent a compensatory response to a reduction of SR store functions. Moreover, Ca^{2+} uptake by the mitochondria is crucial in skeletal and cardiac dysfunction and in programmed cell death (Giacomello et al., 2007; Denton, 2009).

Recent studies have proposed that the mitochondria are located close to Ca^{2+}-release channels of the SR (RyR) (Hayashi et al., 2009; Patron et al., 2013; Williams et al., 2013). This position exposes the mitochondria to the high localized increase of $[Ca^{2+}]$ when the ions are released for contraction event. The high local concentration activates the MCU that sequesters the ions into the mitochondrial matrix (Rizzuto et al., 1999; Scorzeto et al., 2013). Moreover, it has been observed that the mitochondrial Ca^{2+} uptake starts a few milliseconds after the $[Ca^{2+}]_c$ rises during both a single twitch and tetanic contraction (Rudolf et al., 2004).

Summarizing, it is apparent that the mitochondria may play an important role in the regulation of Ca^{2+} homeostasis in skeletal muscle both in physiologic and pathologic situations (Gissel, 2005; Scorzeto et al., 2013).

The Sarco(endo)plasmic Ca^{2+}-ATPases

The Ca^{2+}-ATPase of sarco(endo)plasmic reticulum (SERCA) is a protein of about 110 kDa (MacLennan et al., 1985) member of the P-type ATPases family together with PMCA, Na^+/K^+ATPase, and H^+,K^+ATPase (Sweadner and Donnet, 2001).

The distinctive feature of the P-type ATPases is the transfer of terminal phosphate from ATP to an aspartate residue in the catalytic domain during the reaction cycle. Therefore, the hydrolysis of ATP is coupled to the movement of ions across a biological membrane. In particular, SERCA pumps utilize the energy derived from the hydrolysis of a molecule of ATP to transport two Ca^{2+} ions across the membrane (Aravind et al., 1998; Johnson and Lewis, 2001).

In addition, two functionally homologous small proteins have been found to have regulatory activity on SERCAs: phospholamban (PLB, 52 amino acid residues) and sarcolipin (SLN, 31 amino acid residues). These two proteins regulate SERCAs through physical interactions by lowering their apparent Ca^{2+} affinity (Odermatt et al., 1998; Asahi et al., 2002). Different studies showed that PLB is expressed almost exclusively in cardiac, smooth and slow-twitch skeletal muscle suggesting a sole regulation of SERCA2a (Odermatt et al., 1997; Damiani et al., 2000). Regarding SLN, it was originally hypothesized that SLN would act as a counterpart of PLB by regulating SERCA1a in fast-twitch muscle (Odermatt et al., 1997) although recently it has been demonstrated that SLN can regulate both SERCA2a and SERCA1a in a variety of muscle tissues (Tupling et al., 2011).

A recent study enlightened the pattern of PLB and SLN expression using single fibre Western blotting and immunohisto/fluorescence staining techniques.

The most important findings regarded the co-expression patterns of SLN and PLB with SERCA and MHC isoforms in human *vastus lateralis* fibres. Fast-twitch fibres contain relatively high levels of SLN and SERCA1a proteins and relatively low levels of PLB protein, moreover the 14-18% of these fibres express, at relatively low levels, also SERCA2a protein. Conversely, slow-twitch fibres contain relatively high levels of PLB

and SERCA2a proteins and the 22% also relatively low levels of SLN and SERCA1a proteins. The main conclusion of the study was that SLN and PLB likely preferentially regulate SERCA1a, and SERCA2a, respectively. However, the co-immunoprecipitation patterns suggest that PLB likely also regulates SERCA1a and SLN may also regulate SERCA2a in human skeletal muscle. Moreover, the co-expression of PLB and SLN gives evidences of the super-inhibition as possible regulatory mechanism of $[Ca^{2+}]_c$ in physiological situation (Fajardo et al., 2013).

Three distinct genes encoding for SERCA have been identified in vertebrates. Thus, there are three mainly SERCA isoforms named 1, 2, and 3 (Periasamy and Kalyanasundaram, 2007).

SERCA1 is principally expressed in fast-twitch skeletal muscle; it has been recognized an adult isoform named SERCA1a (994 aa) and a fetal isoform indicated as SERCA1b (1011 aa) (Brandl et al., 1987).

SERCA2 has two main isoforms: SERCA2a (997 aa) is expressed predominantly in cardiac and slow-twitch skeletal muscle (MacLennan et al., 1985; Zarain-herzberg et al., 1990), whereas SERCA2b (1042 aa) expressed at low levels in all tissues, in muscle and non-muscle cells (Gunteski-Hamblin et al., 1988; Lytton and Maclennan, 1988; de la Bastie et al., 1990). In addition, a third isoform, named SERCA2c (999 aa), has been recognized in cardiac muscle (Dally et al., 2006).

SERCA3 is a minor form in muscle fibres although the isoforms 3a, 3b and 3c are highly expressed in the hematopoietic cell lineages, platelets, epithelial cells, fibroblasts, and endothelial cells (Burk et al., 1989; Anger et al., 1993; Bobe et al., 1994; Wuytack et al., 1994; Bobe et al., 2005).

An excessive accumulation of free Ca^{2+} in the cytosol of muscle fibre results in a loss of the control on Ca^{2+} homeostasis. Whether this condition is not solved rapidly, by means of the activation of defensive and/or compensatory mechanisms, it leads to short- and long- term muscle damages.

As mentioned earlier, Ca^{2+} ion is an important second messenger in skeletal muscle and thus, a wide range of processes can be activated by a variation of $[Ca^{2+}]_c$. Therefore, a tightly control $[Ca^{2+}]_c$ is crucial to the muscle fibre. The main structures involved in this process are the SR together with SERCAs, PMCA, Na^+/Ca^{2+} exchangers and

mitochondria. In addition, buffer Ca^{2+}-binding proteins such as parvalbumin seem to have an important buffer effect in fast muscle fibres of lower vertebrates and small mammals although not in humans (Fohr et al., 1993; Gailly, 2002; Gissel, 2005).

When a larger influx of Ca^{2+} ions will occur due to an increased permeability of the sarcolemma or when the Ca^{2+} permanence lasts long after the releasing from the storing compartments, the Ca^{2+} load on the fibre increases. The storage capacity of the SR and the mitochondria is large, therefore the increased $[Ca^{2+}]_c$ can be handled and the excessive Ca^{2+} ions can be stored, whether there is a fibre type-specificity of this feature. However, if the increased influx of Ca^{2+} or the Ca^{2+} permanence in the cytosol persist, an excessive accumulation of free Ca^{2+} may result. Consequently, Ca^{2+}-activated neutral proteases (calpains) and phospholipases (PLA2) can be activated and reactive oxygen species (ROS) production increases. Moreover, mitochondria are activated increasing the Ca^{2+} up-taking. This last event can lead to activation of apoptotic processes (Gissel, 2005).

1.4.*SERCA1 architecture*

Sarco(endo)plasmic Reticulum Ca^{2+}-ATPase isoform 1a (SERCA1a) is the mainly expressed isoform in adult fast-twitch muscle fibres. SERCA1a is both structurally and functionally the best characterized member of the P-type (or E1/E2- type) ion translocating ATPases.

1.4.1.SERCA1a structure and functional conformations

The three-dimensional structure of SERCA1a was solved by Toyoshima et al. (2000). SERCA1a consists of three cytoplasmic domains called A (actuator), N (nucleotide binding) and P (phosphorylation), and a domain M, which includes ten transmembrane helices (M1-M10) along with the short luminal loops (Figure 5).

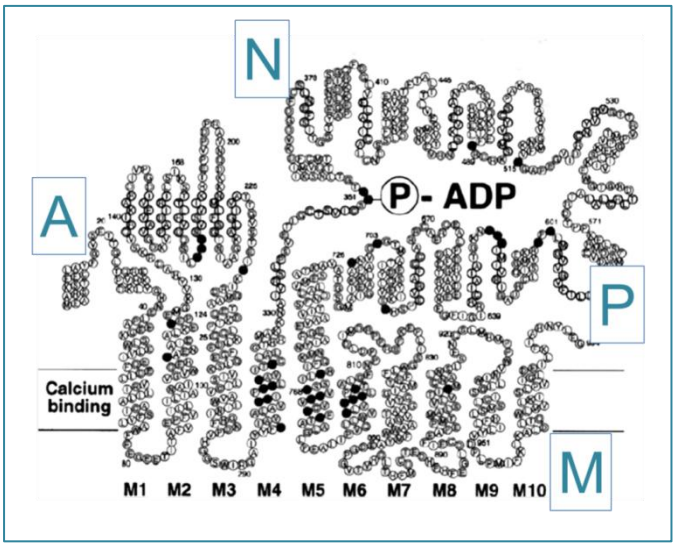

Figure 5. Cartoon representing SERCA1a structure. The three cytoplasmic domains (A, N and P) and the 10 transmembrane helices (domain M) are indicated in the figure. Modified from MacLennan *et al.*, 1997.

The A-domain is connected to the M1–M3 helices with rather long linkers and works as the actuator of the transmembrane gating mechanism that regulates Ca^{2+} binding and release. It seems to play a key role in processing of aspartylphosphate (Ma et al., 2005; Anthonisen et al., 2006).

The P-domain contains Asp351 which is the residue that is phosphorylated during the reaction cycle. The P-domain is wedge shaped and has a flat top surface to allow a large rotation of the A-domain on the top surface of the P-domain (Toyoshima et al., 2007). The Rossmann fold of the P-domain is particularly suited for this purpose. This wedge shape is the key in converting rotational movements of the A-domain to vertical ones of the transmembrane helices. The P-domain can be also bent in two approximately orthogonal directions by the phosphorylation and Mg^{2+}-binding. Such flexibility is a key in realising different domain interfaces. The central β-sheet in the Rossmann fold consisting of two halves allows such bending and is also used as the secondary hinge in SERCA1a to allow an extra 30° not covered by the primary hinge between the N- and P- domains.

The N-domain consists of a long insertion between two parts of the P-domain. It contains the nucleotide-binding site (Phe487 residue) and other residues (e.g. Arg560) that are critical for bridging ATP and the P-domain, although it exhibits no large

structural changes during the enzyme cycle (Toyoshima and Inesi, 2004; Toyoshima, 2008).

The M-domain consists of 10 transmembrane helices, some of them (M2-M5) have long cytoplasmic extensions, while others (M4, M5, M6 and M8) form the two Ca^{2+}-binding sites. Helix M5 can be considered the spine of the molecule because it is 60 Å long and extends from the lumenal surface of the membrane to the end of the P-domain. M4 and M6 helices have proline residues in the middle and are partly unwound throughout the reaction cycle. All helices from M1 to M6 move considerably during the reaction cycle, whereas M7-M10 helices do not. Helix M7 makes a tight couple with M5 and allows the bending of M5 (Toyoshima and Mizutani, 2004).

The SERCA1a protein has been extensively characterized in rabbit where 44 crystal structures have been proposed as possible representations of all the conformational states in the enzyme cycle (Toyoshima and Nomura, 2002; Xu et al., 2002; Sørensen et al., 2004; Toyoshima and Inesi, 2004; Obara et al., 2005; Jensen et al., 2006; Moncoq et al., 2007; Olesen et al., 2007; Takahashi et al., 2007; Laursen et al., 2009; Winther et al., 2010; Toyoshima et al., 2011).

The ion translocating mechanism of the protein has been explained in terms of a cycle characterized by two major conformational states, called E1 and E2. Conformation E1 is the form with the highest affinity for calcium, in this state SERCA1 binds Ca^{2+} from the cytoplasm. Conformation E2 has lower affinity for the ion, in this state SERCA1 releases Ca^{2+} into the lumen of the SR (de Meis and Hasselbach, 1971; Moller et al., 1996). The three cytoplasmic domains (A, P and N) are well separated in the E1 crystal structure although they form a compact headpiece in the other states. This drastic rearrangement follows the aspartate phosphorylation that is the key event to have Ca^{2+} release into the lumen of the SR (Toyoshima and Mizutani, 2004; Toyoshima, 2008). More in detail, two other intermediate conformation states have been proposed as key steps in the transfer of bound Ca^{2+} from cytosol into SR. These intermediates are called E1P and E2P, where ‘P’ indicates that the enzyme is phosphorylated. The transfer takes place through the two phosphorylated intermediates in exchange of H^+ from the SR lumen (Figure 6) (Hua et al., 2002; Toyoshima and Nomura, 2002; Ma et al., 2005; Toyoshima, 2009).

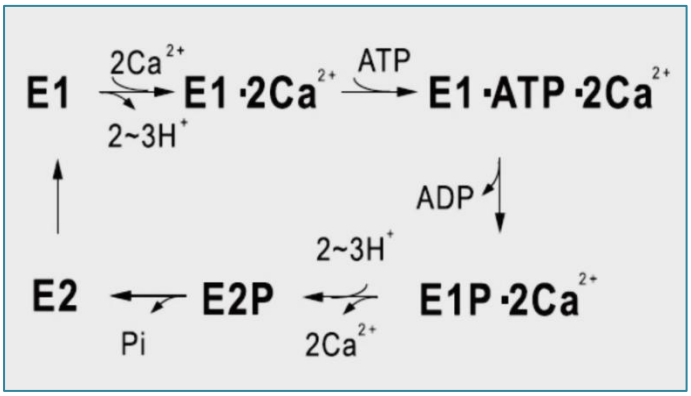

Figure 6. Conformational cycle of SERCA1a. Conformation E1 is the form with the highest affinity for calcium, E2 is the form with the lowest affinity. The others are the most important intermediate steps of the cycle that permits to bind Ca^{2+} from the cytoplasm and free it into the lumen of the SR.

It is well established that SERCA1 has two high affinity transmembrane Ca^{2+}-binding sites, called I and II, located close each other near the cytoplasmic surface (Inesi et al., 1980). The binding of the two Ca^{2+} is sequential. The first ion is bound by site I that is surrounded by M5, M6 and M8 helices. The adjacent M4 helix is the key structure for coordination. When the first Ca^{2+} is bounded at site I, the event is mechanically transmitted to the site II that changes its conformation to receive a second Ca^{2+} ion. Consequently, there is an essential communication between the Ca^{2+}-binding sites and the phosphorylation site. This is possible because the cytoplasmic end of M5 helix (site I) is integrated into the P-domain near the phosphorylation site. Moreover, M5 is hydrogen bounded to the M4 helix (site II) forming a short β-strand. These connections make possible a mechanical transmission of the conformational changes occurring in the sites permitting a coordinate communication (Toyoshima and Nomura, 2002; Toyoshima, 2009).

1.4.2.Bovine SERCA1a

The crystal structure of the Ca^{2+}-bound conformational state (E1) of bovine SERCA includes residues from 1 to 993. A deletion in the bovine enzyme occurs in the position corresponding to rabbit position 504, this generates few disordered amino acids in the stretch 876-880. Consequently, the numbering system of the protein sequence is shifted by 1 compared with the rabbit (Sacchetto et al., 2012).

The amino acid deletion mentioned occurs in a loop connecting α-helices N8 and N9 in the N-domain with no functional effect.

Twenty-two residues have been found different in bovine SERCA comparing with rabbit. Among these 22 substitutions, 12 are conservative (mainly Ser↔Thr or Leu, Ile↔Val) and 10 are non-conservative replacements. Eight of these are located in two areas of the C-terminal of the protein (M-domain) that protrudes in the lumen of the SR. The other two are located in helix M9 in position 937 (Cys→Gly) and 922 (Met→Val). Nevertheless, the last substitutions described appear to be irrelevant from the conformational point of view. At the contrary, six of the eight non-conservative substitutions (residues 863-881) seem to generate a conformational difference between bovine and rabbit enzyme (Sacchetto et al., 2012). The specific region involved is the long loop of M-domain that protrudes into the SR lumen and connects α-helices M7 and M8. It is interesting to note that also this region of the protein undergoes a conformational rearrangement during the cycle E1→E2 as consequence of the large movements of the cytoplasmic domains transmitted through the intermembrane helices. In fact, the movement of the helices M1 and M2 is transmitted to helix M3 causing a shift of the loop connecting helices M3-M4. Simultaneously, helices M7 and M8 undergo a rearrangement that moves them closer to the M3-M4 loop forming a hydrogen bond between Glu877 and Ser287. The amino acidic sequence preceding and following Glu877 is involved in the non-conservative substitutions (Q874K, T876S, D878H, H879S, H881D). These changes could delay the transition from the E1 to the E2 conformation of the bovine enzyme explaining its reduced specific activity when compared with rabbit enzyme (Sacchetto et al., 2012). It is possible that the reported mutations are consequence of an evolutionary process directed by different physiological and behavioural requests that render the bovine enzyme less efficient than the rabbit counterpart. Whilst the binding sites for ions and for the nucleotide are very well conserved, and the calcium binding constant is almost the same for both enzymes (Sacchetto et al., 2012).

1.4.3.SERCA1a mutants for the study of its domains functions

Several studies have been accomplished in order to investigate the importance of this protein in muscle physiology, to understand the role of the different domains in the

functionality of the enzyme and to evaluate the effects of alterations in the different domains. Numerous SERCA1a mutants were built *in vitro* and *in vivo* substituting different amino acids in different sites in accordance with the role that the researchers had planned to highlight.

Dahio and coworkers investigated the role of disulfide bond between Cys876 and Cys888 on the loop M7-M8. In all mutated SERCA1a they built, the disulfide bond was disrupted. As consequence, ATP hydrolyzing activity was maintained at high rates although none of the mutants could transport Ca^{2+} at a detectable rate (Daiho et al., 2001).

Clausen and co-authors studied different Ca^{2+}-ATPase constructs involving the N-domain with mutations of ATP-binding residues. This domain plays a major role in the conversion from E1 to E2 and interfaces with the other cytoplasmic domains (A and P).

The substitutions of amino acids Thr441, Glu442, Lys515, Arg560 and Leu562 introduced in the experiments by Clausen *et al.*, seem crucial primarily to ATP binding step of the enzyme cycle, although also subsequent catalytic steps were affected. In particular, Thr441Ala substitution reduced to 50% both Ca^{2+} transport capacity and ATPase activity comparing with wild type (WT) control levels. Arg560Val substitution displayed approximately 60% of the WT Ca^{2+} transport capacity and only 30% of WT ATPase activity. Interestingly, the Cys561Ala substitution, adjacent to Arg560, reduced Ca^{2+} transport rate to 80% of WT without affecting ATP binding affinity. Among all these observations, it seems that none of the examined residues were very important for the binding of modulatory nucleotide to the phosphoenzyme. On the other hand, all mutations but one slowed the transition from E1P to E2P conformation state decreasing the Ca^{2+} transport activity of the enzyme. On the contrary. the Arg→Val mutation in position 560 enhanced the rate of the Ca^{2+} translocate activity suggesting that Arg560 plays a critical role in optimizing the rate of E1P→E2P conformational transition. (Clausen et al., 2003). Similar inhibiting effect on E1P→E2P transition has been described in presence of point mutations located in the cytoplasmic domains A and P and in the segment connecting M4 with domain P (Vilsen et al., 1989; Clarke et al., 1990a; Clarke et al., 1990b; Vilsen et al., 1991; Clausen et al., 2003). With the use of Circular Dichroism (CD) spectroscopy and ^{15}N-^{1}H heteronuclear single quantum

coherence (HSQC) spectra, Myint *et al.* (2011) demonstrated that little structural perturbation is present in the mutant proteins confirming the hypothesis already proposed by Clausen *et al.* (2003). The results confirmed that these mutants lead to local conformational changes at the binding sites without abolishing completely the catalytic activity (Myint et al., 2011).

The research group of Pan (2003) generated SERCA1-null mice (SERCA1-/-) in order to study the central role of this enzyme and the effects of its completed absence.

SERCA-/- mice were born with normal body weight and normal gross morphology although they developed cyanosis and gasping respiration and died shortly after birth.

The SERCA-/- mouse model of this study has highlighted the importance of maintaining the Ca^{2+} homeostasis for a correct muscle functionality. Moreover, this study underlines the key role of Ca^{2+} ion as starting message to several mechanisms that lead to pathological changes in the tissues (Pan et al., 2003). High levels of cytosolic free Ca^{2+} stimulate glucose transport into skeletal muscle (Youn et al., 1991) where glycogenolysis is inhibited and pyruvate dehydrogenase is stimulated. In addition free Ca^{2+} activates mitochondrial function (McCormack et al., 1990), Ca^{2+}-dependent proteases (Armstrong et al., 1991) and lysosomal proteases (Schwartz and Bird, 1977). All these responses are activated both in physiological (after exercise) and pathological (trauma, disease) situation and generate structural and morphological degradation of the muscular tissue.

At this point, it can be noted that, depending on amino acid mutated and the domain involved, some mutations at SERCA1 sequences lead to a decrease in both protein quantity and activity whereas other mutation can affected the sole pump activity.

Naturally occurring mutations in *ATP2A1* gene have been described in human medicine and referred as cause of a rare inherited myopathy named Brody disease (Brody, 1969; Odermatt et al., 1996). Genetic heterogeneity has been reported in human patients, both in mutation type and in inheritance patterns (A Odermatt et al., 2000; Vattemi et al., 2010; Voermans et al., 2012).

Recently, an inherited condition affecting the skeletal muscles has been described in bovine species and the genetic analyses identified a mutation in *ATP2A1* gene. The disease was named Bovine Congenital Psudomyotonia (Testoni et al., 2008).

1.5.Bovine Congenital Pseudomyotonia

1.5.1.History and epidemiology

Bovine Congenital Pseudomyotonia (PMT) is a recessively inherited disease described for the first time by Prof. Testoni in Italian Chianina cattle breed (Testoni et al., 2008). Clinically, the disorder is characterized by muscle contracture that prevents animals from performing muscular activities but a simple walk at a slow pace. The underlying cause of this pathological condition is a mutation of the *ATP2A1* gene, encoding the fast-twitch Sarco(endo)plasmic Ca^{2+}-ATPase (SERCA1) of the skeletal muscle (Drögemüller et al., 2008). Interestingly, in the same years a similar clinical manifestation has been described in Belgian Blue cattle and named Congenital Muscular Dystonia type I (CMD1). Its causative mutation interests *ATP2A1* gene and leads to an amino acid substitution in the SERCA1 pump. Affected calves show impaired swallowing, fatigue after brief exercise or stimulation associated with muscle myotonia. The contraction results in limbs stiffness and lose of balance. Moreover, CMD1 calves usually have altered growth parameters and die within a few weeks as a result of respiratory complications (Charlier et al., 2008).

Few years later, Grünberg and colleagues reported a single case of muscular disorder in a Dutch improved Red&White crossbred calf (Verbeterd Roodbont, VRB). Clinical and biochemical similarities suggested that the calf was a PMT case although genetic analysis indicated a mutation in *ATP2A1* gene identical to the one of CMD1 affected calves. To solve this incongruence, it has been proposed that PMT and CMD1 refer to the same congenital condition (mutation of *ATP2A1* gene) with a different phenotype expression (Grünberg et al., 2010).

In addition, my group reported recently the typical symptoms of Congenital PMT in four Italian Romagnola cattle breed, another beef breed similar to Chianina. Genetic analysis was performed and the result was the identification of two mutations, one novel and one previously described in Chianina cattle breed. One of the affected calves was homozygous for the novel mutation of *ATP2A1* gene while the others were heterozygous for both mutations. This condition is called "compound heterozygous mutation" and it has been described in bovine species for the first time by my group of research (Murgiano et al., 2012). These Romagnola affected subjects and the Dutch

improved Red&White crossbred case were the object of study in my PhD research project.

The increased frequency of Congenital Pseudomyotonia diagnosis in bovine population may highlight the importance of a correct breeding programs in those animal populations characterized by a stringent selection for high specialization and low genetic variability due to a small effective/reproductive population (Charlier et al., 2008). The University of Berne developed a DNA-based test for the detection of PMT carriers. Since 2008 this test has been used by the Italian Chianina Breeders' Association (ANABIC) in order to identify, within all the top sires indexed in the annual catalogues, the ones that are carriers of the PMT causative mutation. Moreover, also the new young bulls selected for performance test have been tested for the mutation and the carriers excluded from the breeding program. An epidemiologic study has been recently performed to estimate the frequency of the recessive allele (A) causative of PMT in the Italian Chianina cattle breed. Because analyse the entire population of Chianina finds critical logistic and economic difficulties it has been decided to evaluate the carrier prevalence within top sires and selected bull calves. The results showed a frequency of 6.8% of the mutant *ATP2A1* allele within the top sires tested (9 animals on 66 -13.6%- were heterozygous carriers of the PMT mutation), and a frequency of 6.7% among the young bulls (56 animals on 417 -13.4%- tested were heterozygous PMT-carriers)[2] (Murgiano et al., 2013). This high frequency of mutant allele in the population might be correlated with the presence of quantitative trait loci (QTL) for beef traits in the same region. In other words, it could be possible that selection of high performance traits implicates a transmission of other characters (positive or negative) due to co-segregation mechanism. This hypothesis is supported by a work on Angus cattle breed in which two QTL influencing carcass traits were mapped to the *ATP2A1* gene region (McClure et al., 2010; Murgiano et al., 2013).

Because most of the top sires carry important characters for high performances, the current strategy of the ANABIC is to exclude new bulls PMT carriers from the breeding

[2] The allele frequency was estimated using the Hardy-Weinberg equation: $p^2 + 2pq + q^2 = 1$, where p is the frequency of the wild-type allele (G) and q is the frequency of the mutant allele (A). PMT allele frequency (q) was calculated as follows: $q = 1 - [2(GG) + (AG)]/2n$, where n = total number of animals tested, GG = number of PMT non-carrier cattle, and AG = number of PMT carriers.

programme but only to identify the carriers within the actual sires without disabling them from further mating. This means that the PMT carrier prevalence is predicted to be <0.1% only at the seventh generation (Thompson et al., 2006).

1.5.2.Features of Congenital Pseudomyotonia

The clinical approach, the histopathological and biochemical investigations used on the first cases of PMT in Italian Chianina breed have been standardized later in the approach to other cases in other breed. In the following paragraphs I will sum up the clinical features and the main histopathological and biochemical findings published on Chianina cattle breed.

Clinical aspects of PMT in Chianina cattle breed

Bovine Congenital Pseudomyotonia (PMT) is an impairment of muscle relaxation induced by exercise that prevents animals from performing rapid movements.

The medical case was initially defined in Italian Chianina cattle in 2008. The main characteristic was a prolonged muscular contracture that particularly interests the hind limbs skeletal muscles (Figure 7). When the animal was stimulated to move faster than a simple slow-pace walk, the muscles froze-up temporarily leading to a stiff and uncoordinated gate. Whether the animal was obliged to continue the movement, the contracture prevented it to keep the balance and consequently it fell to the ground.

Figure 7. Image sequence of a muscle stiffness attack in two Chianina subjects (a and b).

The animal did not lose consciousness although it lied on the ground in a tetanic-like spasm till the contraction disappeared (within 20-30 seconds) and the animal regained the ability to normally move. The cramp attack was also provoked by walk on irregular ground, when animal dismounted from a track or if it was obliged to a sudden change of walk direction or speed. Moreover, strong external stimuli could frighten the animal and provoke the contraction attack. On the contrary, prolonged walk (at least 30 minutes) at low and regular pace did not provoke any cramp or sign of fatigue (Testoni et al., 2008). Another clinical sign associated with the skeletal muscle contracture was the protrusion of the third eyelid caused by the prolonged contraction of the *retractor bulbi* muscle. This aspect was also described in animals farmed in tie-stall housing in response of external stimuli (sounds or physical interaction) although no generalized muscle contractions were displayed (Testoni et al., 2008).

Routine hematology tests revealed no alterations in the values of the affected animals although biochemistry analysis showed a slight increase in levels of muscle-specific enzymes: creatine-kinase (CK: 8,000 iu/l, reference number <200 iu/l), lactate-dehydrogenase (LDH: 4000 iu/l, <1500 iu/l) and aspartate-aminotransferase (AST: 300 iu/l, <150 iu/l). L-lactate showed physiological values at rest (<2mmoli/l) but these levels increased immediately after the exercise-stimulated cramp attack (8 mmoli/l) (Testoni et al., 2008). Standard needle electromyography revealed no altered myoelectrical activities: spontaneous insertion and voluntary electrical activities were normal in all skeletal muscles observed, in addition no myotonic discharges were recorded after the exercise and the following contracture display. The latter feature led to adopt the term of "psudomyotonia", in contrast to true myotonia, to describe the pathology in the cattle (Testoni et al., 2008).

Histopathological findings of PMT in Chianina cattle

Semimembranosus muscle biopsy sections obtained from Chianina cattle PMT subjects were analysed. Routinely morphological and histochemical stainings were performed on samples collected from animals kept at rest, moved at a slow pace or after an fast-movement exercise test protocol (Sacchetto et al., 2009).

Gomori trichrome morphological staining showed normal fibre diameter, and no evidence of muscle damage when animal was at rest or moved at slow walk were

analysed, while dark giant fibres with large areas of degeneration were observed in the subjects that performed exercise protocol before biopsy. Anti-neonatal MHC immunostaining labelled small or medium size fibres around the degeneration areas suggesting a regenerative activity driven by local satellite cells. Histochemical stainings such as periodic acid-Schiff (PAS), cytochrome oxidase (COX) and succinic dehydrogenase (SDH) did not show morphological alterations and displayed a normal fibre type distribution in all samples. As general observation there was a subject-dependent variation in the severity of damages and in the grade of regenerative response (Testoni et al., 2008; Sacchetto et al., 2009).

Furthermore, monoclonal antibody against SERCA1 isoform was used to analyse fibre type distribution. In *semimembranosus* biopsies, most of the fibres were labelled representing type 2 fibre (fast-twitch), in agreement with the well-establish definition of *semimembranosus* as representative fast-twitch skeletal muscle. The small number of fibres that was unstained with anti-SERCA1, were positive to anti-SERCA2, and antiSERCA2-regulatory protein phospholamban (PLB), both markers of type 1 fibres (slow-twitch). This mutually exclusive protein expression, either SERCA1 or SERCA2 and PLB, was maintained in fibre of both pathological and control animals. Interestingly, comparing with normal, PMT-affected muscle sections revealed a reduction, from mild to severe, of immunoreactivity to SERCA1 suggesting a decrease in SERCA1 content (Sacchetto et al., 2009).

Biochemical characteristics of PMT Chianina cattle

Basing on the histological findings on SERCA1 distribution, biochemical analysis has been performed in order to obtain a protein profile of the disease.

Sarco(endo)plasmic Reticulum (SR) fractions were prepared from pathological and control muscle biopsies and probed with specific antibodies after electrophoresis and blotting. The antibodies used were against protein markers of junctional and non-junctional SR membranes. There were no differences between pathological and control sample in the expression of FKBP12 (junctional) or sarcalumenin and 53-kDa glycoprotein (non-junctional), although SERCA1 content showed a decrease in labelling of PMT-affected samples. In a case of Chianina cattle breed, a protein band of

about 55 kDa corresponding to the slow/cardiac Calsequestrin (CS) isoform was detected suggesting a regenerative process (Sacchetto et al., 2009).
In addition, real-time PCR experiments were performed to investigate whether the reduced levels of SERCA1 might be due to a reduced *ATP2A1* transcriptional activity. The analysis showed comparable mRNA expression levels in all pathological and control samples suggesting that the reduction might be due to post-transcriptional mechanisms (Sacchetto et al., 2009).
The Ca^{2+}-ATPase activity assay was another interesting analysis that has been performed in order to shed light on the functional characteristics of mutated SERCA1. The assay has been achieved on microsomal fractions enriched of SR membranes (Sacchetto et al., 2009). All the tests showed a lower pump activity of affected-subject samples when compared with control-animal samples, although the Ca^{2+}-dependence of pump activity resulted similar between pathological and healthy fractions. In other words, the functional assay indicated a reduction in the activity of SERCA1 in the fast-twitch skeletal muscle but not in the functionality of the enzyme. In conclusion, it has been displayed that the reduction in SERCA1 protein density in immunoblotting consistently correlated with the decrease in Ca^{2+}-ATPase activity. Moreover, this is also correlated with the reduced labelling in immuno-fluorescence histology (Sacchetto et al., 2009). Altogether, the data reported defined PMT mutation of Chianina as an alteration that leads to a decrease in quantity of SERCA1 protein that likely maintains its proper functionality.

After a few years from the first diagnosis of PMT, a 5-month old Dutch improved Red&White calf with a clinical history highly similar to PMT Chianina cases was presented to the Clinic of the Department of Farm Animal Health at Utrecht University. The research were immediately directed to assess the presence of the congenital alteration. Indeed, a DNA test was performed and a mutation in *ATP2A1* gene, different from Chianina mutation, was identified. In order to evaluate whether the functionality of mutant SERCA1 was maintained as in Chianina, Ca^{2+}-ATPase activity assay was performed on the new case and a decrease in activity was reported (Grünberg et al., 2010). Therefore, despite the different genetic background, the Dutch improved Red&White case was incredibly similar to Chianina affected animal.

Genetics of Bovine Congenital Pseudomyotonia

As mentioned before, Congenital PMT is caused by a genetic mutation in *ATP2A1* gene coding for SERCA1. So far, different point mutations have been described in the different breeds that displayed the disease (Figure 8).

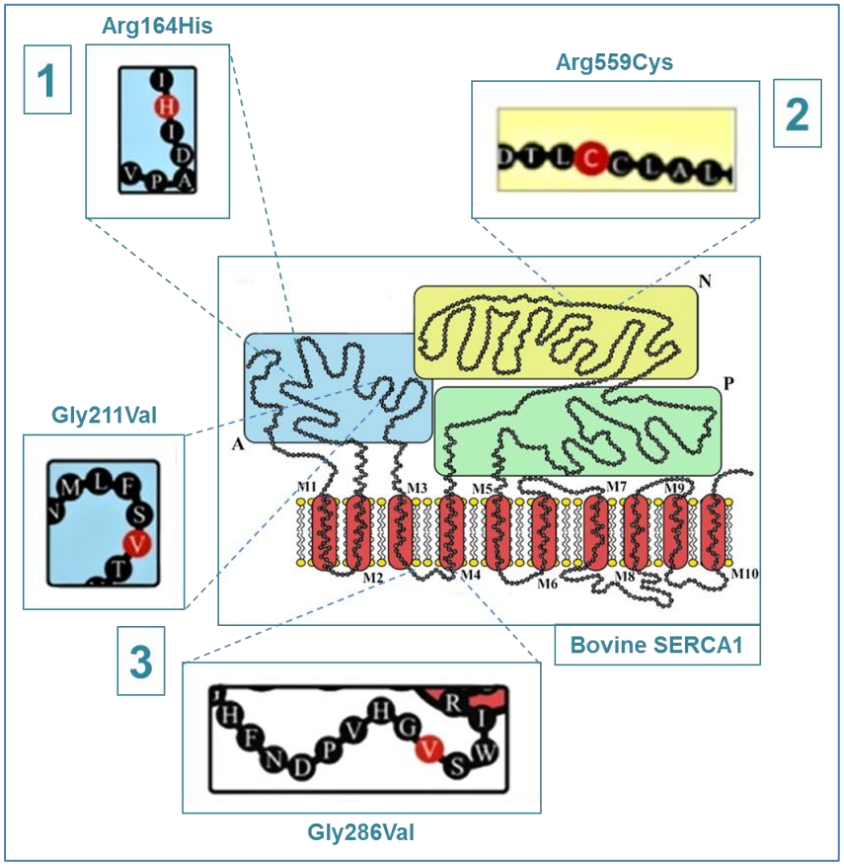

Figure 8. Cartoon model of bovine SERCA1 protein and its mutations reported so far in PMT animals. (1) mutation Arg164His identified in Chianina breed; (2) mutation Arg559Cys reported in CMD1-affected Blue Belgian calves and in the Dutch improved Red&White PMT case; (3) the double point mutation Gly211Val, Gly286Val reported in homozygosis or coumpound heterozygosis with Arg164His in Romagnola breed. Modified from Murgiano *et al.*, 2012.

The affected Chianina cattle carried homozygous a single base transition within exon 6 (c.491G>A), the missense mutation leads to an amino acid exchange in position 164 (Arg164His). In detail, the arginine in position 164 is substituted by an histidine within a highly conserved domain of SERCA1 affecting the actuator domain (domain A) and consequently the Ca^{2+} and ATP binding phases of the pump (Drögemüller et al., 2008).

The DNA sequencing carried on the Belgian Blue calves affected by CMD1 and the Dutch improved Red&White crossbred calf PMT-affected revealed a single base

transition within exon 14 (c.1675 C>T) of *ATP2A1* gene. The alteration leads to a substitution in position 559 in the amino acidic sequence of SERCA1. The arginine in position 559 is substituted by a cystein (Arg559Cys) generating an alteration in the conformation of the nucleotide-binding domain (domain N) of the Ca^{2+}-ATPase pump (Charlier et al., 2008; Grünberg et al., 2010).

In Romagnola cattle breed, a case was homozygous for two single nucleotide variations in *ATP2A1* exon 8 (c.[632 G>T; 857 G>T]) leading to the substitution of the two glycines in position 211 and 286 with two valines (Gly211Val, Gly288Val) in the protein sequence. The first substitution altered the domain A while the second one (286) affected a sarcoplasmic loop of the transmembrane domain (domain M). The other cases in Romagnola cattle breed were heterozygous for this double mutation at the exon 8 and, in addition, they were heterozygous for missense point mutation in exon 6 (c.491 G>A), the same variation identified in Chianina cattle breed. The Romagnola calves carrying all the three single substitutions were the first reported cases of compound heterozygosis for different mutations in a single gene in the bovine species (Murgiano et al., 2012).

Overall, it can be noticed how Pseudomyotonia is characterized by substantial genetic heterogeneity. The phenotypical expression of the disease is influenced by the carried mutation although some other genetic/breed characteristics should be considered for the final manifestation of the pathology, especially in terms of severity. This last proposed hypothesis may explain why the same mutation, Arg559Cys, caused impaired swallowing, abnormal growth and early death in Belgian Blue calves but neither respiratory implication, nor growth alteration were described in the Dutch improved Red&White case (Grünberg et al., 2010). At the same way, it is interesting to notice how different mutations in the same gene may generate severe and lethal changes (in Belgian Blue) or no deleterious symptoms allowing the animal to survive (in Chianina) and, from an economical point of view, to reach an age and a satisfying weight for slaughterhouse (Testoni et al., 2008; Sacchetto et al., 2009).

Finally, an intriguing result of the studies on Bovine PMT is that the observed phenotypes in affected cattle and the particular genetic heterogeneity make this disease a perfect model for a rare human genetic disorder named Brody disease (Brody, 1969;

Drögemüller et al., 2008). This pathological condition of skeletal muscle is caused by various mutations in the human *ATP2A1* gene which produce alterations in the SERCA1. The symptoms of bovine disease closely resembled the symptoms of human. Indeed, Brody disease is characterized by painless muscle contracture and exercise-induced impairment of muscle relaxation due to a defect of calcium re-uptake (Odermatt et al., 1996; Odermatt et al., 1997; Alex Odermatt et al., 2000). Moreover, Brody disease is genetically heterogeneous showing recessively or dominantly inherited forms, different mutations or no mutations in *ATP2A1* in patients displaying the typical symptoms of the muscular disease (Pan et al., 2003; Vattemi et al., 2010; Voermans et al., 2012). Consequently, the PMT affected cattle might be a very helpful and useful model to deepen the pathogenesis of the disease and the role of SERCA1. Indeed, bovine model allows to study naturally occurring mutation in a large animal which displays muscular morphology and biomechanics more similar to human than a traditional small mammal model (Drögemüller et al., 2008). A very intriguing application of bovine model might be the possible use as new target for therapeutic interventions such as injections of recombinant SERCA1 protein or inhibitors of the protein quality control systems (Drögemüller et al., 2008; Bianchini et al., 2014).

1.6.*Objectives*

The main objective of my PhD project was to complete the characterization of Bovine Congenital Pseudomyotonia by mean of analysing Italian Romagnola cattle breed cases and deepening the Dutch improved Red&White crossbred case from a morphological, histochemical and biochemical point of view. The bases of my research were the studies on Italian Chianina cattle breed (Testoni et al., 2008; Sacchetto et al., 2009; Murgiano et al., 2012) that since the first diagnosis of PMT enlightened the genetic cause, the pathogenic mechanisms and the main clinical, histopathological and biochemical appearance of PMT. Since Chianina PMT cattle was proposed as animal model for the study of human Brody disease, the report of novel *ATP2A1* gene mutations in different breeds reinforced the definition of PMT as the truly counterpart of the human muscular dysfunction. Consequently, the interest on this disease and its effects on the muscle tissue increased and the research progressed to understand whether the different genetic background lead to a similar phenotype.

Therefore, the main goal of my study was to integrate the data on Chianina cattle with the analysis of other PMT-affected animals in order to increase the knowledge on morphological and biochemical effects of the disease on the muscle tissue, to evaluate the phenotypic variability of the disease and to identify possible adaptive/compensatory mechanisms (Hypothesis 1). Moreover, comparative histological and biochemical analyses between Dutch improved Red&White and Italian Piedmontese cattle purebred subjects were performed in order to evaluate genetic influences or compensatory mechanisms that lead to the particular phenotype of Dutch improved Red&White case (Hypothesis 2).

Hypothesis	
1	Bovine Congenital Pseudomyotonia (PMT) in Italian Romagnola cattle breed shows the same features described in Italian Chianina cattle breed: i) degeneration of fibres always associated with regenerative phenomena; ii) no variation in fibre type distribution, fibre dimension or metabolic alteration; iii) exclusive decrease in SERCA1a quantity and activity.
2	The increase of mitochondria number in the fibres of the affected Dutch improved Red&White crossbred calf is a compensatory response of the muscular cells to the prolonged Ca^{2+} permanence in the cytoplasm.

2.MATERIALS AND METHODS

2.1.Animals recruitment

The animal used in this study were: a 5-month old female Dutch improved Red&White crossbred affected calf and two healthy control animals of same phenotype, gender and age; four Italian Romagnola cattle purebred affected calves (two males and two females, 2- or 3-month old) and three healthy control of the same breed. Figure 9 synthesizes graphically the genealogical tree of Dutch improved Red&White and Romagnola affected animals showing how the mutate alleles spread in heterozygosis through the generations till they cause clinical manifestation in homozygosis or in compound heterozygosis.

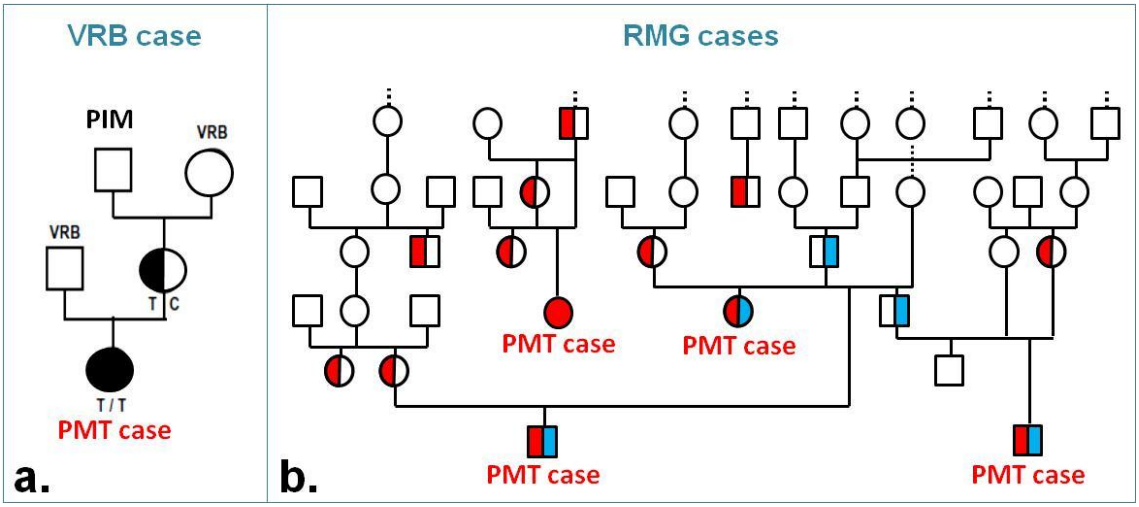

Figure 9. (a) Part of pedigree of the PMT-affected Dutch improved Red&White calf, the half-filled symbol represents the Arg559Cys mutant allele that was present in homozygosis (filled symbol) in PMT case and in heterozygosis in the dam. The genotype of the sire of PMT case was unknown (VRB=Verbeterd Roodbont or Dutch improved Red&White; PIM=Piedmontese). (b) Part of pedigree of the PMT cases in Italian Romagnola cattle breed (RMG), the red halves symbols represent the double point mutation Gly211Val, Gly286Val that was reported in homozygosis in one subject (red filled circle). The light blue halves symbols represent the Arg164His mutant allele reported also in Chianina. Three PMT-cases of Romagnola were compound heterozygous for this two mutations (half red and half light blue symbols). Image modified from (a) Grünberg *et al.*, 2010; (b) Murgiano *et al.*, 2012.

Additionally, three Italian Piedmontese purebred subjects were included in the study for a comparative evaluation. Two of these animals showed double-muscled phenotype, between class S and E according to S.E.U.R.O.P.[3] assessment grid of the EU carcass classification system (European Community, 1991; European Community, 2006). One was a 16-month old male, the other was a 22-month old female. The third animal was a female 27-month old with no extreme development of the muscles in the regions of the proximal fore and hind quarters like in the other two. This latter animal was indicated as non-hypertrophic, a condition that characterizes less than 4% of the population in Piedmonte Region in Italy (Miretti et al., 2013).

Biopsies of *semimembranosus* muscle, a representative fast-twitch muscle, were obtained under epidural anesthesia from Romagnola and the Dutch improved Red&White crossbred subjects (Grünberg et al., 2010; Murgiano et al., 2012).

Piedmontese samples were collected from the animals immediately after they were slaughtered at "Manzo Carni S.n.c." slaughterhouse in Rocca Dè Baldi (Cuneo-Italy).

Piedmontese breed was chosen because the Dutch improved Red&White crossbred affected calf was an offspring of a purebred Dutch improved Red&White sire and a crossbred (Piedmontese × Dutch improved Red&White) dam. Given that the affected Dutch improved Red&White displayed some intriguing morphological alterations when compared with the healthy controls, a complementary comparison with purebred Piedmontese could enlighten whether the reported changes were consequent to disease or phenotypic characters introduced by Piedmontese genetic line. Basing on various studies present in literature (Wegner et al., 2000; Wang et al., 2009), I speculated whether Piedmontese genetic line might confer phenotypic characters which could improve symptomatic outcomes in the affected crossbred animal.

2.2.*Preparation of the samples*

All muscle biopsies were frozen in cold isopentane and mounted upright for a cross-sectional cut on cork-disc with OCT (Optimal Cutting Temperature compound). Transverse sections (8µm) were cut in a cryostat. The obtained series of sections were used to perform histological, histochemical and immunohistochemical staining

[3] S.E.U.R.O.P., EU carcass classification system: S = super; E = excellent; U = abundant; R = good; O = fair; P = poor.

protocols. Moreover, part of the biopsies were frozen and stored at -80°C for further procedure of total protein and microsomal fraction extractions.

2.3.Histology, Histochemistry and Immunoistochemistry

Hematoxylin and eosin staining protocol (H&E) was accomplished for a general morphological analysis. Comparative α-napthyl acetate protocol for esterase staining was performed to underline the presence of macrophages inside and around the fibres degenerated or in degeneration (Miller et al., 1984).

Histochemical stains for cytochrome oxidase (COX) and succinic dehydrogenase (SDH) were performed to evaluate mitochondria distribution and possible metabolic alterations. Periodic acid shiff (PAS) stain was used to evaluate the glycogen content and its distribution in relation to the SR.

In order to characterize fibre types, myofibrillar ATPase (m-ATPase) stain was performed as previously described (Latorre et al., 1993). M-ATPase staining followed either alkaline pre-incubation at pH 10.2, 10.3 and 10.4 (sodium barbital 0.075M, sodium acetate 0.07M, calcium cloride 0.1M) or acid pre-incubation at pH 4.4, 4.5 and 4.6 (sodium acetate 0.2M). For the classification of fibres, we referred to the work of Maccatrozzo *et al.* (2004). In all slides, it was easily possible to distinguish type 1 from type 2 fibres. At pH 4.6 and 10.2, it was possible to separate type 2A fibres and 2X fibres (conventional 2B fibres). Some 2C fibres were also identified. All the histological and histochemical protocols are synthetically described in Table 1 along with the general immunostaining procedure used for the immunohistochemical analysis.

The primary antibodies used were:

_polyclonal anti neonatal (α) myosin heavy chain isoform (αMHC dilution 1:5000, Sigma St. Louis MO);

_monoclonal antibody against sarco(endo)plasmic reticulum calcium ATPase 1a (SERCA 1a, dilution 1:500, Biomol Plymouth Meeting PA);

_monoclonal antibody against sarco(endo)plasmic reticulum calcium ATPase 2 (SERCA 2, dilution 1:200, Biomol Plymouth Meeting);

_monoclonal antibody anti-phospholamban (PLB, dilution 1:200, Affinity BioReagents, Golden CO);

_monoclonal antibody against myosin heavy chain isoform I (MHCI dilution 1:200, Sigma);

_polyclonal antibody anti-mitochondrial preprotein traslocases of the outer membrane 20 (Tom20, dilution 1:100, Santa Cruz biotechnology, Texas US).

Immunostained slides were then incubated either with secondary antibody conjugated with TRITC (Dako, Milano, Italy) and visualized with Laica TCS-SP2 confocal laser scanning microscope, or with secondary antibody conjugated with biotin (Sigma) and the reaction was visualized with Olympus Vanox AH-3 bright field microscope after Envision Method (Vector, Burlingame US).

Staining	Procedure
H&E	1.Rinse in deionized water; 2.Stain 1x12min in haematoxylin, rinse 1x3min in deionized water, rinse 1x5min in running tap water, dip few seconds in HCl-ethanol (1/70), rinse 1x3min in deionized water; 3.Stain 1x40 seconds in eosin, dehydrate in alcohol 2x95%>2x100% (3min each), 3x5min in xylene; 4.Mount slides and dry ON in the hood.
Esterase	1.Stain 1x5min in Staining Solution (prepared fresh: 5mg α-naphtyl acetate, 0.75 ml acetone, mix, add 12.5ml 0.2M sodium phosphate, mix, add azotized pararosaniline -0.4ml 4% pararosaniline HCl and 4ml 4% sodium nitrite); 2.Rinse for several minutes in running tap water; 3.Dehydrate in alcohol 1x50%>1x70%>2x95%>2x100% (5min each), and 3x5min in xylene; 4.Mount slides and dry ON in the hood.
COX	1.Stain 1x30min at RT in Incubating Solution (prepared fresh: 750mg sucrose in 7.5ml deionized water, add 2.5ml 0.2M phosphate buffer pH7.6, add 5mg DAB, 10mg cytochrome C, 20µg catalase); 2.Rinse 2x5min in deionized water; 3.Dehydrate in alcohol 1x50%>1x70%>2x95%>2x100% (3min each), 3x5min in xylene; 4.Mount slides and dry ON in the hood.
SDH	1.Stain 1x30min at 37°C in Incubating Solution (prepared fresh: in 10ml 0.2M phosphate buffer pH7.6 dissolve 270mg sodium succinate and 10mg NBT-nitro blue tetrazolium-); 2.Rinse 2x5min in deionized water; 3.Rinse in 30%-60%-90% acetone/water solution in increasing and decreasing concentration (3min each; 4.Rinse several times in deionized water; 5.Mount slides with aqueous mounting media and dry ON in the hood.
PAS	1.Incubate 1x15min in Carnoy' fixative (60% ethanol, 30% chloroform, 10% acetic acid); 2.Rinse 3x3min in deionized water; 3.Incubate 5min in 0.5% periodic acid solution; 4.Rinse 3x3min in deionized water; 5.Incubate 15min with Shiff reagent; 6.Rinse 1x5min in tap water and 1x5min in deionized water; 7.Stain 1min in haematoxylin; 8.Rinse 1x5min in tap water and 1x5min in deionized water; 9.Dehydrate in alcohol 1x50%>1x70%>2x95%>2x100% (3min each), 3x5min in xylene; 10.Mount slides and dry ON in the hood.

m-ATPase	1.Incubate 1x15min in alkalin pre-incubation buffer or 1x5min in acid pre-incubation buffer; 2.Rinse twice in deionized water; 3.Rinse twice in Wash Solution (0.075M Na-barbital, 0.07M Na-acetate, 0.1M Ca-chloride, pH9.45); 4.Incubate 30min (after alkaline pre-incubation) or 60min (after acid pre-incubation) in ATP-incubation Solution (1mg/ml ATP in Wash Solution); 5.Rinse 3x30seconds in Ca-chloride; 6.Incubate 1x3min in Co-chloride and rinse in deionized water; 7.Incubate 1min in Ammonium sulfid and wash in deionized water; 8.Dehydrate in alcohol 2x95%>2x100% (3min each), 3x5min in xylene; 9.Mount slides and dry ON in the hood.
HIC	1.[For Tom20 Ab, permeabilization step 15min in 0.15%Triton in PBS]; 2.Block 1x60min in 1%BSA-PBS; 3.Incubate primary antibody 60-90min; 4.Wash 3x5min in PBS; 5.Incubate 60min with secondary antibody; 6.Wash 3x5min in PBS; -If biotin-conjugated (diluted 1:200): 7.Incubate 60min with ABCkit (Avidin-Biotin Complex, Vector); 8.Wash 1x5min in PBS; 9.Stain with DAB (3, 3'diaminobenzidine, Vector) from 45seconds till 1min and 45seconds depending on the signal; 10.Rinse in deionized water, dehydrate in alcohol 2x95%>2x100% (3min each), 3x5min in xylene, mount slides and dry ON in the hood. -If TRITC-conjugated (diluted 1:100): 7.Mount slides with special mounting media (Vectrasin) and fix the coverslip with polish, store in dark.

Table 1. Synthetic explanation of the staining protocols used in this project.

Additionally, measurements of fibre areas were recorded using software Adobe Photoshop CS4 on COX stained slides images (magnification 10X) of Dutch improved Red&White and Piedmontese subjects. Fibres were chosen randomly among 20 images per sample and a total of 200 light labelled fibres and 200 dark labelled fibres per animal were measured. The fibres were then grouped in classes of dimension to build a distribution curve using Microsoft Excel 2010 software (Microsoft corporation).

2.4.Biochemical analysis

2.4.1.Microsomal fractions preparative procedures

For Romagnola and Dutch improved Red&White crossbred subjects, a crude microsomal fraction enriched in content of SR membranes was isolated using differential centrifugation method previously described (Sacchetto et al., 2005; Sacchetto et al., 2009). Briefly, tissue samples were homogenized in 10 mM/L HEPES, pH 7.4, 20 mM/L KCl containing 1 µg/ml leupeptin and 100 µM/L phenylmethylsulfonyl fluoride. The first centrifugation at 650×g for 10 minutes at 4°C removed the myofibrils (sedimented). Afterwards, ultracentrifugation at 120,000×g for 90 minutes at 4°C was performed on the previous supernatant. The obtained pellet consisted in the crude SR fraction. These membrane fractions were resuspended in 0.3 M/L sucrose, 5 mM/L imidazole, pH 7.4, containing 1 µg/ml leupeptin and 100 µM/L phenylmethylsulfonyl fluoride and stored at -80°C. Protein concentration was determined by the method of Lowry *et al.* (1951) using bovine serum albumin as standard.

2.4.2.ATPase biochemical assay

ATPase activity of the microsomal fractions (20 µg/ml) was measured by spectrophotometric determination of NADH oxidation coupled to an ATP regenerating system, as previously described (Sacchetto et al., 2009). The assay was performed at 37^{o}C in the presence of 2 µg/ml A23187 Ca^{2+}-ionophore at pCa5.

2.4.3.Total homogenates preparative procedures

Roughly 100 mg of the biopsies from Dutch improved Red&White crossbred and Piedmontese subjects were used to prepare total muscle homogenates that were used in electrophoresis and immunoblotting as explained further below.

The biopsy was first wetted with 5 µl of leupeptin (1µg/ml) and phenylmethylsulfonyl fluoride (100 µM/L) and then minced into small pieces with scissors. Finally, the minced muscle was collected in a 5 ml tissue grinder vessel (Potter). After 600 µl of Lysis buffer (62.5 mM Tris/HCl, pH 6.8, 10% glycerol, 2% SDS containing 1µg/ml leupeptin and 100 µM/L phenylmethylsulfonyl fluoride) were added, the sample was homogenized up and down until the tissue appeared completely homogenized. The

liquid part was removed with a glass pipet and placed in a clean 1.5 ml test tube (eppendorf). Using other 400 µl of Lysis Buffer, the sample was homogenized a second time, the liquid part was removed and placed in the test tube. The homogenates were then centrifuged 10,000 rpm for 10 minutes and the supernatant was carefully removed, placed in a clean 1.5 ml test tube and stored at -80°C. Protein concentration was determined by the method of Lowry *et al.* (1951) using bovine serum albumin as standard.

2.4.3.Gel Electrophoresis and Immunoblotting

Equal quantities of crude sarcoplasmic reticulum microsomal fractions were separated by 5-10% SDS-polyacrylamide gel electrophoresis (SDS-PAGE) as previously described (R Sacchetto et al., 2012). On the other hand, total proteins fractions were separated by 10-15% SDS-PAGE. Slab gels were either stained with EZblue Gel Staining Reagent or cationic dye Stains-All (Sacchetto et al., 2009), or proteins were electroblotted to Protran Nitrocellulose transfer membrane (Schleicher&Schuell Bioscience GmbH Whatman Group, Dassel Germany) for subsequent immunoblotting survay.

Immunoblotting was performed using the following primary antibodies:

_monoclonal antibody against sarco(endo)plasmic reticulum calcium ATPase 1a (SERCA 1a, dilution 1:500, Biomol Plymouth Meeting PA);

_monoclonal antibody against sarco(endo)plasmic reticulum calcium ATPase 2 (SERCA 2, dilution 1:200, Biomol Plymouth Meeting);

_monoclonal antybody anti-ryanodin receptor (RyR, dilution 1:5000, Thermo scientific);

_monoclonal antibody anti-sarcalumenin and glycoprotein53 splice variant (GP53, dilution 1:4000, Affinity Bioreagents, Golden CO);

_monoclonal antibody anti-plasma membrane calcium ATPase (PMCA, dilution 1:2500, Thermo Fisher scientific);

_polyclonal antibody anti-mitochondrial preprotein traslocases 20 of the outer membrane (Tom20, dilution 1:1000, Santa Cruz biotechnology).

The transfer membrane was incubated with secondary antibody alkalin phosphatase-conjugated (Sigma) and premixed BCIP/NBT solution (Sigma-Aldrich) was used to visualize the reaction.

2.5.*RNA preparation and Quantitative Real-Time PCR*

SERCA1 mRNA levels were quantified by real-time PCR (RT PCR). The procedures to extract RNA, to synthetize cDNA and to perform RT PCR were the same described in Sacchetto *et al.* (2009). Briefly, total RNA was isolated from *semimembranosus* muscles using TRIzol reagent (Invitrogen, Milano, Italy). Two micrograms of total RNA from each sample were subjected to random hexamer primed first-strand cDNA synthesis in a volume of 20 µl using Superscript II reverse transcriptase (Invitrogen), according to manufacturer's instructions. Real-time PCR was performed by the SYBR Green method with an Applied Biosystems 7,500 Fast Real Time PCR System (Patruno et al., 2008). Real-time PCR amplification was performed in a total volume of 20 µl. Reaction conditions were as follows: 2 minutes at 50°C, 10 seconds at 95°C, and 40 cycles of 15s at 95°C, 1 minute at 60°C. Oligonucleotide primers used were:

SERCA1

5′-GCACTCCAAGACCACAGAAGA-3′ (sense);

5′-GAGAAGGATCCGCACCAG-3′ (antisense);

glyceraldehydes-3-phosphate dehydrogenase

5′-GGTCACCAGGG CTGCTTTTA-3′ (sense),

5′- GAAGATGGTGATGGCCTTTCC-3′ (antisense).

3.**RESULTS**

3.1.*Clinical features of Congenital Pseudomyotonia in Romagnola and Dutch improved Red&White affected animals*

The first approach to the animals manifesting signs of neuromuscular dysfunction was a deep clinical examination that put in differential diagnosis several possible disease, PMT included.

The Romagnola animals analysed in this study were four young calves that, at clinical examination, were bright, alert and in good body condition. Since their birth, all were showing exercise-induced muscle contraction that prevented them from performing muscular activities of greater intensity than a simple walk at a slow pace. When forced to move faster, the muscles 'froze up' temporarily, inducing rigidity and uncoordinated gait without signs of pain. When forced to continue the movement animals reach a stiffness condition so pronounced that made impossible any further action and they fell to the ground. After a few seconds, the muscles relaxed and the animals regained their ability to get up and move. At the same way, when the calves were startled by an operator that rapidly approached them or was making sudden noises and movements, a cramp attack showed up (Figure 10a and b). One of the calf had a character particularly active and curious, moving and scouting during the whole clinical evaluation. This subject was also characterized by an hyper-reactivity to the external stimulations showing stronger intensity in the attacks (Figure 10b).

As already reported (Grünberg et al., 2010) the Dutch improved Red&White calf was bright, alert and responsive with normal mentation and behaviour. It was normally developed for its age with good body condition and, being the offspring of two doubled-muscling cattle breeds (Dutch improved Red&White and Piedmontese), it had the characteristic muscle development. In contrast with Romagnola calves, this animal was moving slowly, making short strides and carrying the head low (dorsal line of the neck parallel to the ground). Pushing the calf from either side to induce a corrective movement to maintain equilibrium induced a generalized sudden muscle spasm of the whole body resulting in a saw-horse type position and a consequent loss of balance. The

calf flipped over with extended legs and remaining in lateral recumbency with stiffened limbs for 20 to 30 seconds (Figure 10c). The relaxation of the limb musculature occurred after this period of time allowing the animal to regain sternal recumbency first, and to get up later. During these episodes the animal remained bright and alert without losing consciousness. At the same way, forcing the calf to walk at a faster pace rapidly induced an increase in muscle tone of body and limbs leading to a bunny-hopping type gait, and as stiffness progressed, making further strides or even movements of head or neck impossible. Whether the animal was left at rest after this forced exercise, the muscle stiffness shortly resolved (Grünberg et al., 2010).

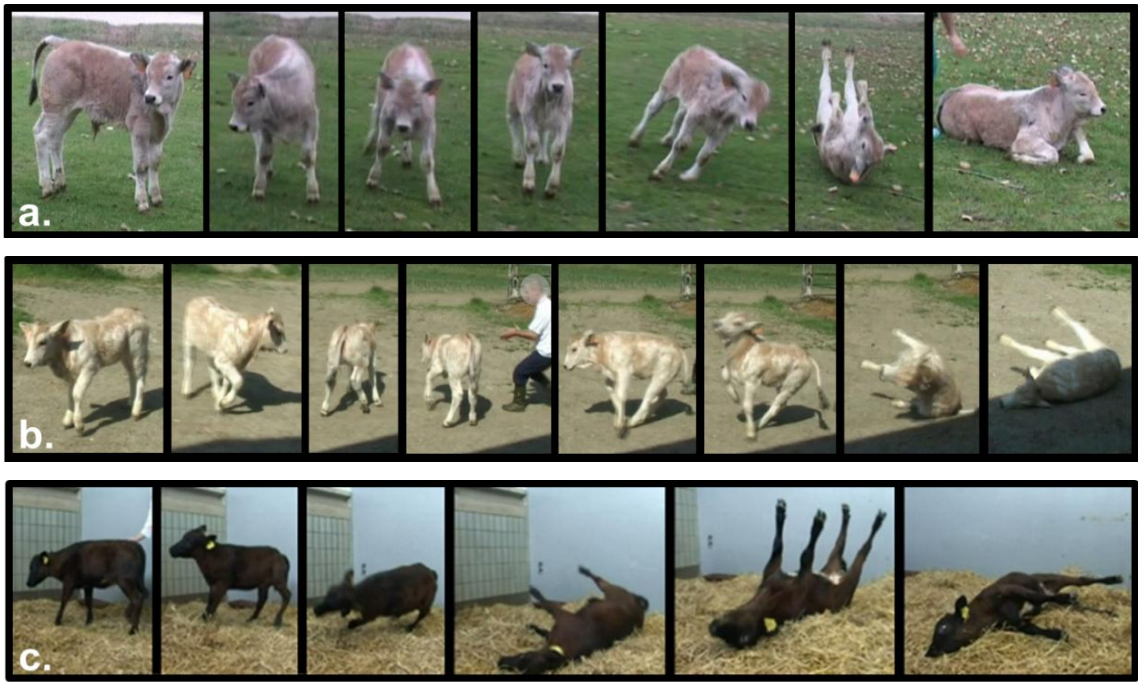

Figure 10. Sequential images of a muscle stiffness attack in (a, b) two Romagnola calves and in (c) the Dutch improved Red&White calf affected by PMT.

In all the animals electromyography (EMG) investigation performed at rest on muscles of forelimb (*paraspinalis* of the thoracic region, *deltoid* muscles) as well as of hind limb (*triceps surae* and *gluteobiceps* muscles, *quadriceps femoris* muscles) showed no spontaneous activity. A part from the muscular symptoms no other clinical signs were reported. Consequently, the absence of myotonic discharges and the specific sequence of events in a cramp attack leaded the diagnosis to PMT. Indeed, the clinical symptoms reported in the Dutch improved Red&White case and in the four Romagnola affected calves, strongly resembled the Chianina cases of PMT (Testoni et al., 2008) even if the Dutch improved Red&White calf displayed more severe clinical appearance when

compared with the other PMT subjects. Indeed, the Dutch improved Red&White affected calf was unable to get up without assistance till three days of life and it always showed a certain level of muscle stiffness that obliged it to move slowly or limited some simple movements (e.g. lift the head, belt the neck).
Regardless the different grade of severity, genetic analyses confirmed the clinical suspects of PMT locating novel point mutations in *ATP2A1* gene, different from the one found in Chianina (Grünberg et al., 2010; Murgiano et al., 2012).

3.2.*Histopathological characterization of Congenital Pseuodomyotonia in Romagnola and Dutch improved Red&White calves*

Despite the different *ATP2A1* gene mutation, the close clinical similarities between Chianina and Romagnola PMT subjects lead to speculate whether the two breeds share also the histopathological consequences of the genetic alteration. The histological, histochemical and immunohistochemical analyses performed on Romagnola animals aimed to collect information of the disease effects on muscle tissue in this breed.
The Dutch improved Red&White affected subject had a particular genetic background being a crossbred of two different double-muscled breeds (Dutch improved Red&White and Piedmontese). Indeed, Dutch improved Red&White cattle is closely related with Belgian Blue cattle breed since it was used to increase the muscle development in a breed primarily characterized by dairy attitude (Dutch Red&White). The double-muscling phenotype in Belgian Blue is caused by a deletion of eleven bases in the gene coding for Growth Differentiation Factor 8 (GDF8) or Myostatin that leads to a complete inactivation of the protein (Kambadur et al., 1997). This mutation was introduced in Dutch improved Red&White cattle breed to improve the beef production. At the same way, it could be possible that also the mutation in *ATP2A1* gene, causing the substitution Arg559Cys in the SERCA1a, was accidentally introduced in Dutch improved Red&White genetic line in the inbreeding process. This last consideration may provide an explanation on the fact that the identical mutation at *ATP2A1* gene was found in Belgian Blue calves affected by Congenital Muscular Dystonia 1 (CMD1) and in the Dutch improved Red&White crossbred calf affected by PMT. The other double-muscled breed present in the genealogic tree of Dutch improved Red&White crossbred calf was the Piedmontese cattle breed, an Italian breed characterized by a missense

mutation in the gene coding for GDF8 that leads to a substitution of a cysteine by a tyrosine in protein sequence (Kambadur et al., 1997). As consequence of the mutation, GDF8 decreases its inhibiting activity and causes an increased muscle development.
The Dutch improved Red&White calf represents a result of a combination of two mutations at GDF8 and this might influence the clinical and pathological outcome of SERCA1a mutation. Indeed, since the mutations in Belgian Blue CMD1-calves and in Dutch improved Red&White PMT-calf were the same, the severity of manifestation in the two breeds was different. A comparative study between Dutch improved Red&White and Piedmontese animals was performed in order to highlight common phenotypic characteristics that might improve the response to the disease in the Dutch improved Red&White subject.

3.2.1.Morphological profile of Congenital Pseudomyotonia in Romagnola cattle breed and immunofluorescence analysis of SERCA1, SERCA2 and PLB expression in pathological muscle

Biopsies of *semimembranosus* muscle were collected from affected and control animals kept at rest. No exercise protocols were performed before the sampling in order to avoid the influence of the physical activity (and of eventual muscle stiffness attack) in the histological appearance and obtain a picture of the disease in "normal" (non-stressed) condition. Indeed, in a previous study my group demonstrate an exercise-dependence in the severity of histopathological signs in muscle of Chianina PMT-affected animals (Sacchetto et al., 2009). The histopathological examination achieved on Romagnola animals used in this study revealed the presence of degenerated fibres in pathological subjects. The degree of alteration was generally mild with some fibres in degeneration followed by fibre regeneration and no other major morphological changes (e.g. central nuclei). Nevertheless, a Romagnola case appeared more severe than the other subjects displaying frequent degenerative fibres with enlarged and pale cytoplasm often surrounded or filled by mononuclear cells. The labelling for non-specific esterase suggested that these cells were macrophages (Figure 11a-d) (Cosford et al., 2008). This higher severity in histopathological signs might be relate to a major activity of the subject before the sampling procedure. The immunostaining of the serial section using anti-neonatal myosin heavy chain (αMHC) marked positively small-size fibres in the

proximity of degenerating/ed fibres and proved the presence of regenerative phenomena in all the affected animals analysed (Figure 11e-i).

In addition, combined COX-SDH staining was performed to evaluated possible metabolic alterations. Sections from all Romagnola animals used in this project were analysed with this stain and no alterations were noticed (Figure 12a and b-da aggiungere). Also PAS stain revealed no changes in glycogen distribution displaying a typical honeycomb-like staining pattern and consequently indicating a normal association between glycogen and SR membranes (Figure 12c, d and e).

Furthermore, in order to enlighten whether the mutation caused a decrease in SERCA1 expression, sections of all Romagnola subjects were incubated with the corresponding antibody. Moreover, antibodies against SERCA1, SERCA2 and PLB were used on serial section to investigate the distribution pattern of the three proteins. *Semimembranosus* muscle is a predominantly fast-twitch muscle, consequently most of the fibres were immunostained for SERCA1 and few for SERCA2 and PLB. The evaluation of SERCA1 expression revealed a decrease in fibre immunoreactivity for SERCA1 in the affected animals compared with the healthy controls (Figure 13a, b). Moreover, immunofluorescence showed a mutually exclusive labelling for SERCA1 or SERCA2 along with PLB in all the sample. However, in pathological animals some fibres faintly labelled with SERCA1 were also faintly reactive for SERCA2, and some fibres were immunoreactive for both SERCA1 and PLB displaying a novel pattern of co-expression of the three proteins (Figure 14a-f).

3.2.2.Morphological characterization of the Dutch improved Red&White PMT-affected subject and comparative analysis between Dutch improved Red&White calves and Piedmontese cattle

The morphological analysis on Dutch improved Red&White crossbred case revealed to be a further support to the definition of a general PMT case. Indeed, the histopathological analyses described a picture similar to Chianina and Romagnola with some fibres in degeneration surrounded by macrophages and always accompanied with regenerative phenomena (Figure 11g-k). No metabolic alterations in terms of glycogen SR-association or oxidative enzymes distribution were reported. Although, an increased intensity for the oxidative enzymes staining was described in PMT case along with

hypertrophy of a particular fibre population (Dorotea *et al.*, submitted for publication). These observations will be better described later in this paragraph.

To complete the morphological investigation, serial sections of Dutch improved Red&White subjects were incubated with antibodies against SERCA1, SERCA2 and PLB in order to evaluate the expression levels and the distribution pattern of these proteins. As for Chianina and Romagnola, Dutch improved Red&White *semimembranosus* muscle sections showed almost complete immunostaining for SERCA1 and only few fibres positive for SERCA2 and PLB. In addition, the immunoreactivity for SERCA1 in the affected animals was relative minor when compared with the healthy controls (Figure 13c and d). Finally, also Dutch improved Red&White subjects displayed a classical mutually exclusive labelling for SERCA1 or SERCA2 along with PLB, although in pathological animals some fibres co-expressed the two isoforms or SERCA1 and PLB (Figure 14g-m).

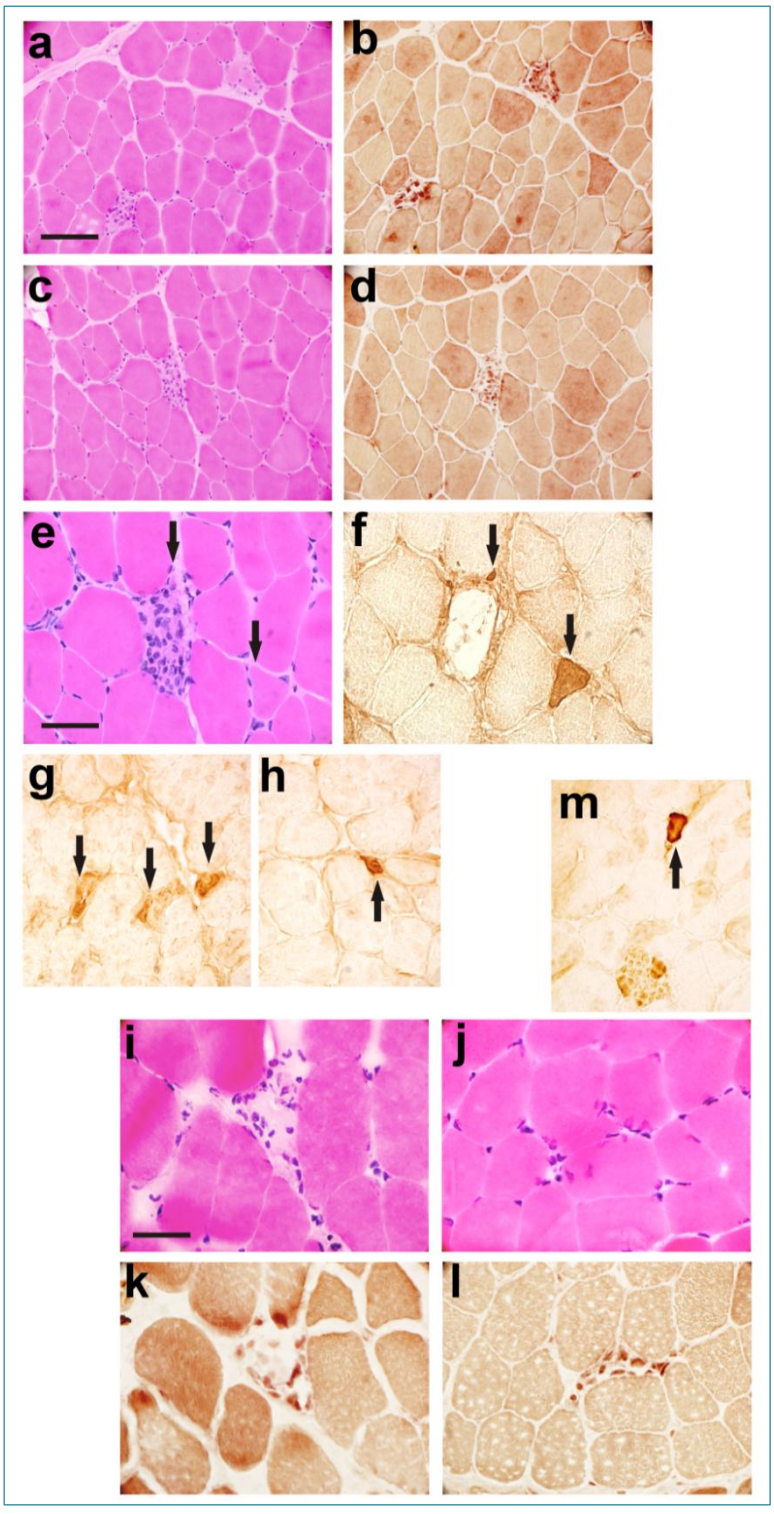

Figure 11. Histological and immunohistochemical stainings on *semimembranosus* muscle cryosections from Romagnola (a-h) and Dutch improved Red&White (i-m) affected calves. Serial sections were stained with H&E (a, c, e, i, j) to identify areas of myonecrosis and phagocytosis, or with esterase reaction (b, d, k, l) to highlight the lysosomal activity within macrophages clearing necrotic debris. Arrows in (f, g, h, m) indicate small fibres positive for immunostained with antibodies to neonatal MHC isoform. Scale bars: 100 µm (a-d), 50 µm (e-m).

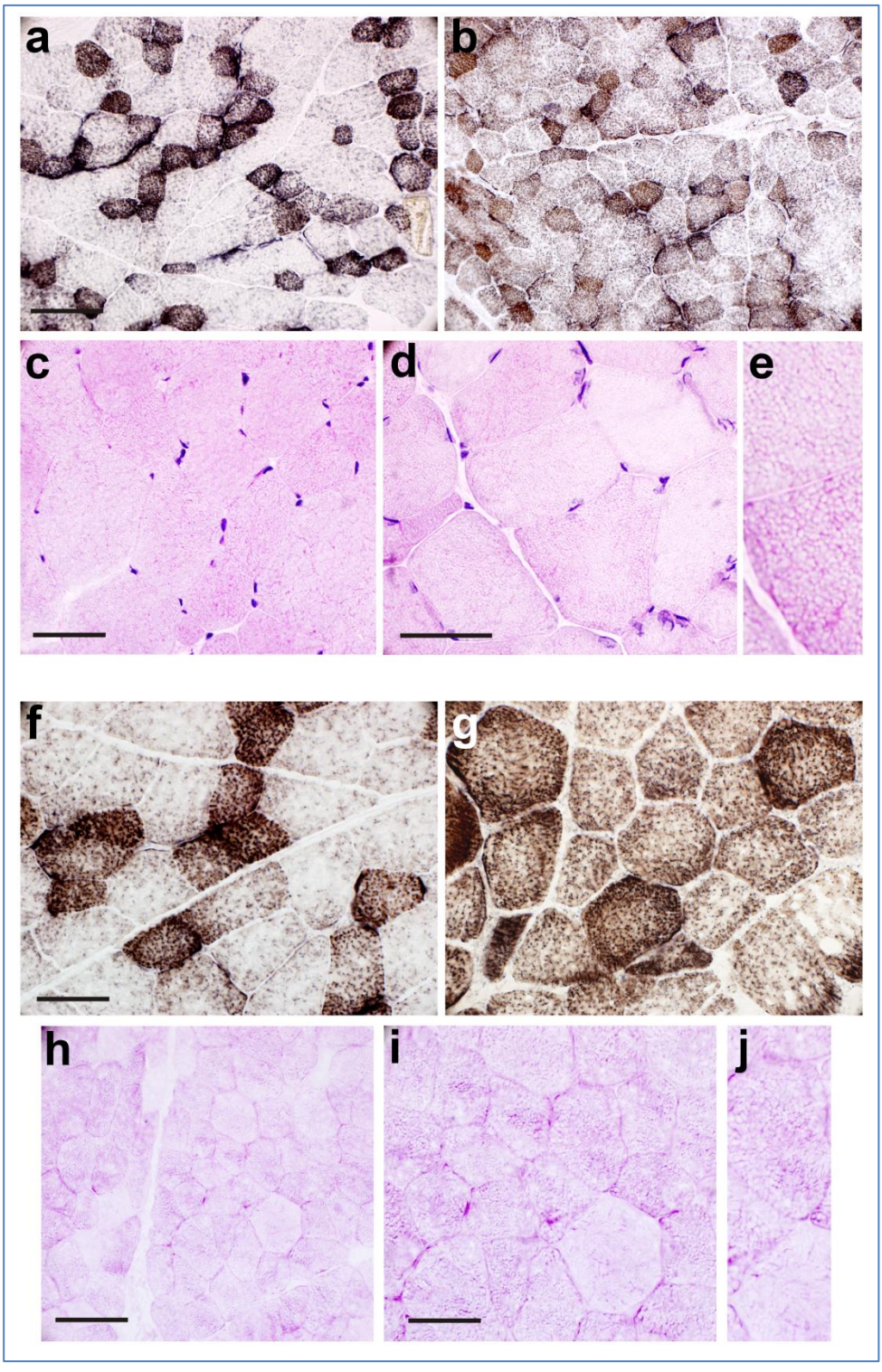

Figure 12. Representative histochemical staining on *semimembranosus* muscle cryosections from Romagnola and Dutch improved Red&White healthy and affected calves. Combined COX-SDH staining shows no alteration in the distribution of mitochondria nor in healthy (a, f) nor in pathological (b, g) animals. PAS staining reveals a normal association of glycogen to SR membranes both in controls (c, h) and affected (d, i) subjects displaying the typical polygonal honeycomb-like staining pattern (e, j). Scale bar: 100 µm (a, b, h), 50 µm (c, d, f, g, i).

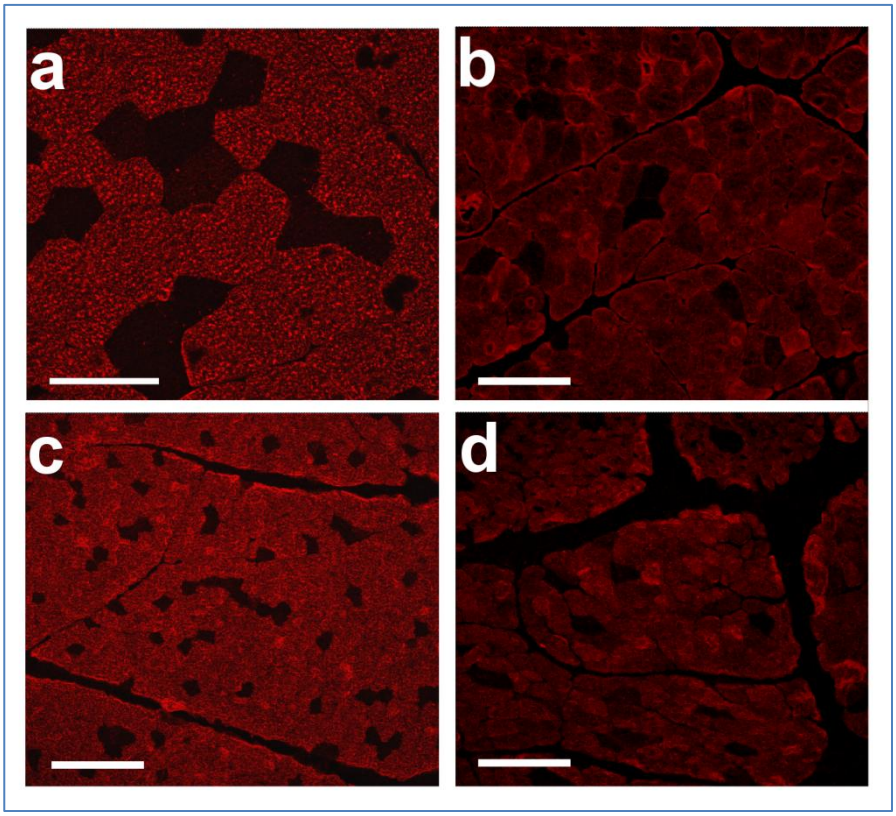

Figure 13. Confocal microscopy of *semimembranosus* muscle cryosections. (a) Control and (b) PMT affected Romagnola subjects; (c) healthy and (d) pathological Dutch improved Red&White animals. Transverse sections from were immunolabelled with monoclonal antibodies to SERCA1 and then incubated with TRITC-conjugated anti-mouse secondary antibodies. Control sections display a more intense immunoreactivity when compared to affected sections. Scale bars: 100 µm (a), 150 µm (b-d).

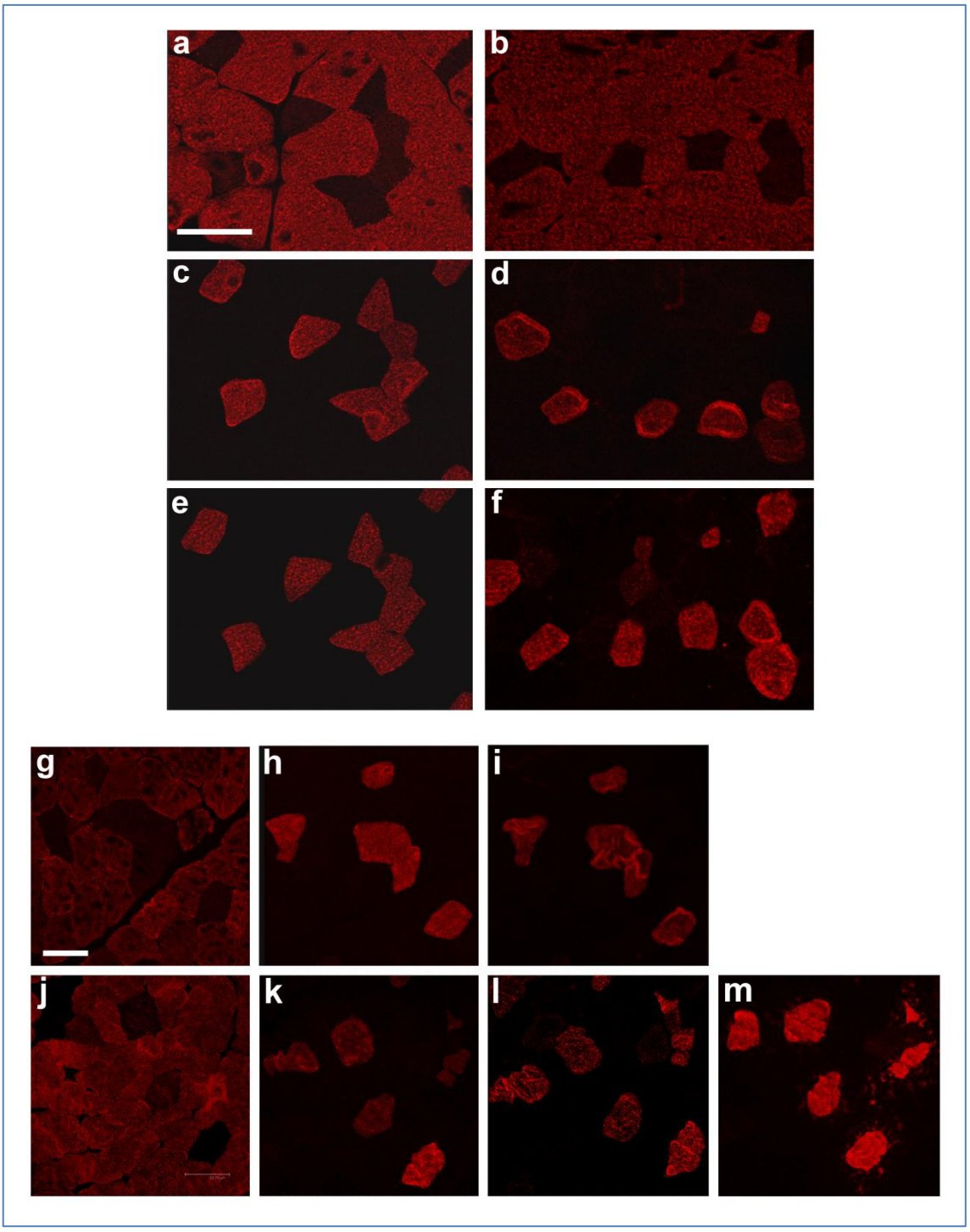

Figure14. Representative confocal microscopy of *semimebranosus* muscle cryosections from Romagnola (a-f) and Dutch improved Red&White (g-m) subjects. Serial sections were immunolabelled with monoclonal antibody against SERCA1 (a, b, g, j), SERCA2 (c, d, h, k) and PLB (e,f, i, l).The three proteins display a mutually exclusive pattern of expression although some fibres co-express the two SERCA isoforms or SERCA1 and PLB (b, d, f and j,k,l). Monoclonal antibody to MHC I (m).was used to identify fibres type 1. Scale bar: 100 µm.

Moreover, cross sections of Dutch improved Red&White and Piedmontese subjects were stained for COX. Using the microscope images obtained from these slides, I measured the cross-section areas of a representative sample of the two fibre populations that this protocol easily differentiates: oxidative (dark labelled) and glycolytic (lightly or no labelled) fibres (Figure 15). Integrated fibre classifications described three types of fibre: large-size fast-twitch glycolytic fibres (type 2X), intermediate-size fast-twitch oxidative fibres (type 2A) and small-size slow-twitch oxidative fibres (type 1) (Schiaffino and Reggiani, 2011).

As mentioned earlier, Piedmontese cattle breed is characterized by a great muscular mass development named double-muscling that is caused by a missense mutation in the gene coding for GDF8 (Kambadur et al., 1997). Generally, double-muscled animals have increased number and dimension of fast glycolytic fibre (conventional 2B or 2X type) that consequently are more frequent than slow fibre and have marked hypertrophy. In addition, different grades of hypertrophy and hyperplasia are described between and within double-muscled breeds (Wegner et al., 2000). The comparative analysis performed in this study showed that the largest glycolytic fibres were identified in Piedmontese subjects according to their pure double-muscled phenotype. The Dutch improved Red&White subjects had relatively smaller glycolytic fibre and, within them, the affected Dutch improved Red&White had the smallest. Interestingly, in all the healthy subjects, oxidative fibres are always smaller than the corresponding glycolytic fibres, on the contrary in the affected Dutch improved Red&White this proportion is inverted showing the oxidative fibres broadly larger than the glycolytic ones (Figure 15d).

Staining protocol for sole COX or SDH was used to evaluate the presence and distribution of mitochondria. In all the healthy animals used in the comparison study (Dutch improved Red&White and Piedmontese), COX and SDH stain showed a similar pattern with a restricted labelling to a specific population of fibres: oxidative (dark labelled) and glycolytic (lightly or non-labelled) fibres. Interestingly, the sections of the affected Dutch improved Red&White subject showed a more homogeneous stain for COX and SDH in all the fibres with no clear difference between the two population (Figure 16a, e and i). This increased staining level for oxidative enzymes might suggest a possible increase in mitochondria activity and/or number. To clarify this observation,

immunohistochemistry with an antibody against a structural protein of the mitochondrion (Tom20) was performed (Figure 16m-p). The stained sections of the healthy controls displayed an immunoreactivity mostly restricted to a population of fibres whereas in the affected Dutch improved Red&White subject the sections showed a diffuse immunofluorescence throughout all the fibres (Figure 16 q-v) supporting a possible increase in mitochondria presence.

In addition, fibre type characterization was performed on sections of Dutch improved Red&White and Piedmontese using m-ATPase staining protocol. Comparing acid and alkaline pre-incubated serial sections, it was possible to unambiguously distinguish fibre type 1 (slow-oxidative), type 2A (fast-oxidative) and 2X (fast-glycolytic) in all the subjects (Figure 17). Few type 2C fibres (Maccatrozzo et al., 2004) were also identify (arrows in Figure 17g-i).

A comparative analysis between serial slides stain with COX and m-ATPase allowed to combine the complementary information of these procedures. The comparison revealed that in healthy Dutch improved Red&White and in Piedmontese subjects the large-size fibres, light in COX stain, are type 2X fibres, the intermediate-size fibres, dark in COX stain, are type 2A fibres and the small, dark fibres are type 1 fibres (Figure 17a-i). Interestingly, in affected Dutch improved Red&White subject the fibres that displayed an increased labelling for COX resulted to be type 2X fibres (Figure 17j-l). Moreover, the large dark fibres of affected Dutch improved Red&White corresponded to type 2A fibres (Figure 17j-l).

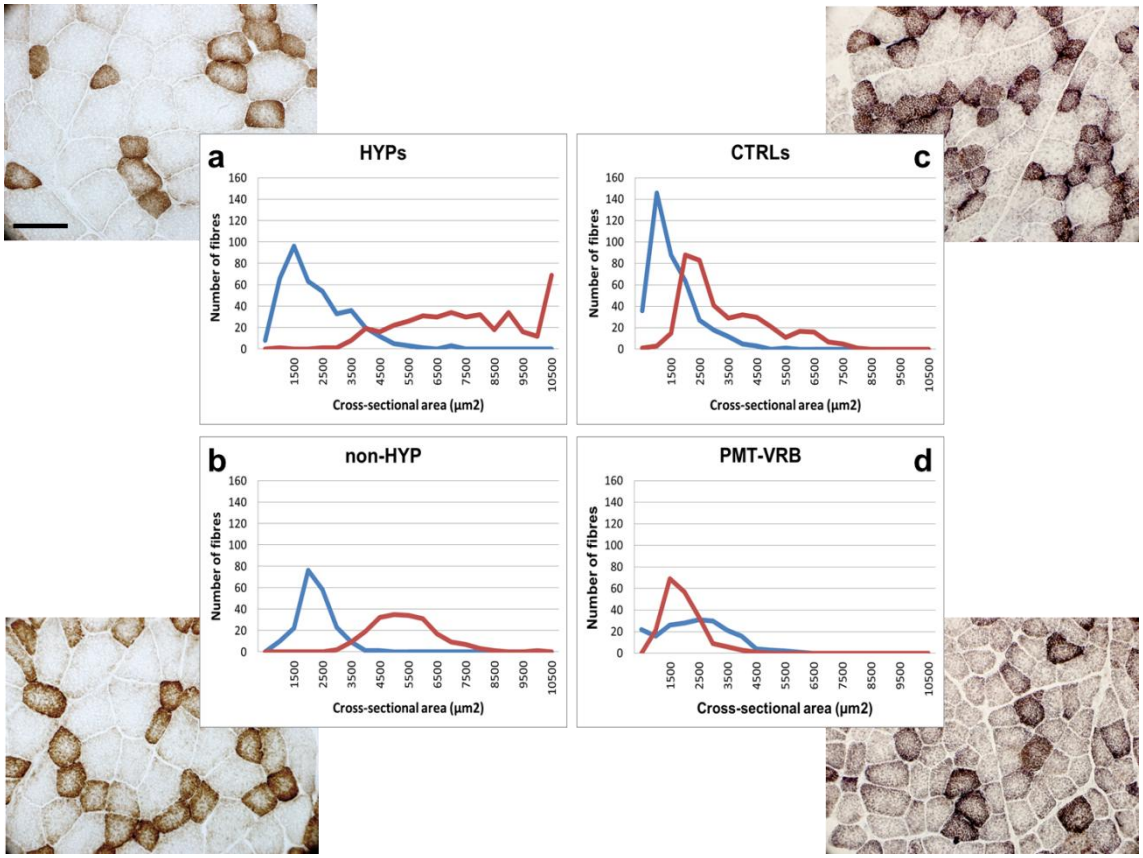

Figure 15. Measurements of fibre cross-sectional areas in the comparative analysis between Piedmontese and Dutch improved Red&White subjects. (a) Distribution of areas in hypertrophic subjects (mean between the two animals). (b) Distribution of areas in non-hypertrophic subject. (c) Distribution of areas in Dutch improved Red&White control subjects (mean between the two animals). (d) Distribution of areas in Dutch improved Red&White PMT-affected animal. The blue line represents oxidative fibre population, the red line glycolytic fibre population. Each graph is associated with a representative 10X microphotograph of COX-stained sections. Bar scale = 100 µm.

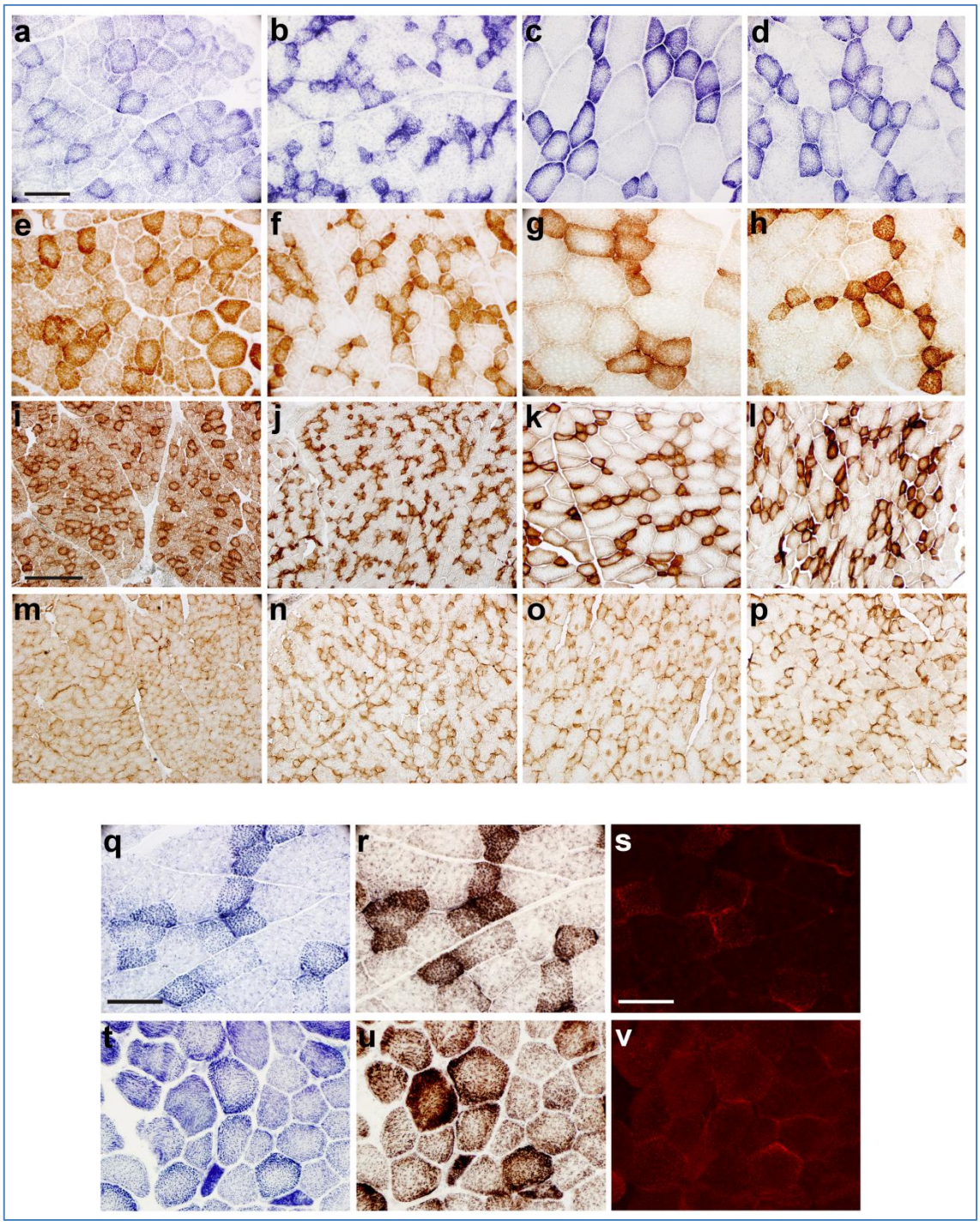

Figure 16. Histochemical stainings on *semimembranosus* muscle sections from Dutch improved Red&White PMT affected calf, from an healthy control and two Piedmontese healthy animals. Transverse sections from muscle biopsies were stained for mitochondrial specific reactions, succinic dehydrogenase (SDH) (a-d) and cytochrome oxidase (COX) (e-h, i-l). Scale bar: 100 µm (a-h), 500 µm (i-l). The sections were also immunolabelled with polyclonal antibodies against Tom20. Sections were then incubated with antibodies conjugated with biotin and the reaction was revealed with the Envision method (m-p). Scale bar: 500 µm. (q-s) Healthy and (t-v) pathological Dutch improved Red&White serial section stained for SDH, COX and immunolabelled for Tom20. Scale bar: 50 µm.

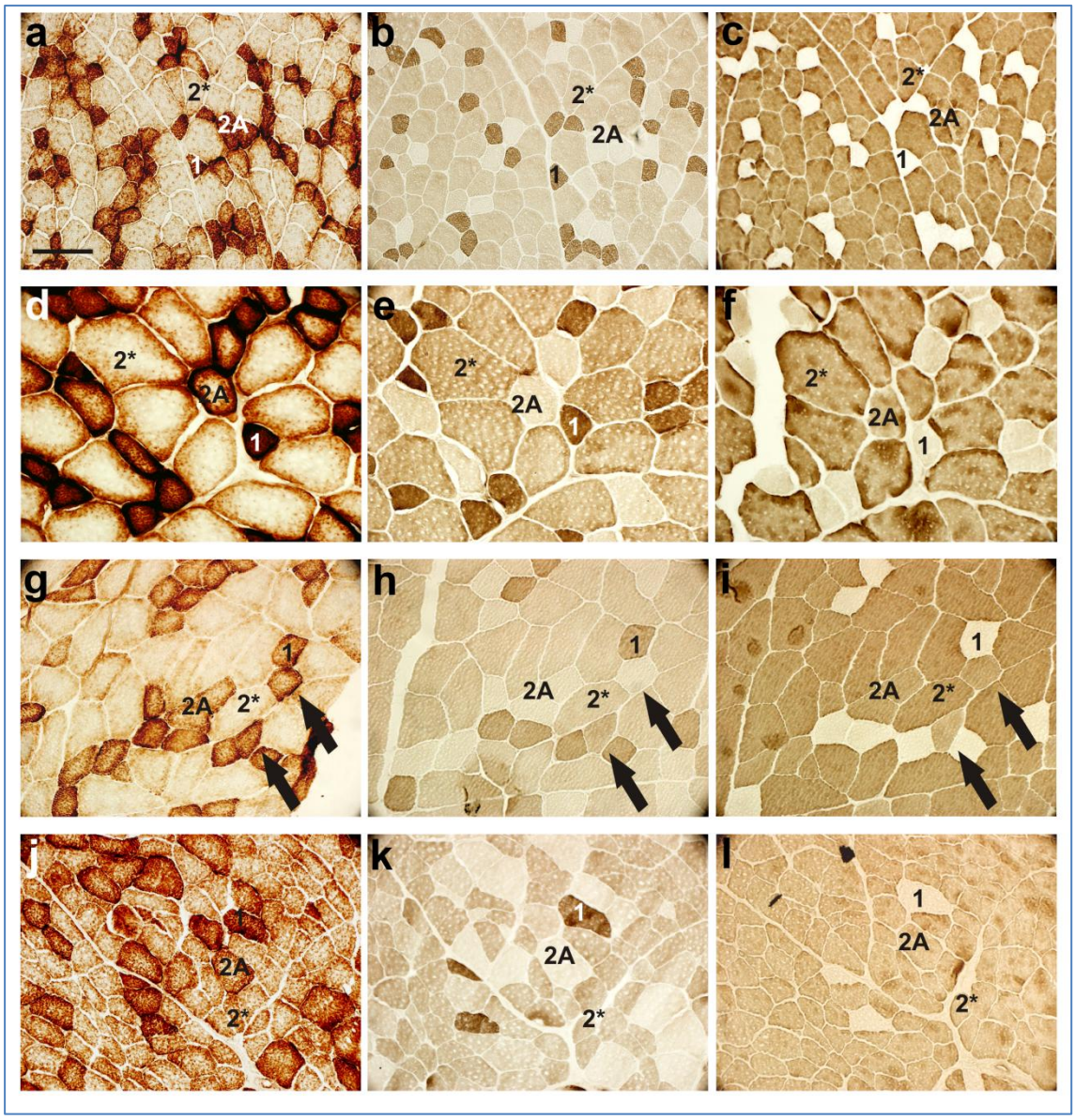

Figure 17. Histochemical stainings on *semimembranosus* muscle from control Dutch improved Red&White (a-c), Piedmontese healthy animals (d-f, g-i) and affected Dutch improved Red&White calf (j-l). Transverse serial sections were stained for COX (a, d, g,j) and for mATPase at pH 4.6 (b, e, h, k) or pH 10.2 (c, f, i,l). In the figure the fibre types are indicated (1=type 1; 2A=type 2A; 2*=type 2X). The arrows in (g-i) indicate type 2C fibres. Scale bar: 100 µm.

3.3.*Biochemical characterization of Congenital Pseudomyotonia in Romagnola and Dutch improved Red&White calves*

In parallel with the histopathological investigation, biochemical characterization of the disease was performed in order to evaluate the effects of PMT on muscle proteomic profile in Romagnola cattle breed and in the Dutch improved Red&White crossbred case.

3.3.1.Muscle proteomic profile of Congenital Pseudomyotonia in Romagnola and Dutch improved Red&White calves

Crude microsomal fractions enriched in content of SR membranes were obtained through differential ultra-centrifugations from *semimembranosus* muscle biopsies of Romagnola and Dutch improved Red&White pathological and healthy subjects. The subfractions obtained by differential centrifugations of muscle homogenates prepared in a low-ionic strength medium (Sacchetto et al., 2005; Sacchetto et al., 2009) were a soluble surnatant (Sp), a myofibrillar pellet (MP) and total membranes (TM). In order to control the final content, all the fractions were saved during the separation procedure and store for further investigations. Indeed, all the fractions collected were loaded onto a gel and the protein profile were analysed after staining with EZblue Gel Staining Reagent or cationic dye Stains-All (Figure 18a and 19a). Results clearly confirmed that Sp fraction contained soluble proteins similarly in all the samples. The MP fraction showed a large band on top of the gel that corresponded to myosin filaments. This band was present in traces in the other fraction suggesting an efficient first purification step in the differential centrifugation process. Therefore, from the total muscle it was possible to obtain a fraction (TM) purified from the high content of contractile and soluble proteins. This fraction exclusively displayed a protein band of about 63 kDa corresponding to calsequestrin 1 (CS1), an established marker of junctional SR, that selectively stained blue with Stains-All (Figure 19a) (Sacchetto et al., 1999). Another intense protein band at about 110 kDa was present only in TM fractions, the immunoblot subsequently performed on these fractions revealed that this protein corresponded to SERCA1. In conclusion, these observations provided evidence that the TM fraction was constituted mostly of SR membranes and that was almost free of muscle structural proteins.

The sole TM microsomal fractions of all the animals analysed here were probed with specific antibodies against SERCA1a and SERCA2. In parallel, immunoblotting analyses were performed using antibodies against a representative protein of junctional SR (RyR) and a protein of non-junctional SR (SL and GP53) SR. The immunoblots showed a decrease in the amount of SERCA1 in Romagnola affected subjects (Figure 18b) and in the Dutch improved Red&White case (Figure 19b). On the contrary, no differences were observed in content of junctional or non-junctional proteins suggesting that only SERCA1 protein was selectively affected by the mutation. In addition, SERCA2 did not show any notable variation in content excluding its involvement in a compensatory response to the decrease of SERCA1 neither in Romagnola nor in Dutch improved Red&White affected animals.

The Dutch improved Red&White affected calf displayed a more severe clinical condition than Romagnola calves although not so severe to become life threatening as it was in Belgian Blue CMD1-affected calves. This intermediate situation prompted to focus the attention on possible compensatory mechanisms put to use by the Dutch improved Red&White PMT subject. Excluded the augmentation of SERCA2 expression, TM fractions of Dutch improved Red&White animals were probed with an antibody against PMCA, another important ion pump involved in Ca^{2+} homeosatasis. The immunoblot displayed an increased PMCA band density in the affected samples when compared with the controls (Figure 20a) suggesting a compensatory increase of this membrane pump. Furthermore, in order to integrate and reinforce the histological findings, muscle total protein extracts obtained from Dutch improved Red&White subjects were used to evaluate mitochondria content using an antibody against a structural protein of the cellular organelle (Tom20). The immunoblots revealed that the samples from the PMT-affect Dutch improved Red&White showed a more intense band of Tom20 when compared to the healthy controls (Figure 20b).

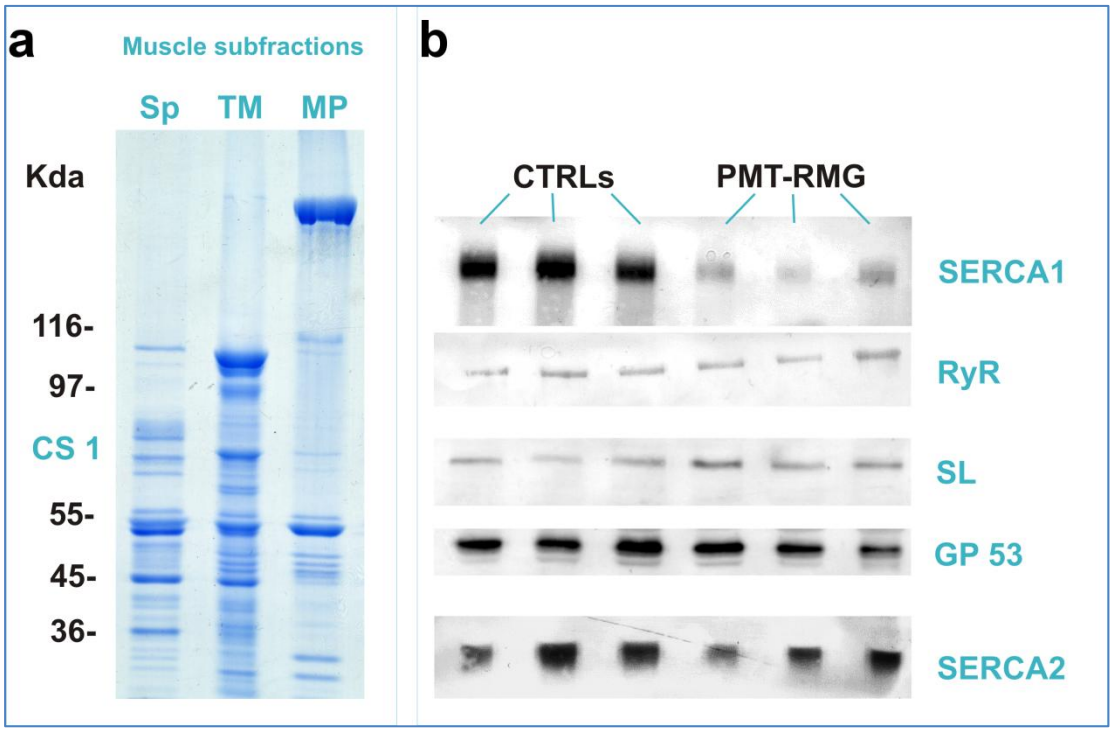

Figure 18. Protein profile of muscle subfractions and immunodetection of SERCA1 and membrane protein markers in crude microsomal fractions from Romagnola controls and pathological animals. (a) Representative muscle subfractions from a Romagnola control sample: Sp=soluble surnatant, MP=myofibrillar pellet,TM=total membranes, CS1=cal-sequestrina 1. (b) An equal quantity of protein from TM fractions from controls (CTRLs) and Romagnola PMT affected calves (PMT-RMG) was separated by SDS-PAGE and subjected to immunoblot analysis with antibodies specific to SERCA1, calcium release channel/ryanodine receptor (RyR1), sarcalumenin (SL) and 53 kDa glycoprotein (GP53) and SERCA2, as indicated. Only the pathological samples show lower intense bands selectively for SERCA1.

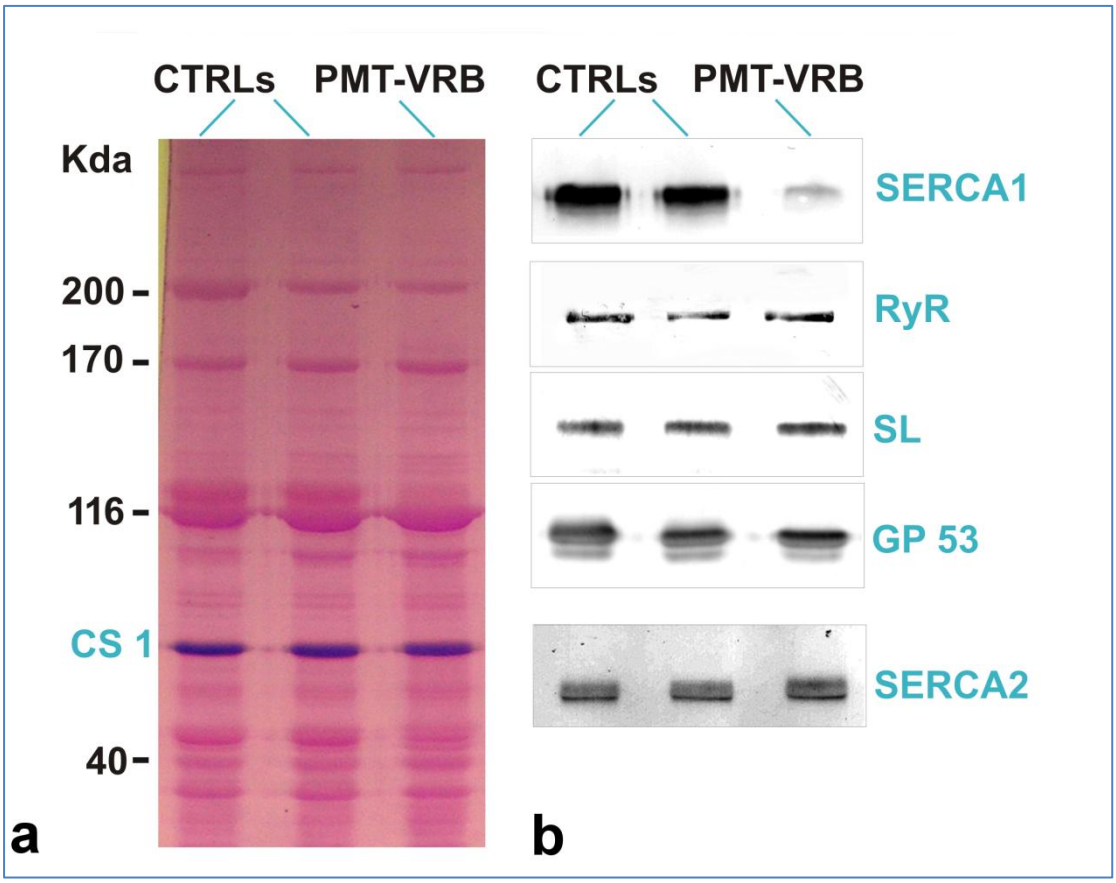

Figure 19. Protein profile of membrane isolated from control and pathological muscle and immunodetection of SERCA1 and membrane protein markers. (a) Crude microsomal fractions (50 µg/lane) from *semimembranosus* muscle obtained from controls (CTRLs) and PMT-affected Dutch improved Red&White calf (PMT-VRB), were resolved using 5–10% gradient gel and stained with Stains-All. This stain identify Ca^{2+} binding protein calsequestrin (CS1) as a dark blue band of about 63kDa in contrast with all the other proteins that stain purple. (b) An equal quantity of protein from crude microsomal fractions from controls (CTRLs) and PMT affected calf (PMT-VRB), was separated by SDS-PAGE and subjected to immunoblot analysis with antibodies specific to SERCA1, calcium release channel/ryanodine receptor (RyR1), sarcalumenin (SL) and 53 kDa glycoprotein (GP53) and SERCA2, as indicated.

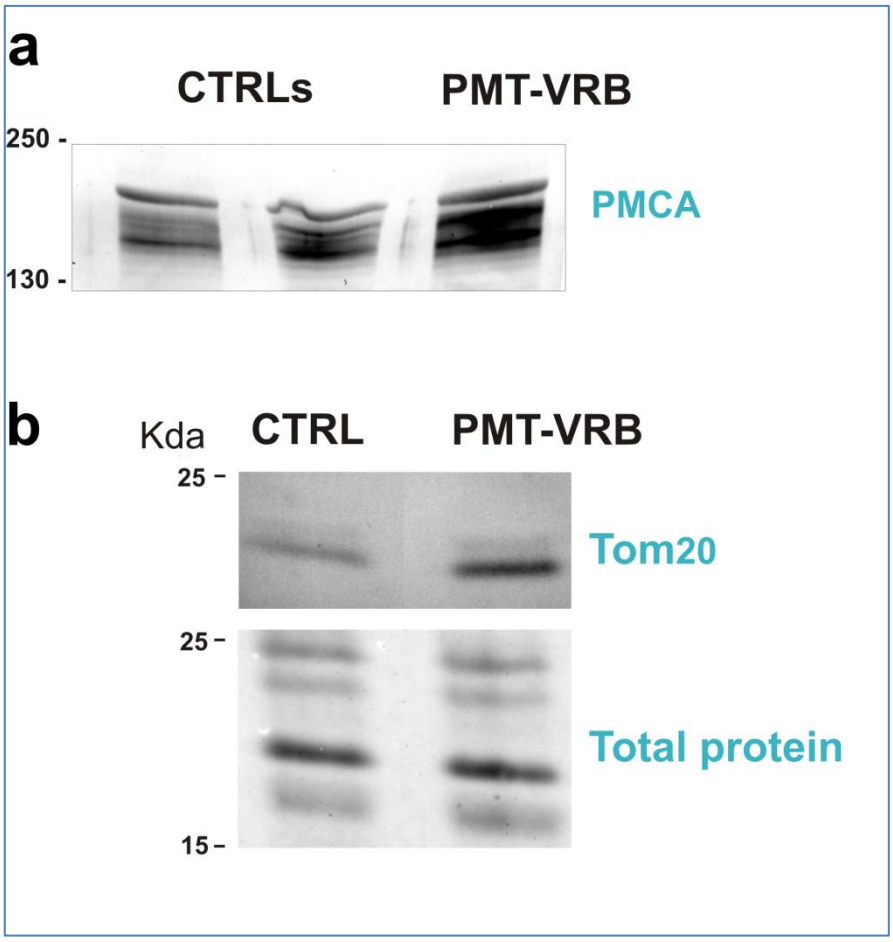

Figure 20. Specific immunoblot analyses on crude microsomal fractions (a) and total protein extracts (b) from controls and PMT-affected Dutch improved Red&White calf. (a) Total membrane fractions from controls (CTRLs) and affected (PMT-VRB) calves were separated by SDS-PAGE and then probed with antibody against plasma membrane Ca^{2+}-ATPase. (b) Bundles of fibres from muscle biopsies from control and PMT-VRB subjects were homogenized and equal quantity of protein was separated by SDS-PAGE. Immunoblot analysis with antibodies specific to Tom20 shows a more intense band in the pathological sample. Lower panel in (b) is Ponceau Red staining of muscle total lysates, used as loading control.

3.3.2.Ca^{2+}ATPase activity assay and SERCA1 mRNA expression in Romagnola and Dutch improved Red&White calves

To complete the biochemical investigation, Ca^{2+}ATPase activity assay was performed on SR microsomal fractions obtained from PMT-affected and control animals. In all the pathological cases the Ca^{2+} dependence of the SERCA pump activity was considerably lower in the SR membranes fractions from pathological muscle comparing to the ones from healthy controls. Figure 21 shows the results of the Ca^{2+}ATase activity assay performed on samples of Dutch improved Red&White and Romagnola calves [Grunberg, 2010; Murgiano, 2012]. These results were in full agreement with the data recorded for Chianina affected animals (Sacchetto et al., 2009). Consequently, like in Chianina, also in Dutch improved Red&White and Romagnola cases, SERCA1a showed a lower activity that is correlated to a decrease in the content of the protein.

Finally, in order to investigate the possibility that the reduced content of SERCA1 displayed histologically and biochemically might be due to a reduced *ATP2A1* transcriptional activity, Real Time RT-PCR experiments were performed on Dutch improved Red&White and Romagnola subjects. The attention were focussed on the homozygous animals with the aim to enlighten whether the mutation (c.1675 C>T, Arg559Cys) of the Dutch improved Red&White and the double point mutation (c.[632 G>T; 857 G>T], Gly211Val Gly286Val) of the Romagnola might affect the transcriptional activity of the gene. The analyses showed that SERCA1 mRNA expression levels in pathological samples were comparable to those of controls (Figure 22). Also the Romagnola in compound heterozygosis displayed a normal mRNA expression confirming that the two mutation had effects on the protein but not on the mRNA levels in both homozygosis and heterozygosis.

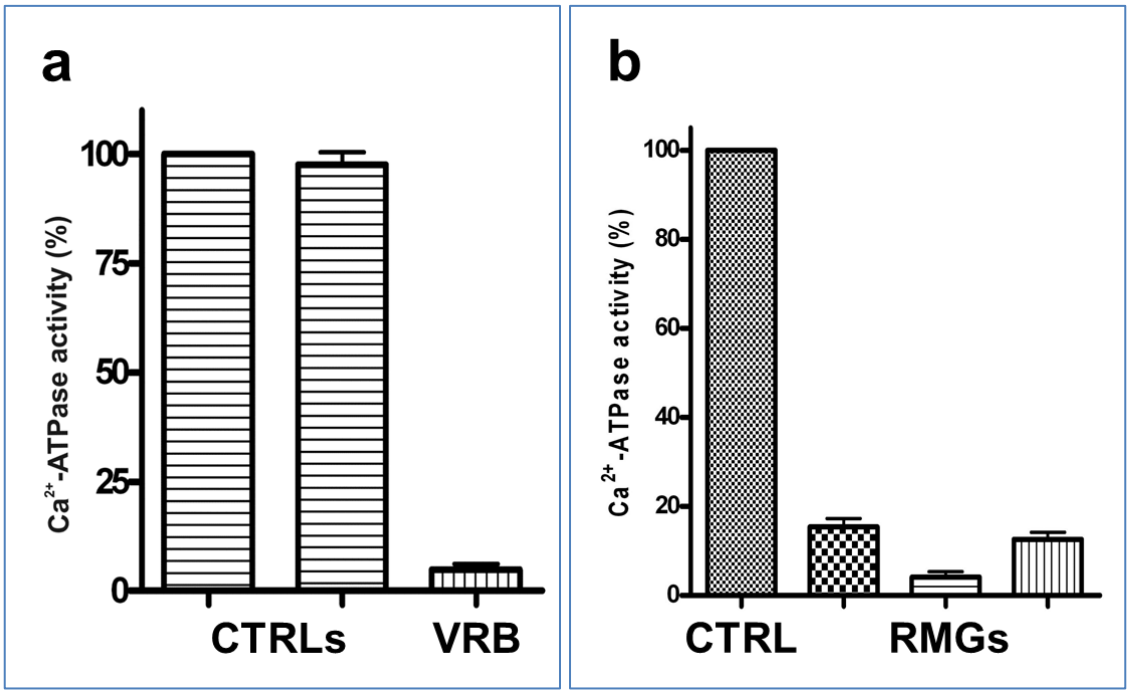

Figure 21: Ca^{2+}-ATPase activity in (a) control (CTRLs) and PMT affected Dutch improved Red&White calf (VRB) and (b) control (CTRL) and PMT cases of Romagnola breed (RMG). The Ca^{2+}-ATPase activity was determined by a spectrophotometric enzyme-coupled assay at optimum pCa (pCa 5) in the presence of ionophore A23187. Values were obtained from different preparations of microsomes obtained from the same muscle specimens. Data are expressed as percent of control value, considered 100%, and are the mean ± SD of several independent experiments.

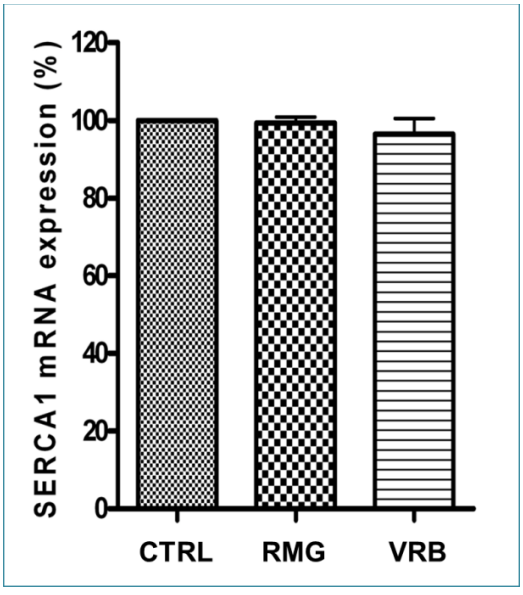

Figure 22: Expression levels of SERCA1 mRNA in a control (CTRL), a Romagnola case (RMG) and the PMT affected Dutch improved Red&White calf (VRB). SERCA1 mRNA levels were quantified by Real Time RT-PCR. Data are reported as the relative expression on control value. Data were obtained from different mRNA extractions from the same muscle specimens.

4.DISCUSSION and CONCLUSIONS

The main goal of my PhD was to complete and deepen the knowledge on the histopathological and biochemical characteristics of Bovine Congenital Pseudo-myotonia (PMT). Chianina PMT-affected cattle has been proposed and accepted as truly counterpart of human Brody disease due to the strong similarities in clinical and histological manifestations along with the mutation at *ATP2A1* gene encoding for SERCA1a. Brody disease is usually transmitted as an autosomal recessive trait but a few families line showed an autosomal dominant inheritance without mutation at *ATP2A1* gene. Despite this latter situation, several different mutations (deletions and point mutation) in *ATP2A1* have been described in human patients indicating the genetic heterogeneity of Brody disease (Vattemi et al., 2010; Voermans et al., 2012). Chianina cattle displayed only a single point mutation, therefore when a PMT case was diagnosed in a Dutch improved Red&White crossbred calf that carried another point mutation in *ATP2A1* gene, the idea of bovine as animal model was reinforced. This definition was further supported by the diagnosis of PMT in Romagnola cattle with the location of a novel double mutation and a compound heterozygosis of this double mutation and the one described in Chianina. Consequently, PMT became an inherited muscular dysfunction characterized by genetic heterogeneity like Brody disease. This project started from this concept and developed a series of experiments to evaluate whether the different genetic background has similar phenotype and/or leads to various responses to the alteration.

As previously mentioned, PMT cases have been diagnosed for the first time in Italian Chianina cattle breed that became the reference for all the following diagnoses. The starting point of my research was the morphological and biochemical profile of PMT-affected Chianina subjects. Indeed, the first hypothesis I worked on prompted me to perform various analyses to verify whether PMT phenotype of Italian Romagnola cattle breed was the same described in Italian Chianina breed in spite of the different genetic background.

The clinical presentation of Romagnola calves was closely similar to Chianina affected animals. The animals were bright and alert, well-developed with no alteration in growth. The sole pathological symptom was the increased muscular tone exercise-induced, although the animal did not show any sign of pain during and after the attacks and did not lose consciousness. Altogether, these data suggests that, leaving the animal quite without forcing it to move fast, PMT affected subjects could have a life comparable with a normal animal. Consequently, PMT is not considered a life-threatening disease, therefore an attention in terms on management of PMT subjects could permit to reach a satisfying weight for slaughtering without particular difficulties.

As a general consideration, the histopathological analyses performed on affected muscle found no dramatic alterations in fibres morphology. H&E staining showed some fibres degenerated or with degenerative changes in all the pathological samples, although these fibres were not extremely frequent and they were always accompanied with regenerative phenomenon. Interestingly, a Romagnola case showed a more severe histopathological picture characterized by frequent degenerated fibres and an acute/intense macrophages infiltration. All together these observations suggest that the muscular tissue is able to handle the mutation without suffering large damages or fibres loss, in addition the tissue maintains and actives the regenerative response. The difference in severity of histopathological alterations might depend on the animal condition when the biopsy was collected. Indeed, it could be possible that the Romagnola subject with more severe histopathological signs was subjected to the biopsy sampling after a cramp attack not observed by the operators or a particular intense activity independently performed by the animal. Furthermore, it should be noted that the Romagnola animals were all young calves basically more active (due to playing and scouting aptitudes) than an adult. Thus, these considerations could explain the alterations grading found in the samples analysed in this study, in agreement with the work by Sacchetto *et al.* (2009) in which the histopathological findings of Chianina affected animals undergone exercise protocols were more severe than affected subject maintained at rest (Sacchetto et al., 2009). Combined COX-SDH staining protocol displayed no alteration in oxidative metabolism showing an expression of both the oxidative enzymes in the same specific fibre population. At the same way, PAS stain did not show any alteration in glycogen content or distribution. In accordance with the

findings in Chianina cattle breed, the disease seems to do not cause any alteration in metabolism in Romagnola cases, indeed all fibres that expressed COX, expressed also SDH and the glycogen was normally associated to SR membranes.

The biochemical analyses performed on Romagnola animals, both pathological and healthy, revealed that PMT-affected animals had lower Ca^{2+}-ATPase activity than the controls and that this decrease was closely correlated to lower quantity of SERCA1 demonstrated through immunoblotting and immunofluorescence. On the contrary, no alteration in *ATP2A1* gene expression was reported. These data indicate that the protein is correctly encoded by the gene although, due to the substitution in the sequence, it might assume an incorrect folded conformation that makes SERCA1 mutant more susceptible to the protein quality control systems of the fibres, as for SERCA1 mutant in Chianina cattle (Bianchini et al., 2014). Consequently, because no gene over-expression is activated, the final result is a reduction in SERCA1 content in the fibres. Interestingly the other proteins included in the immunostaining assays did not show any alteration in expression. Indeed, nor proteins of junctional SR (RyR) nor proteins of non-junctional SR (SL-GP53) displayed decrease in quantity. It has been proposed that an ectopic expression of other SERCA isoforms could act as a compensatory mechanism (Odermatt et al., 2000) in affected fibres, although no differences were reported in SERCA2 expression between pathological and control samples of Romagnola. Altogether, Bovine Congenital Pseudomyotonia in Romagnola seems to show histopathological alteration strongly similar to Chianina affected animals. In addition, pathological Romagnola calves display the same biochemical characteristics described in Chianina with the sole decrease in SERCA1 content.

All the analyses performed on Romagnola animals allowed to obtain a detailed picture of the PMT in these breed and proved the first working hypothesis of my PhD research project providing morphological and biochemical evidences along with the clinical picture of the general similarity between PMT phenotype in Chianina and the signs displayed by the Romagnola affected animals. Moreover, the clinical, histological and preliminary biochemical data referred to the Dutch improved Red&White case were confirmed and integrate with deep analyses here. Consequently, this study afforded to define a complete general histopathological and biochemical case of PMT which previously has been described referring to only one breed.

In addition, a reported collateral finding integrated and enriched the general picture of PMT. An intriguing observation was the evidence of co-expression patterns within SERCA1, SERCA2 and PLB in both Romagnola and Dutch improved Red&White affected animals. Indeed, pathological animals revealed some fibres expressing SERCA1 and SERCA2 and some fibres co-expressing SERCA1 and PLB. These kind of fibres were never described before nor in Chianina affected animals nor in healthy controls where the three proteins showed the typical mutually exclusive expression manner. Recently, co-expression pattern has been described in physiologically normal human fibres (Fajardo et al., 2013). The authors of this last work explained the co-existence of both SERCA isoforms as a possible advantageous tool in human skeletal muscle to increase the versatility in Ca^{2+} homeostasis handling. Moreover, they suggested a possible, even if non preferential, regulation of SERCA1 by PLB. At the same way, the observations of SERCA isoforms co-expression in PMT affected muscle of this study might be explained as an attempt of the fibres to handle the Ca^{2+} overload. However, this event was described only in pathological situation prompting to consider it as a possible compensatory mechanism. Independent of the latter, bovine muscle showed evidence of a potential muscle plasticity like in human supporting, once again, its use as animal model. Despite the immunohistological data on SERCA2 expression together with SERCA1, there were no evidence of increased SERCA2 content from biochemical analysis. The immunoblotting assays showed no differences between affected and control SERCA2 bands although it should be noted that the number of "hybrid" fibres might be insufficient to alter the total content. Future studies that will evaluate the expression pattern of these proteins in single bovine fibres might enlighten the preliminary report of this research.

The Dutch improved Red&White case displayed a histological and biochemical picture similar to Chianina and Romagnola. The morphological analysis described some fibres in degeneration surrounded by macrophages and always associated with regeneration phenomena, the immunofluorescence showed a general decrease in immunoreactivity for SERCA1 in the pathological section and highlighted the presence of some fibre that co-expressed the two SERCA isoforms or SERCA1 and PLB. The biochemical profile was characterized by a sole reduction of SERCA1 content confirming the

immunohistological data, whereas the other SR markers (RyR, SL-GP53) and SERCA 2 did not display any variation. Moreover, a curious observation was reported in the pathological Dutch improved Red&White sections: COX and SDH staining displayed an increased intensity that involved especially type 2A fibres. One interpretation for this stronger intensity of labelling might be an increase in oxidative enzymes activity due to a variation in energy demand by the affected muscle. The use of the antibody Tom20 in the various immuno-surveys (IHC, fluorescence and blotting) confirmed an augmentation in mitochondria content when compare with both healthy Dutch improved Red&White controls and Piedmontese purebred subjects. These latter animals were chosen for a complementary analysis after the increase in oxidative staining was noted between the affected Dutch improved Red&White and the healthy controls. Basing on the collateral findings of Wang et al. (2009) that reported an increased expression of mitochondrial genes in Piedmontese crossbred offspring (Wang et al., 2009), the intent of this part of the research was to roll out whether the increase number of mitochondria was a compensatory mechanisms of the fibres rather than a result of the genetic background of the Dutch improved Red&White affected calf. The involvement of mitochondria in Ca^{2+} uptake was one of the first compensatory mechanisms proposed along with the ectopic expression of other SERCA isoforms, the Na^{+}/Ca^{2+} exchangers and the plasma membrane Ca^{2+}-ATPases (Carafoli, 1987; Odermatt et al., 2000).

The comparative assessment performed between the Dutch improved Red&White and the Piedmontese subjects revealed that the increased labelling for oxidative enzymes or the reactivity in immunostaining were noticed only in the affected Dutch improved Red&White sections or in the total homogenates obtained from this subject. The absence of any alteration regarding mitochondria in the Piedmontese sections leads to exclude the possible influence of the pure Piedmontese genetic line on the particular phenotype of the affected Dutch improved Red&White. Consequently, the increase of mitochondria in the crossbred calf might be a compensatory mechanism put to use by the affected muscular fibres attempting to solve the Ca^{2+} overload. It is interesting to note that the fibres mainly involved in the adaptive changes were type 2 fibres (fast-twitch, glycolytic) that were the population affected by the SERCA1 mutation. Among these, type 2A fibres seemed to respond with hypertrophy whereas type 2X fibres did not show volume changes but they responded with a clear increase in mitochondria

content. These findings point out the high plasticity potential of muscle tissue which is able to adapt and to shift its classical characteristics in order to respond to pathological situations. In this particular case, affected muscle of Dutch improved Red&White crossbred subject responded to the increase of free Ca^{2+} levels in the cytosol increasing the number of mitochondria in fast-twitch fibres population that was selectively affected by the mutation. Indeed, mutation in *ATP2A1* gene leads to alteration in SERCA1a which is expressed primarily in fast-twitch fibres. Taken together, these observations might explain the entire picture in which affected muscle respond to the decrease of SERCA1a (in quantity and activity) through the activation of a compensatory mechanism that in this case involved the Ca^{2+} buffer capacity of mitochondria. The phenotypic effects of this adaptive change are the hypertrophy of type 2A (fast-oxidative) fibres and the increased mitochondria content in type 2X (fast-glycolitic) fibres. Besides, another possible compensatory mechanism was described in Dutch improved Red&White affected calf. Immunoblot using antibody against PMCA displayed an increased presence of this sarcolemma ATPase pump suggesting that a further (or primary) response to the Ca^{2+} increase in the cytosol was put to use by the muscle fibre.

The point mutation that underlied PMT in the Dutch improved Red&White crossbred calf was identified by my group in a previous case report (Grünberg et al., 2010). The transitional mutation in *ATP2A1* gene leads to a substitution of an arginine with a cystein in position 559 of SERCA1a amino acids sequence. The mutation identified in the Dutch improved Red&White case was identical to a mutation reported in Belgian Blue cattle breed which was considered the aetiological cause of a disease named Congenital Muscular Distonia 1 (CMD1) (Charlier et al., 2008). After this case report, the two distinct pathological conditions were referred to the same congenital condition with a different phenotype expression. Indeed, CMD1-affected animals suffered from exercise-induced muscle spasms along with impaired swallowing, decreased growth rates and death within few weeks of age caused by respiratory insufficiency. The Dutch improved Red&White crossbred case showed no such severe symptoms resembling PMT clinical features in Chianina. It survived several months, growing normally with no changes in the clinical presentation. Its sudden death was attributed to a cervical trauma caused by longer and excessive muscle contraction (Grünberg et al., 2010). The

compensatory mechanisms described here might be the reason why the Dutch improved Red&White affected calf did not die after few weeks of ages like the Belgian Blue calves despite the same deleterious mutation.

My research provided histochemical and biochemical evidences to support the hypothesis of the mitochondria involvement in the Ca^{2+} homeostasis (Yi et al., 2011) during the pathological condition caused by PMT mutation. In addition, also PMCA seems to be recruited in the attempt to decrease the lasting high $[Ca^{2+}]_c$ (Odermatt et al., 2000). The substantial difference between the two mechanism is that PMCA pumps the ions out of the fibre and thus the Ca^{2+} pool decreases with the consequent effects on the muscle functionality. At the contrary mitochondrial mechanism preserves the Ca^{2+} pool inside (even if not in the physiological compartment) the fibre with the possibility to release it later. Therefore, this latter response seems more effective in maintaining a functional muscle although the Ca^{2+} load in mitochondria could initiate other cellular mechanisms including apoptosis.

Overall, the Dutch improved Red&White crossbred affected calf was the first case in which compensatory mechanisms has been described. Indeed, my project provided the objective evidences of the possible activation of two different although complementary adaptive response of the muscle tissue to the Ca^{2+} overload in the cytosol consequent to SERCA1 failure. Despite the fact that the pathological Dutch improved Red&White crossbred was a single isolated case in that breed line, it was an intriguing and clear example of possible compensatory reactions. Therefore the reported data contributed to enlighten the pathological response to PMT mutation and provided an approaching platform for further investigations.

A further characteristic of PMT, described first in Chianina and confirmed here in Romagnola and Dutch improved Red&White, was that the SERCA1a mRNA levels were the same in healthy and pathological animals. This suggested that *ATP2A1* gene did not alter its transcriptional activity and correctly encoded for SERCA1a. A recent study by my group (Bianchini et al., 2014) provided evidence that in Chianina cattle the Arg164His mutation in the amino acids sequence generates an alteration in the shape of the protein that is recognized incorrect by the protein quality control pathway named ubiquitin-proteosome system (UPS). This particular situation classify Chianina cattle

PMT in the group of Unfolded Protein Disease (UPDs). UPDs are characterized by a pathological condition caused by a mutation in a protein that is not folded correctly and consequently is more susceptible to the action of protein quality control systems. The mutated protein maintains the catalytic activity but the quality control systems reduce its half-life leading to a reduction in content that causes the pathological manifestations. This could be the case for Romagnola as well as Dutch improved Red&White PMT, in which mutations lead to a selective reduced expression of SERCA1 protein. Nevertheless, in Romagnola cattle breed the aminoacids substitutions occur in the A domain, at the N terminus of SERCA1 protein, a region described as critical for the correct folding and for maintenance of the three dimensional structure of SERCA1, but not for the catalytic activity (Daiho et al., 1999). By contrast, in Dutch improved Red&White PMT the mutation replaces the amino acid at position 559 (corresponding to R560 in rabbit SERCA1 isoform). Functional consequences of R560 mutations have been extensively studied by using heterologous cell expression systems. It has been reported that replacement of R560 with different amino acids affects the nucleotide binding and phosphoryl transfer, producing a strong inhibition of Ca^{2+}-ATPase activity (Hua et al., 2002). In conclusion only Romagnola PMT could be ascribed to UPDs group. Further analyses of the Ca^{2+} dependence of the Ca^{2+} ATPase activity and/or of the ability of the mutant to counteract cytosolic Ca^{2+} transients, will clarify the functional properties of SERCA1 mutant expressed in Romagnola PMT affected muscles. The experiments performed by our group on heterologous HEK293 cellular model overexpressing the Arg164His mutant of SERCA1 and muscular explants from affected Chianina cattle using inhibitors of the UPS, demonstrated the rescue of mutated SERCA1 to SR membrane which can re-establish resting cytosolic Ca^{2+} concentration. The data suggested a therapeutic approach against PMT. It will be interesting to reproduce the experiments on heterologous system using the other mutation reported in Romagnola in order to deepened and integrated the first study on Chianina mutation. In particular it will be useful to evaluate the involvement of UPS or other protein quality control systems in the degradation of the other mutants of SERCA1a and the efficiency of the inhibitors to block the degradation process. A further step might be *in vivo* tests of the molecules to afford the therapeutic use in animal as well as in human.

5.**BIBLIOGRAPHY**

Anger, M., J. Samuel, F. Marotte, F. Wuytack, L. Rappaport, and A. Lompré. 1993. The sarco(endo)plasmic reticulum Ca^{2+}-ATPase mRNA isoform, SERCA3, is expressed in endothelial and epithelial cells in various organs. FEBS Lett. 334:45–48.

Anthonisen, A. N., J. D. Clausen, and J. P. Andersen. 2006. Mutational analysis of the conserved TGES loop of sarcoplasmic reticulum Ca^{2+}-ATPase. J. Biol. Chem. 281:31572–82.

Aravind, L., M. Y. Galperin, and E. V Koonin. 1998. The catalytic domain of the P-type ATPase has the haloacid dehalogenase fold. TIBS - Protein Seq. motifs 23:127–129.

Armstrong, R. B., G. L. Warren, and J. A. Warren. 1991. Mechanisms of exercise-induced muscle fibre injury. Sport. Med. 12:184–207.

Asahi, M., K. Kurzydlowski, M. Tada, and D. H. MacLennan. 2002. Sarcolipin inhibits polymerization of phospholamban to induce superinhibition of sarco(endo)plasmic reticulum Ca^{2+}-ATPases (SERCAs). J. Biol. Chem. 277:26725–26728.

Balnave, C. D., and D. G. Allen. 1998. Evidence for Na^{+}/Ca^{2+} exchange in intact single skeletal muscle fibers from the mouse. Am. Physiol. Soc. 274:C940–C946.

Barany, M. 1967. ATPase activity of myosin correlated with speed of muscle shortening. J. Gen. Physiol.:197–218.

Baughman, J. M., F. Perocchi, H. S. Girgis, M. Plovanich, C. A. Belcher-Timme, Y. Sancak, X. R. Bao, L. Strittmatter, O. Goldberger, R. L. Bogorad, V. Koteliansky, and V. K. Mootha. 2011. Integrative genomics identifies MCU as an essential component of the mitochondrial calcium uniporter. Nature 476:341–345.

Beard, N. a, D. R. Laver, and a F. Dulhunty. 2004. Calsequestrin and the calcium release channel of skeletal and cardiac muscle. Prog. Biophys. Mol. Biol. 85:33–69.

Berchtold, M. W., H. Brinkmeier, and M. Muntener. 2000. Calcium ion in skeletal muscle: its crucial role for muscle function , plasticity , and disease. Physiol. Rev. 80:1215–1266.

Berg, J. S., B. C. Powell, and R. E. Cheney. 2001. A millennial myosin census. Mol. Biol. Cell 12:780–794.

Bianchini, E., S. Testoni, A. Gentile, T. Calì, D. Ottolini, A. Villa, M. Brini, R. Betto, F. Mascarello, P. Nissen, D. Sandonà, and R. Sacchetto. 2014. Inhibition of Ubiquitin Proteasome System Rescues the Defective Sarco(endo)plasmic Reticulum Ca^{2+}-ATPase (SERCA1) Protein Causing Chianina Cattle Pseudomyotonia. J. Biol. Chem.:1–20.

Bobe, R., R. Bredoux, E. Corvazier, C. Lacabaratz-Porret, V. Martin, T. Kovács, and J. Enouf. 2005. How many Ca^{2+}-ATPase isoforms are expressed in a cell type? A growing family of membrane proteins illustrated by studies in platelets. Platelets 16:133–150.

Bobe, R., R. Bredoux, F. Wuytack, R. Quarck, T. Kovacs, B. Papp, E. Corvazier, C. Magnier, and J. Enouf. 1994. The rat platelet 97-kDa Ca^{2+}ATPase isoform is the Sarcoendoplasmic Reticulum Ca^{2+}ATPase 3 protein. J. Biol. Chem. 269:1417–1424.

Bottinelli, R., R. Betto, S. Schiaffino, and C. Reggiani. 1994. Unloaded shortening velocity and myosin heavy chain and alkali light chain isoform composition in rat skeletal muscle fibres. J. Physiol. 478:341–349.

Bottinelli, R., M. Canepari, C. Reggiani, and G. J. M. Stienent. 1994. Myofibrillar ATPase activity during isometric contraction and isomyosin composition in rat single skinned muscle fibres. J. Physiol. 481:663–675.

Bottinelli, R., S. Schiaffino, and C. Reggiani. 1991. Force-velocity relations and myosin heavy chain isoform compositions of skinned fibres from rat skeletal muscle. J. Physiol. 437:655–672.

Brandl, C. J., S. DeLeon, D. R. Martin, and D. H. MacLennan. 1987. Adult forms of the Ca2+-ATPase of Sarcoplasmic Reticulum. J. Biol. Chem. 262:3768–3774.

Brandt, N. R., A. H. Caswell, S. A. Carl, D. G. Ferguson, T. Brandt, J. P. Brunschwig, and A. L. Bassett. 1993. Detection and localization of triadin in rat ventricular muscle. J. Membr. Biol. 131:219–228.

Brody, A. I. 1969. Muscle contracture induced by exercise. A syndrome attributable to decreased relaxing factor. N. Engl. J. Med. 281:187–192.

Brooke, M. H., and K. K. Kaiser. 1970. Muscle Fiber Types: How Many and What Kind? Arch. Neurol. 23:369–379.

Brooks, S. V. 2003. Current Topics for Teaching Skeletal Muscle Physiology. Adv. Physiol. Educ. 27:171–182.

Burk, S. E., J. Lytton, D. H. Maclennan, and G. E. Shull. 1989. cDNA cloning , functional expression , and mRNA tissue distribution of a third organellar Ca^{2+} pump. J. Biol. Chem. 264:18561–18568.

Carafoli, E. 1987. Intracellular calcium homeostasis. Annu. Rev. Biochem. 56:395–433.

Charlier, C., W. Coppieters, F. Rollin, D. Desmecht, J. S. Agerholm, N. Cambisano, E. Carta, S. Dardano, M. Dive, C. Fasquelle, J.-C. Frennet, R. Hanset, X. Hubin, C. Jorgensen, L. Karim, M. Kent, K. Harvey, B. R. Pearce, P. Simon, N. Tama, H. Nie, S. Vandeputte, S. Lien, M. Longeri, M. Fredholm, R. J. Harvey, and M. Georges. 2008. Highly effective SNP-based association mapping and management of recessive defects in livestock. Nat. Genet. 40:449–454.

Clarke, D. M., T. W. Loo, and D. H. MacLennan. 1990a. Functional consequences of alterations to amino acids located in the nucleotide binding domain of the Ca^{2+}-ATPase of Sarcoplasmic Reticulum. J. Biol. Chem. 265:22223–22227.

Clarke, D. M., T. W. Loo, and D. H. MacLennan. 1990b. Functional consequences of mutations of conserved amino acids in the beta strand domain of the Ca^{2+}-ATPase of Sarcoplasmic Reticulum. J. Biol. Chem. 265:14088–14092.

Clausen, J. D., D. B. McIntosh, B. Vilsen, D. G. Woolley, and J. P. Andersen. 2003. Importance of conserved N-domain residues Thr441, Glu442, Lys515, Arg560, and Leu562 of sarcoplasmic reticulum Ca2+-ATPase for MgATP binding and subsequent catalytic steps. Plasticity of the nucleotide-binding site. J. Biol. Chem. 278:20245–20258.

Close, R. 1967. Properties of motor units in fast and slow skeletal muscle of the rat. J. Physiol. 193:45–55.

Cosford, K. L., S. M. Taylor, L. Thompson, and G. D. Shelton. 2008. Case Report: A possible new inherited myopathy in a young Labrador retriever. Canine Vet. J. 49:393–397.

Cummings, B. 2006. InterActive Physiology: Anatomy Review: Skeletal Musle Tissue. Chapter 9. Pearson Educ.

Daiho, T., K. Yamasaki, T. Saino, M. Kamidochi, K. Satoh, H. Iizuka, and H. Suzuki. 2001. Mutations of either or both Cys876 and Cys888 residues of sarcoplasmic reticulum Ca^{2+}-ATPase result in a complete loss of Ca^{2+} transport activity without a loss of Ca^{2+}-dependent ATPase activity. Role of the CYS876-CYS888 disulfide bond. J. Biol. Chem. 276:32771–32778.

Daiho, T., K. Yamasaki, H. Suzuki, T. Saino, and T. Kanazawa. 1999. Deletions or specific substitutions of a few residues in the NH(2)-terminal region (Ala(3) to Thr(9)) of sarcoplasmic reticulum Ca^{2+}-ATPase cause inactivation and rapid degradation of the enzyme expressed in COS-1 cells. J. Biol. Chem. 274:23910–23915.

Dally, S., R. Bredoux, E. Corvazier, J. P. Andersen, J. D. Clausen, L. Dode, M. Fanchaouy, P. Gelebart, V. Monceau, F. Del Monte, J. K. Gwathmey, R. Hajjar, C. Chaabane, R. Bobe, A. Raies, and J. Enouf. 2006. Ca2+-ATPases in non-failing and failing heart: evidence for a novel cardiac sarco/endoplasmic reticulum Ca^{2+}-ATPase 2 isoform (SERCA2c). Biochem. J. 395:249–258.

Damiani, E., R. Sacchetto, and A. Margreth. 2000. Variation of phospholamban in slow-twitch muscle sarcoplasmic reticulum between mammalian species and a link to the substrate specificity of endogenous Ca^{2+}-calmodulin-dependent protein kinase. Biochim. Biophys. Acta 1464:231–241.

Denton, R. M. 2009. Regulation of mitochondrial dehydrogenases by calcium ions. Biochim. Biophys. Acta 1787:1309–1316.

Deval, E., G. Raymond, and C. Cognard. 2002. Na^{+}-Ca^{2+} exchange activity in rat skeletal myotubes: effect of lithium ions. Cell Calcium 31:37–44.

Dorotea, T., W. Grünberg, F. Mascarello, and R. Sacchetto. 2014. Fast-twitch skeletal muscle fibers response to SERCA1 deficiency in a Dutch improved Red and White calf pseudomyotonia case. Cell Tissue Res. (submitted for pubblication).

Drögemüller, C., M. Drögemüller, T. Leeb, F. Mascarello, S. Testoni, M. Rossi, A. Gentile, E. Damiani, and R. Sacchetto. 2008. Identification of a missense mutation in the bovine ATP2A1 gene in congenital pseudomyotonia of Chianina cattle: an animal model of human Brody disease. Genomics 92:474–477.

European Community, E. U. 2006. Council Regulation No 1183/2006 of 24 July 2006 concerning the Community scale for the classification of carcases of adult bovine animals (codified version). Off. J. Eur. Communities 214.

European Community, E. 1991. Council Regulation No 1026/91 of 22 April 1991 amending regulation (EEC) No 1208/81 determining the Community scale for the classification of carcases of adult bovine animals. Off. J. Eur. Communities 106.

Fajardo, V. a, E. Bombardier, C. Vigna, T. Devji, D. Bloemberg, D. Gamu, A. O. Gramolini, J. Quadrilatero, and a R. Tupling. 2013. Co-expression of SERCA isoforms, phospholamban and sarcolipin in human skeletal muscle fibers. PLoS One 8.

Fohr, U. C., B. R. Weber, M. Muntener, W. Staudenmann, G. J. Hughes, S. Frutiger, D. Banville, B. W. Schafer, and C. W. Heizmann. 1993. Human alfa and beta parvalbumins: structure and tissue-specific expression. Eur. J. Biochem. 215:719–727.

Franzini-Armstrong, C., and A. O. Jorgensen. 1994. Structure and development of E-C coupling units in skeletal muscle. Annu. Rev. Physiol. 56:509–534.

Franzini-Armstrong, C., and F. Protasi. 1997. Ryanodine receptors of striated muscles: a complex channel capable of multiple interactions. Physiol. Rev. 77:699–729.

Franzini-Armstrong, C. 1996. Functional significance of membrane architecture in skeletal and cardiac muscle. Soc. Gen. Physiol. Ser. 51:3–18.

Fryer, M. W., and D. G. Stephenson. 1996. Total and sarcoplasmic reticulum calcium contents of skinned fibres from rat skeletal muscle. J. Physiol. 493:357–370.

Gailly, P. 2002. New aspects of calcium signaling in skeletal muscle cells: implications in Duchenne muscular dystrophy. Biochim. Biophys. Acta 1600:38–44.

Geeves, M. A., and K. C. Holmes. 1999. Structural mechanism of muscle contraction. Annu. Rev. Biochem. 68:687–728.

Giacomello, M., I. Drago, P. Pizzo, and T. Pozzan. 2007. Mitochondrial Ca^{2+} as a key regulator of cell life and death. Cell Death Differ. 14:1267–1274.

Gissel, H. 2005. The role of Ca^{2+} in muscle cell damage. Ann. N. Y. Acad. Sci. 1066:166–180.

Gorza, L. 1990. Identification of a novel type 2 fiber population in mammalian skeletal muscle by combined use of histochemical myosin ATPase and anti-myosin monoclonal antibodies. J. Histochem. Cytochem. 38:257–265.

Grünberg, W., R. Sacchetto, I. Wijnberg, K. Neijenhuis, F. Mascarello, E. Damiani, and C. Drögemüller. 2010. Pseudomyotonia, a muscle function disorder associated with an inherited ATP2A1 (SERCA1) defect in a Dutch Improved Red and White cross-breed calf. Neuromuscul. Disord. 20:467–470.

Gunn, H. M. 1989. Heart weight and running ability. J. Anat. 167:225–233.

Gunter, T. E., and D. R. Pfeiffer. 1990. Mechanisms by which mitochondria transport calcium. Am. Physiol. Soc.:755–786.

Gunteski-Hamblin, A.-M., J. Greeb, and G. E. Shull. 1988. A novel Ca^{2+} pump expressed in brain , kidney , and stomach is encoded by an alternative transcript of the slow-twitch muscle Sarcoplasmic Reticulum Ca^{2+}-ATPase gene. J. Biol. Chem. 263:15032–15040.

Guo, W., A. O. Jorgensen, and K. P. Campbell. 1996. Triadin, a linker for calsequestrin and the ryanodine receptor. Soc. Gen. Physiol. Ser. 51:19–28.

Guth, L., and F. J. Samaha. 1969. Qualitative differences between actomyosin ATPase of slow and fast mammalian muscle. Exp. Neurol. 25:138–152.

Hayashi, T., R. Rizzuto, G. Hajnoczky, and T.-P. Su. 2009. MAM: more than just a housekeeper. Trends Cell Biol. 19:81–88.

Hidalgo, C., M. E. González, and A. M. García. 1986. Calcium transport in transverse tubules isolated from rabbit skeletal muscle. Biochim. Biophys. Acta 854:279–286.

Hua, S., H. Ma, D. Lewis, G. Inesi, and C. Toyoshima. 2002. Functional role of “N” (nucleotide) and “P” (phosphorylation) domain interactions in the sarcoplasmic reticulum (SERCA) ATPase. Biochemistry 41:2264–2272.

Inesi, G., M. Kurzmack, C. Coan, and D. E. Lewis. 1980. Cooperative calcium binding and ATPase activation in sarcoplasmic reticulum vesicles. J. Biol. Chem. 255:3025–3031.

Jensen, A.-M. L., T. L.-M. Sørensen, C. Olesen, J. V. Møller, and P. Nissen. 2006. Modulatory and catalytic modes of ATP binding by the calcium pump. EMBO J. 25:2305–2314.

Johnson, L. N., and R. J. Lewis. 2001. Structural basis for control by phosphorylation. Chem. Rev. 101:2209–2242.

Julian, F. J., R. L. Moss, and M. R. Sollins. 1978. The mechanism for vertebrate striated muscle contraction. Circ. Res. 42:2–14.

Kambadur, R., M. Sharma, T. P. L. Smith, and J. J. Bass. 1997. Mutations in myostatin (GDF8) in Double-Muscled Belgian Blue and Piedmontese Cattle. Genome Res. 7:910–915.

De la Bastie, D., D. Levitsky, L. Rappaport, J. J. Mercadier, F. Marotte, C. Wisnewsky, V. Brovkovich, K. Schwartz, and a. M. Lompre. 1990. Function of the sarcoplasmic reticulum and expression of its Ca^{2+}-ATPase gene in pressure overload-induced cardiac hypertrophy in the rat. Circ. Res. 66:554–564.

LaFramboise, W. A., M. J. Daood, R. D. Guthrie, P. Moretti, S. Schiaffino, and M. Ontell. 1990. Electrophoretic separation and immunological identification of type 2X myosin heavy chain in rat skeletal muscle. Biochim. Biophys. Acta 1035:109–112.

Lamboley, C. R., R. M. Murphy, M. J. McKenna, and G. D. Lamb. 2013. Endogenous and maximal sarcoplasmic reticulum calcium content and calsequestrin expression in type I and type II human skeletal muscle fibres. J. Physiol. 591:6053–6068.

Lamboley, C. R., R. M. Murphy, M. J. McKenna, and G. D. Lamb. 2014. Sarcoplasmic reticulum Ca2+ uptake and leak properties, and SERCA isoform expression, in type I and type II fibres of human skeletal muscle. J. Physiol. 592:1381–1395.

Latorre, R., F. Gil, J. M. Vazquez, F. Moreno, F. Mascarello, and G. Ramirez. 1993. Skeletal muscle fibre types in the dog. J. Anat. 182:329–337.

Laursen, M., M. Bublitz, K. Moncoq, C. Olesen, J. V. Møller, H. S. Young, P. Nissen, and J. P. Morth. 2009. Cyclopiazonic acid is complexed to a divalent metal ion when bound to the sarcoplasmic reticulum Ca^{2+}-ATPase. J. Biol. Chem. 284:13513–13518.

Lowry, O. H., N. J. Rosebrough, L. Farr, and R. J. Randall. 1951. Protein measurement with the folin phenol reagent. J. Biol. Chem. 193:265–275.

De Luca, H. F., and G. W. Engstrom. 1961. Calcium uptake by rat kidney mitochondria. Biochemistry 47:1744–1750.

Lytton, J., and D. H. Maclennan. 1988. Molecular cloning of cDNAs from human kidney coding for two of the cardiac Ca^{2+}-ATPase gene. J. Biol. Chem. 263:15024–15031.

Lyttons, J., M. Westlin, S. E. Burk, G. E. Shull, and D. H. Maclennan. 1992. Functional comparisons between isoforms of the sarcoplasmic or Endoplasmic Reticulum family of calcium pumps. J. Biol. Chem. 267:14483–14489.

Ma, H., D. Lewis, C. Xu, G. Inesi, and C. Toyoshima. 2005. Functional and Structural Roles of Critical Amino Acids within the " N ", " P ", and "A" Domains of the Ca^{2+} ATPase (SERCA) Headpiece. Biochemistry 44:8090–8100.

Maccatrozzo, L., M. Patruno, L. Toniolo, C. Reggiani, and F. Mascarello. 2004. Myosin heavy chain 2B isoform is expressed in specialized eye muscles but not in trunk and limb muscles of cattle. Eur. J. Histochem. 48:357–366.

MacLennan, D. H., C. J. Brandl, B. Korczak, and N. M. Green. 1985. Amino-acid sequence of a Ca^{2+} Mg^{2+}-dependent ATPase from rabbit muscle sarcoplasmic reticulum, deduced from its complementary DNA sequence.

MacLennan, D. H., W. J. Rice, and N. M. Green. 1997. The Mechanism of Ca^{2+} Transport by Sarco(Endo)plasmic Reticulum Ca^{2+}-ATPases. J. Biol. Chem. 272:28815–28818.

MacLennan, D. H., and P. T. S. Wong. 1971. Isolation of a Calcium-Sequestering Protein from Sarcoplasmic Reticulum. Proc. Natl. Acad. Sci. 68:1231–1235.

McClure, M. C., N. S. Morsci, R. D. Schnabel, J. W. Kim, P. Yao, M. M. Rolf, S. D. McKay, S. J. Gregg, R. H. Chapple, S. L. Northcutt, and J. F. Taylor. 2010. A genome scan for quantitative trait loci influencing carcass, post-natal growth and reproductive traits in commercial Angus cattle. Anim. Genet. 41:597–607.

McCormack, J. G., A. P. Halestrap, and R. M. Denton. 1990. Role of calcium ions in regulation of mammalian intramitochondrial metabolism. Physiol. Rev. 70:391–425.

De Meis, L., and W. Hasselbach. 1971. Acetyl Phosphate as substrate for Ca^{2+} uptake in skeletal muscle microsomes : inhibition by alkali ions. J. Biol. Chem. 246:4759–4763.

Meissner, G., and X. Lu. 1995. Dihydropyridine receptor-ryanodine receptor interactions in skeletal muscle excitation-contraction coupling. Biosci. Rep. 15:399–408.

Meissner, G. 1994. Ryanodine receptor/Ca^{2+} release channels and their regulation by endogenous effectors. Annu. Rev. Physiol. 56:485–508.

Michalak, M., K. Famulski, and E. Carafoli. 1984. The Ca^{2+}-pumping ATPase in skeletal muscle sarcolemma. J. Biol. Chem. 259:15540–15547.

Miller, S. C., B. M. Bowman, and L. K. Roberts. 1984. Identification and characterization of mononuclear phagocytes isolated from rat testicular interstitial tissues. J. Leukoc. Biol. 36:679–687.

Miretti, S., E. Martignani, P. Accornero, and M. Baratta. 2013. Functional effect of mir-27b on myostatin expression: a relationship in Piedmontese cattle with double-muscled phenotype. BMC Genomics 14:194.

Moller, J. V, B. Juul, and M. le Maire. 1996. Structural organization, ion transport, and energy transduction of P-type ATPases. Biochim. Biophys. Acta 1286:1–51.

Moncoq, K., C. a Trieber, and H. S. Young. 2007. The molecular basis for cyclopiazonic acid inhibition of the sarcoplasmic reticulum calcium pump. J. Biol. Chem. 282:9748–9757.

Monteith, G. R., and B. D. Roufogalis. 1995. The plasma membrane calcium pump - a physiological perspective on its regulation. Cell Calcium 18:459–470.

Murgiano, L., R. Sacchetto, S. Testoni, T. Dorotea, F. Mascarello, R. Liguori, A. Gentile, and C. Drögemüller. 2012. Pseudomyotonia in Romagnola cattle caused by novel ATP2A1 mutations. BMC Vet. Res. 8:186.

Murgiano, L., S. Testoni, C. Drögemüller, M. Bolcato, and A. Gentile. 2013. Frequency of bovine congenital pseudomyotonia carriers in selected Italian Chianina sires. Vet. J. 195:238–240.

Murphy, R. M., N. T. Larkins, J. P. Mollica, N. a Beard, and G. D. Lamb. 2009. Calsequestrin content and SERCA determine normal and maximal Ca^{2+} storage levels in sarcoplasmic reticulum of fast- and slow-twitch fibres of rat. J. Physiol. 587:443–460.

Myint, W., Q. Gong, J. Ahn, and R. Ishima. 2011. Characterization of sarcoplasmic reticulum Ca^{2+} ATPase nucleotide binding domain mutants using NMR spectroscopy. Biochem. Biophys. Res. Commun. 405:19–23.

De Nardi, C., S. Ausoni, P. Moretti, L. Gorza, M. Velleca, M. Buckingham, and S. Schiaffino. 1993. Type 2X-myosin heavy chain is coded by a muscle fiber type-specific and developmentally regulated gene. J. Cell Biol. 123:823–835.

Needham, D. M. 1926. Red and white muscle. Physiol. Rev. 6:1–27.

Obara, K., N. Miyashita, C. Xu, I. Toyoshima, Y. Sugita, G. Inesi, and C. Toyoshima. 2005. Structural role of countertransport revealed in Ca^{2+} pump crystal structure in the absence of Ca^{2+}. PNAS 102:14489–14496.

Odermatt, A., K. Barton, V. K. Khanna, J. Mathieu, D. Escolar, T. Kuntzer, G. Karpati, and D. H. MacLennan. 2000. The mutation of Pro789 to Leu reduces the activity of the fast-twitch skeletal muscle sarco(endo)plasmic reticulum Ca^{2+} ATPase (SERCA1) and is associated with Brody disease. Hum. Genet. 106:482–91.

Odermatt, A., K. Barton, V. K. Khanna, J. Mathieu, D. Escolar, T. Kuntzer, G. Karpati, and D. H. Maclennan. 2000. The mutation of Pro789 to Leu reduces the activity of the fast-twitch skeletal muscle sarco(endo)plasmic reticulum Ca^{2+}ATPase (SERCA1) and is associated with Brody disease. Hum. Genet. 106:482–491.

Odermatt, A., S. Becker, V. K. Khanna, K. Kurzydlowski, E. Leisner, D. Pette, and D. H. MacLennan. 1998. Sarcolipin Regulates the Activity of SERCA1, the Fast-twitch Skeletal Muscle Sarcoplasmic Reticulum Ca^{2+}-ATPase. J. Biol. Chem. 273:12360–12369.

Odermatt, A., P. E. Taschner, V. K. Khanna, H. F. M. Busch, G. Karpati, C. K. Jablecki, M. H. Breuning, and D. H. MacLennan. 1996. Mutations in the gene-encoding SERCA1, the fast-twitch skeletal muscle sarcoplasmic reticulum Ca^{2+} ATPase, are associated with Brody disease. Nat. Publ. Gr.:191–194.

Odermatt, A., P. E. Taschner, S. W. Scherer, B. Beatty, V. K. Khanna, D. R. Cornblath, V. Chaudhry, W. C. Yee, B. Schrank, G. Karpati, M. H. Breuning, N. Knoers, and D. H. MacLennan. 1997. Characterization of the gene encoding human sarcolipin (SLN), a proteolipid associated with SERCA1: absence of structural mutations in five patients with Brody disease. Genomics 45:541–553.

Olesen, C., M. Picard, A.-M. L. Winther, C. Gyrup, J. P. Morth, C. Oxvig, J. V. Møller, and P. Nissen. 2007. The structural basis of calcium transport by the calcium pump. Nature 450:1036–1042.

Palty, R., W. F. Silverman, M. Hershfinkel, T. Caporale, S. L. Sensi, J. Parnis, C. Nolte, D. Fishman, V. Shoshan-Barmatz, S. Herrmann, D. Khananshvili, and I. Sekler. 2010. NCLX is an essential component of mitochondrial Na^{+}/Ca^{2+} exchange. Proc. Natl. Acad. Sci. USA 107:436–441.

Pan, Y., E. Zvaritch, a R. Tupling, W. J. Rice, S. de Leon, M. Rudnicki, C. McKerlie, B. L. Banwell, and D. H. MacLennan. 2003. Targeted disruption of the ATP2A1 gene encoding the sarco(endo)plasmic reticulum Ca2+ ATPase isoform 1 (SERCA1) impairs diaphragm function and is lethal in neonatal mice. J. Biol. Chem. 278:13367–13375.

Paolini, C., M. Quarta, L. D'Onofrio, C. Reggiani, and F. Protasi. 2011. Differential effect of calsequestrin ablation on structure and function of fast and slow skeletal muscle fibers. J. Biomed. Biotechnol. 2011:634075.

Patron, M., A. Raffaello, V. Granatiero, A. Tosatto, G. Merli, D. De Stefani, L. Wright, G. Pallafacchina, A. Terrin, C. Mammucari, and R. Rizzuto. 2013. The mitochondrial calcium uniporter (MCU): molecular identity and physiological roles. J. Biol. Chem. 288:10750–10758.

Patruno, M., S. Sivieri, C. Poltronieri, R. Sacchetto, L. Maccatrozzo, T. Martinello, B. Funkenstein, and G. Radaelli. 2008. Real-time polymerase chain reaction, in situ hybridization and immunohistochemical localization of insulin-like growth factor-I and myostatin during development of Dicentrarchus labrax (Pisces: Osteichthyes). Cell Tissue Res. 331:643–658.

Peachey, L. D. 1965. Transverse tubules in excitation-contraction coupling. Fed. Proc. 24:1124–34.

Periasamy, M., and A. Kalyanasundaram. 2007. SERCA pump isoforms: their role in calcium transport and disease. Muscle Nerve 35:430–442.

Peter, J. B., R. J. Barnard, V. R. Edgerton, C. A. Gillespie, and K. E. Stempel. 1972. Metabolic profiles of three fiber types of skeletal muscle in guinea pigs and rabbits. Biochemistry 11:2627–2633.

Pette, D., H. Peuker, and R. S. Staron. 1999. The impact of biochemical methods for single muscle fibre analysis. Acta Physiol. Scand. 166:261–277.

Protasi, F., C. Franzini-Armstrong, and P. D. Allen. 1998. Role of ryanodine receptors in the assembly of calcium release units in skeletal muscle. J. Cell Biol. 140:831–842.

Protasi, F., X. H. Sun, and C. Franzini-Armstrong. 1996. Formation and maturation of the calcium release apparatus in developing and adult avian myocardium. Dev. Biol. 173:265–278.

Reggiani, C., and F. Mascarello. 2004. Fibre type identification and functional characterization in adult livestock animals. In: H. P. Haagsmann, M. F. W. Te Pas, and M. E. Everts, editors. Muscle Development of Livestock Animals: Physiology, Genetics and Meat Quality. CABI publishing, Wallingford, Oxfordshire. p. 39–68.

Rizzuto, R., P. Pinton, M. Brini, A. Chiesa, L. Filippin, and T. Pozzan. 1999. Mitochondria as biosensors of calcium microdomains. Cell Calcium 26:193–199.

Rudolf, R., M. Mongillo, P. J. Magalhães, and T. Pozzan. 2004. In vivo monitoring of Ca^{2+} uptake into mitochondria of mouse skeletal muscle during contraction. J. Cell Biol. 166:527–536.

Rüegg, C., C. Veigel, J. E. Molloy, S. Schmitz, J. C. Sparrow, and R. H. A. Fink. 2002. Molecular Motors: Force and Movement Generated by Single Myosin II Molecules. News Physiol. Sci. 17:213–218.

Sacchetto, R., I. Bertipaglia, S. Giannetti, L. Cendron, F. Mascarello, E. Damiani, E. Carafoli, and G. Zanotti. 2012. Crystal structure of sarcoplasmic reticulum Ca^{2+}-ATPase (SERCA) from bovine muscle. J. Struct. Biol. 178:38–44.

Sacchetto, R., E. Bovo, A. Donella-Deana, and E. Damiani. 2005. Glycogen- and PP1c-targeting subunit GM is phosphorylated at Ser48 by sarcoplasmic reticulum-bound Ca^{2+}-calmodulin protein kinase in rabbit fast twitch skeletal muscle. J. Biol. Chem. 280:7147–7155.

Sacchetto, R., E. Sharova, M. Patruno, L. Maccatrozzo, E. Damiani, and F. Mascarello. 2012. Overexpression of histidine-rich calcium binding protein in equine ventricular myocardium. Vet. J. 193:157–161.

Sacchetto, R., S. Testoni, A. Gentile, E. Damiani, M. Rossi, R. Liguori, C. Drögemüller, and F. Mascarello. 2009. A defective SERCA1 protein is responsible for congenital pseudomyotonia in Chianina cattle. Am. J. Pathol. 174:565–573.

Sacchetto, R., F. Turcato, E. Damiani, and A. Margreth. 1999. Interaction of triadin with histidine-rich Ca^{2+}-binding protein at the triadic junction in skeletal muscle fibers. J. Muscle Res. Cell Motil. 20:403–415.

Schiaffino, S., V. Hanzltkova, and S. Pierobon. 1970. Relations between structure and function in rat skeletal muscle fibers. J. Cell Biol. 47:107–119.

Schiaffino, S., and C. Reggiani. 2011. Fiber types in mammalian skeletal muscles. Physiol. Rev. 91:1447–1531.

Schiaffino, S. 2010. Fibre types in skeletal muscle: a personal account. Acta Physiol. 199:451–463.

Schwartz, B. W. N., and J. W. C. Bird. 1977. Degradation of Myofibrillar Proteins by Cathepsins B and D. Biochem. J. 167:811–820.

Scorzeto, M., M. Giacomello, L. Toniolo, M. Canato, B. Blaauw, C. Paolini, F. Protasi, C. Reggiani, and G. J. M. Stienen. 2013. Mitochondrial Ca2+-handling in fast skeletal muscle fibers from wild type and calsequestrin-null mice. PLoS One 8:e74919.

Sørensen, T. L. M., J. V. Møller, and P. Nissen. 2004. Phosphoryl transfer and calcium ion occlusion in the calcium pump. Science (80). 304:1672–1675.

De Stefani, D., A. Raffaello, E. Teardo, I. Szabò, and R. Rizzuto. 2011. A forty-kilodalton protein of the inner membrane is the mitochondrial calcium uniporter. Nature 476:336–340.

Sweadner, K. J., and C. Donnet. 2001. Structural similarities of Na, K-ATPase and SERCA, the Ca^{2+}-ATPase of the sarcoplasmic reticulum. Biochem. J. 356:685–704.

Takahashi, M., Y. Kondou, and C. Toyoshima. 2007. Interdomain communication in calcium pump as revealed in the crystal structures with transmembrane inhibitors. PNAS 104:5800–5805.

Talmadge, R. J., M. J. Castro, D. F. Apple, and G. a Dudley. 2002. Phenotypic adaptations in human muscle fibers 6 and 24 wk after spinal cord injury. J. Appl. Physiol. 92:147–154.

Termin, A., R. S. Staron, and D. Pette. 1989. Myosin heavy chain isoforms in histochemically defined fiber types of rat muscle. Histochemistry 92:453–457.

Testoni, S., P. Boni, and A. Gentile. 2008. Congenital Psudomyotonia in Chianina cattle. Vet. Rec. 163:252.

Thompson, P. N., J. a P. Heesterbeek, and J. a M. van Arendonk. 2006. Changes in disease gene frequency over time with differential genotypic fitness and various control strategies. J. Anim. Sci. 84:2629–2635.

Toniolo, L., M. Patruno, L. Maccatrozzo, M. A. Pellegrino, M. Canepari, R. Rossi, G. D'Antona, R. Bottinelli, C. Reggiani, and F. Mascarello. 2004. Fast fibres in a large animal: fibre types, contractile properties and myosin expression in pig skeletal muscles. J. Exp. Biol. 207:1875–1886.

Toyoshima, C., and G. Inesi. 2004. Structural basis of ion pumping by Ca^{2+}-ATPase of the sarcoplasmic reticulum. Annu. Rev. Biochem. 73:269–292.

Toyoshima, C., and T. Mizutani. 2004. Crystal structure of the calcium pump with a bound ATP analogue. Nature 430:529–535.

Toyoshima, C., M. Nakasako, H. Nomura, and H. Ogawa. 2000. Crystal structure of the calcium pump of sarcoplasmic reticulum at 2.6 A resolution. Nature 405:647–655. Available from: http://www.ncbi.nlm.nih.gov/pubmed/10864315

Toyoshima, C., and H. Nomura. 2002. Structural changes in the calcium pump accompanying the dissociation of calcium. Nature 418:605–611.

Toyoshima, C., Y. Norimatsu, S. Iwasawa, T. Tsuda, and H. Ogawa. 2007. How processing of aspartylphosphate is coupled to lumenal gating of the ion pathway in the calcium pump. PNAS 104:19831–19836.

Toyoshima, C., S. I. Yonekura, J. Tsueda, and S. Iwasawa. 2011. Trinitrophenyl derivatives bind differently from parent adenine nucleotides to Ca^{2+}-ATPase in the absence of Ca^{2+}. PNAS 108:1833–1838.

Toyoshima, C. 2008. Structural aspects of ion pumping by Ca^{2+}-ATPase of sarcoplasmic reticulum. Arch. Biochem. Biophys. 476:3–11.

Toyoshima, C. 2009. How Ca^{2+}-ATPase pumps ions across the sarcoplasmic reticulum membrane. Biochim. Biophys. Acta 1793:941–946.

Tupling, A. R., E. Bombardier, S. C. Gupta, D. Hussain, C. Vigna, D. Bloemberg, J. Quadrilatero, M. G. Trivieri, G. J. Babu, P. H. Backx, M. Periasamy, D. H. MacLennan, and A. O. Gramolini. 2011. Enhanced Ca^{2+} transport and muscle relaxation in skeletal muscle from sarcolipin-null mice. Am. J. Physiol. Cell Physiol. 301:841–849.

Vale, R. D. 2000. The Way Things Move: Looking Under the Hood of Molecular Motor Proteins. Science (80). 288:88–95.

Vattemi, G., F. Gualandi, A. Oosterhof, M. Marini, P. Tonin, P. Rimessi, M. Neri, V. Guglielmi, A. Russignan, C. Poli, T. H. van Kuppevelt, A. Ferlini, and G. Tomelleri. 2010. Brody disease: insights into biochemical features of SERCA1 and identification of a novel mutation. J. Neuropathol. Exp. Neurol. 69:246–252.

Vilsen, B., J. P. Andersen, D. M. Clarke, and D. H. Maclennan. 1989. Functional consequences of proline mutations in the cytoplasmic and transmembrane sectors of the Ca2+-ATPase of Sarcoplasmic Reticulum. J. Biol. Chem. 264:21024–21030.

Vilsen, B., J. Peter, and D. H. Maclennan. 1991. Functional consequences of alterations to hydrophobic amino acids located at the M4S4 boundary of the Ca^{2+}-ATPase of Sarcoplasmic Reticulum. J. Biol. Chem. 266:18839–18845.

Voermans, N. C., a E. Laan, A. Oosterhof, T. H. van Kuppevelt, G. Drost, M. Lammens, E. J. Kamsteeg, C. Scotton, F. Gualandi, V. Guglielmi, L. van den Heuvel, G. Vattemi, and B. G. van Engelen. 2012. Brody syndrome: a clinically heterogeneous entity distinct from Brody disease: a review of literature and a cross-sectional clinical study in 17 patients. Neuromuscul. Disord. 22:944–954.

Wang, Y. H., N. I. Bower, A. Reverter, S. H. Tan, N. De Jager, R. Wang, S. M. McWilliam, L. M. Cafe, P. L. Greenwood, and S. A. Lehnert. 2009. Gene expression patterns during intramuscular fat development in cattle. J. Anim. Sci. 87:119–130.

Wegner, J., E. Albrecht, I. Fiedler, F. Teuscher, H. J. Papstein, and K. Ender. 2000. Growth- and breed-related changes of muscle fiber characteristics in cattle. J. Anim. Sci. 78:1485–1496.

Williams, G. S. B., L. Boyman, A. C. Chikando, R. J. Khairallah, and W. J. Lederer. 2013. Mitochondrial calcium uptake. PNAS 110:10479–10486.

Winther, A. M. L., H. Liu, Y. Sonntag, C. Olesen, M. le Maire, H. Soehoel, C.-E. Olsen, S. B. Christensen, P. Nissen, and J. V Møller. 2010. Critical roles of hydrophobicity and orientation of side chains for inactivation of sarcoplasmic reticulum Ca^{2+}-ATPase with thapsigargin and thapsigargin analogs. J. Biol. Chem. 285:28883–28892.

Wu, K. D., and J. Lytton. 1993. Molecular cloning and quantification of sarcoplasmic reticulum Ca^{2+}-ATPase isoforms in rat muscles. Am. J. Physiol. 264:333–341.

Wuytack, F., B. Papp, H. Verboomen, L. Raeymaekers, L. Dode, E. Bobe, J. Enouf, S. Bokkala, K. S. Authi, and R. Casteels. 1994. A Sarco/endoplasmic Reticulum Ca^{2+}-ATPase 3-Type Ca^{2+} pump is expressed in platelets , in lymphoid cells , and in mast cells. J. Biol. Chem. 269:1410–1416.

Xu, C., W. J. Rice, W. He, and D. L. Stokes. 2002. A structural model for the catalytic cycle of Ca^{2+}-ATPase. J. Mol. Biol. 316:201–211.

Yi, J., C. Ma, Y. Li, N. Weisleder, E. Ríos, J. Ma, and J. Zhou. 2011. Mitochondrial calcium uptake regulates rapid calcium transients in skeletal muscle during excitation-contraction (E-C) coupling. J. Biol. Chem. 286:32436–32443.

Youn, J. H., E. A. Gulve, and J. O. Holloszy. 1991. Calcium stimulates glucose transport in skeletal muscle by a pathway independent of contraction. Am. J. Physiol. 260:C555–561.

Zarain-herzberg, A., D. H. Maclennang, and M. Periasamy. 1990. Characterization of rabbit cardiac Sarco(endo)plasmic Ca^{2+}-ATPase gene. J. Biol. Chem. 265:4670–4677.

Side project

Extra Cellular Matrix responses to tendon injury:

A.Biochemical analysis of cartilage oligomeric matrix (COMP) fragmentation levels in injury-predisposed sites

B.Morphological analysis of deep digital flexor tendon (DDFT) with naturally occurring tear-type lesion

1.GENERAL INTRODUCTION

1.1.*Tendon anatomy: cell population and collagen organization*

Tendons are anatomic structures interposed between muscles and bones transmitting the force created in the muscle to bone, and, in this way, making joint movement possible. Basically, each muscle has two tendons, proximal and distal. The point of union with a muscle is called myotendinous junction (MTJ), and the point of union with a bone osteotendinous junction (OTJ) (Kannus, 2000).

When healthy, tendons appear brilliant white and they consist of a dense fibrous extracellular matrix (ECM) with a high water content. This matrix is synthetized and maintained by a small population of tenoblasts and tenocytes (Sharma and Maffulli, 2006; C T Thorpe et al., 2010).

Cell population: The cellular elements of the tendon consist of tenoblasts and tenocytes for about 90–95% on the total cell population. The other 5-10% includes: i) chondrocytes located at the pressure and insertion sites, ii) synovial cells of the tendon sheath, and iii) vascular cells (endothelial and smooth muscle cells). Inflammatory cells, macrophages and myofibroblasts are observed within the tendon tissue in pathological conditions (Józsa and Kannus, 1997; Kannus, 2000).

Tenoblasts and tenocytes are fibroblastic cells responsible for synthesis and turnover of the matrix. They are arranged in parallel rows between collagen fibril bundles within fascicles, where most lack direct contact with the vasculature located in the endotenon. The tenocytes extend long cytoplasmic processes within and between rows and are linked into complex three-dimensional networks by gap junctions and actin-associated adherens junctions that facilitate coordinated responses to mechanical loading. Gap junctional intercellular communication may also facilitate transfer of nutrients between cells within the avascular matrix (Patterson-Kane and Firth, 2009).

In Veterinary medicine, an histological classification based on nuclear morphology do not describe tenoblasts in adult tissue although divides tenocytes in type 1, 2 or 3. Type 1 tenocytes have long, thin spindle-shaped nuclei, and type 2 cells plump, cigar-shaped

nuclei. Type 3 cells are round with pale basophilic matrix immediately surrounding them (similar to chondrocytes) and are found in fibrocartilaginous regions of tendons (Smith and Webbon, 1996). Comparing the description above with the classification of tendon cells in human medicine, types 2 tenocytes are the 'tenoblasts' (Dowling et al., 2000; Kannus, 2000).

Type 2 cells ('tenoblasts') contain larger amounts of synthetic organelles suggesting an high metabolism which means high synthesis of extracellular matrix components. Type 1 cells ('tenocytes') still have well-developed rough endoplasmic reticulum and Golgi apparatus, as well as an high quantity of free ribosomes, suggesting that tenocytes are metabolically active cells although not at the same level as the tenoblasts. Moreover, it is documented that an age-related increase in the proportion of type 1 on type 2 tenocytes along with a reduction in total cellularity and levels of cellular activity (Kannus, 2000; Patterson-Kane and Firth, 2009).

All the three main pathways of energy metabolism (aerobic Krebs' cycle, anaerobic glycolysis, and pentose phosphate shunt) are used by tendon cell. In young tendon, all the three pathways of energy production are highly active while, with increasing age, there is a decrease in aerobic metabolism (Krebs' cycle and the pentose phosphate shunt) and the anaerobic glycolysis becomes the main metabolic pathway for the tenocytes. In general, the synthetic activity is high during growth and diminishes with age. However, the activity pattern may change drastically in many pathological conditions (Kannus, 2000).

The characteristic low metabolic rate of adult tendon tissue is well suited for the main purpose of the tendon. The low metabolic rate with well-developed anaerobic energy production is essential if the tendon is to carry loads and remain in tension for periods of time without the risk of ischemia and necrosis. The drawback of this low metabolic rate is the slow rate of recovery after activity and of healing after injury (Kannus, 2000).

Collagen organization and tendon architecture: Tendons consist of collagen and elastin embedded in a proteoglycan-water matrix. Collagen is mostly type I collagen and it represents about 65–80% of the dry mass of the tendon, whereas elastin approximately the 1–2%. These elements are produced by tenoblasts and tenocytes (Kannus, 2000).

Collagen is arranged in hierarchical levels of increasing complexity (Figure 1), beginning with tropocollagen, a triple-helix polypeptide chain, which unites into fibrils; fibrils group in fibres or subfascicle (primary bundle); a group of primary bundles forms a fascicle (secondary bundle); a group of secondary bundles forms a tertiary bundle and these shape the tendon itself (Kannus, 2000; Sharma and Maffulli, 2006).

In general, collagen fibres are mainly oriented longitudinally, although fibres also run transversely and horizontally, forming spirals and plaits. Under a polarized light microscope, four types of fibre crossing can be demonstrated simply crossing two fibres, crossing of two fibres with one straight-running fibre, a plait formation with three fibres, and up-tying of parallel running fibres with one fibre (Józsa et al., 1984; Kannus, 2000). In addition, all these fibres form spirals (Kastelic et al., 1978; Rowe, 1985; Jozsa et al., 1991).

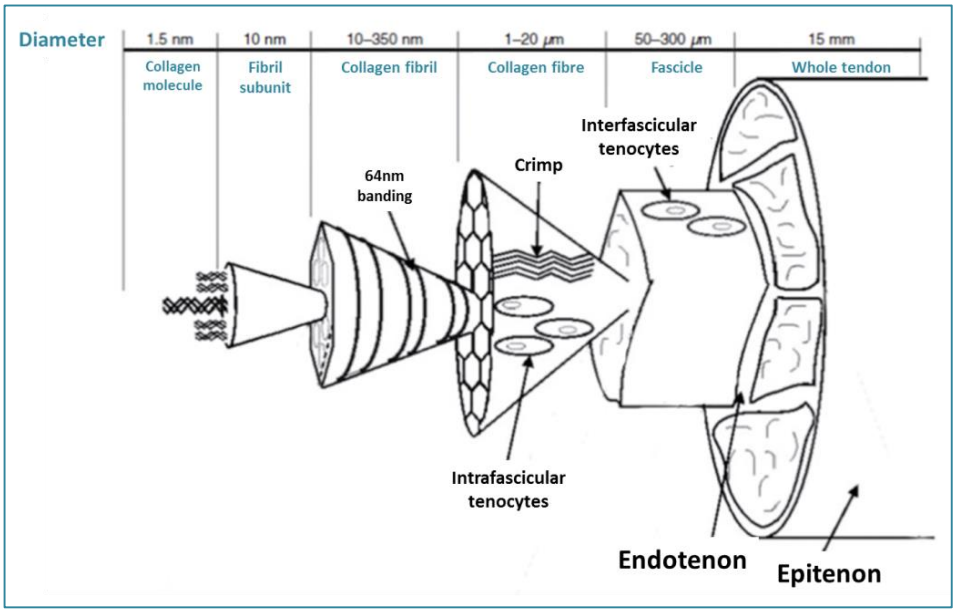

Figure 1. Representation of hierarchical architecture of tendon. Image modified from original in Thorpe *et al.* (2010).

Collagen bundles are divided by a series of sheaths: paratenon, epitenon and endotenon. The epitenon contains vascular, lymphatic, and nerve supply to the tendon. It is a fine, loose connective-tissue sheath that covers the whole tendon and extends deep within it between the tertiary bundles as the endotenon. The endotenon is a thin reticular network of connective tissue which originates from the epitenon and invests each tendon fibre. The paratenon sorrounds superficially the epitenon, and it consists of a loose areolar connective tissue with type I and III collagen fibrils, some elastic fibrils, and an inner

lining of synovial cells. In areas subjected to increased mechanical stress, synovial tendon sheaths are described. They consist of an outer fibrotic sheath, and an inner synovial sheath which invests the tendon body and functions as an ultrafiltration membrane to produce synovial fluid (conferring efficient lubrication) (Sharma and Maffulli, 2006).

1.2.*Tendon biomechanics*

The basic function of the tendon is to transmit the force created by the muscle to the bone, and, in this way, make joint movement possible. Moreover, the tendon provides skeletal support, increases the efficiency of locomotion by storing and releasing energy and withstand high-tensile forces(Kannus, 2000; Dahlgren, 2007).

In the resting state, the collagen fibres and fibrils of a tendon show a wavy or crimping configuration which appears already under the light microscope as regular bands across the fibre surface. Crimping is, however, a rather varying, irregular phenomenon, the crimp angle varying between 0° and 60° (Józsa and Kannus, 1997). This may be due to varying contribution of the proteoglycan cross-linking to the crimp (Kannus, 2000).

This configuration disappears if the tendon is stretched slightly corresponding to a straightening of the collagen fibres. When the tensile force is released, the tendon resumes its normal wavy appearance.

Below about 4% elongation, the stress–strain curve of a tendon is reproducible by a sequence of stretches, but as soon as this limit is exceeded the wavy form will not reappear and subsequent deformations will not reproduce the original curve. If an acute stress causes an elongation of 8% or more, the tendon is likely to rupture (Figure 2) (Józsa and Kannus, 1997).

Interestingly, in vivo measurement of equine SDFT strain at the gallop ranges from 11.5% to 16.6%, which is in close agreement with measured in vitro ultimate strains of 12–21% (Wilson et al., 2001; Dowling and Dart, 2005). Furthermore, during the movement, tendons are exposed not only to longitudinal (stretch) but also to transversal and rotational forces. In addition, they must be prepared to withstand direct contusions and pressures. The internal architecture of the tendon with the typical hierarchical organization of collagen fibres within the ECM forms a sort of buffer medium against

forces of various directions and prevent damages of the structure and disconnections between the components (Józsa and Kannus, 1997; Kannus, 2000).

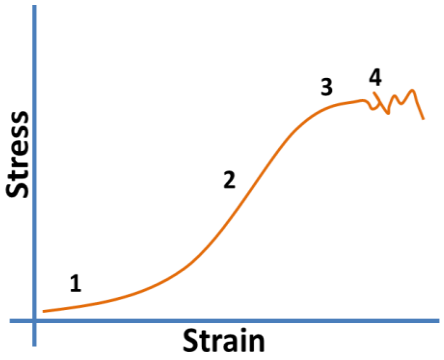

Figure 2. Simplified stress–strain curve for the SDFT (from Goodship et al., 1994). 1 = toe region; 2 = linear deformation; 3 = yield, elongation >4% (microscopic failure); 4 = rupture, elongation ≥ 8% (macroscopic failure).

Experimental studies demonstrate how exercise and different training protocols can influence tendon composition and biomechanics. More in detail, training results in improved tensile strength, elastic stiffness, weight and cross-sectional area of tendons. These effects can be explained by an increase in tenocyte activity with new synthesis of collagen and ECM components such as proteoglycans and COMP (Cartilage Oligomeric Matrix Protein) (Smith et al., 2002). Oppositely, immobilization reduces the water and proteoglycan content of tendons, and increases the number of reducible collagen cross-links resulting in tendon atrophy (Dowling and Dart, 2005; Maganaris et al., 2006).

Also age influences tendon biomechanical properties and functions. Indeed, adult tendon tissue loses the typical high metabolism of young tendon becoming a slow synthesis tissue. Adult tendon shows an aging-related decrease in cellularity, cell activity and matrix synthesis that lead to an increase tendon stiffness, disruption of matrix and loss of matrix components. Interestingly, studies on SDFT in the horse show how these modifications affect primarily only levels that would not endanger the functional competence of the tissue, even if excessive exercise could exacerbate those alterations and lead to a clinical manifestation (Smith et al., 2002; Dowling and Dart, 2005; Sharma and Maffulli, 2006).

1.3. Extracellular Matrix (ECM) of tendon

1.3.1.*Composition and roles of tendon extracellular matrix*

The extracellular tendon matrix (ECM) is composed of the collagen fibres, elastic fibres, the anorganic components and the ground substance.

Collagen and elastic fibres: As described in paragraph "1.1.", collagen fibres are the 65-80% of total dry mass of tendon while elastic fibres account only for approximately 1-2%. Nevertheless, this elastic component may contribute to the recovery of the wavy configuration of the collagen fibres after stretch movement (Kannus, 2000).

Anorganic components: Anorganic components represent less than 0.2% of the tendon dry mass. Calcium is found in the highest concentrations, between 0.05-0.1% in the insertion sites and between 0.001-0.01% in the tensional area of a normal tendon. In particular, pathological conditions (calcifying tendinopathy) calcium concentrations can increase a 10- to 20-fold. Magnesium, manganese, cadmium, cobalt, copper, zinc, nickel, lithium, lead, fluoride, phosphor, and silicon are other components detected in the tendon matrix although their role is not well known (Kannus, 2000).

Ground substance: The tendinous ground substance consists of proteoglycans (PGs), glycosaminoglycans (GAGs), structural glycoproteins, and other small molecules. PGs and GAGs have considerable water-binding capacity which make the ground substance a perfect hydrophilic gel suited to improve the biomechanical tendon properties.

Proteoglycans are large, negatively-charged hydrophilic molecules composed of a protein core in which one or more glycosaminoglycans are covalently attached. They are mostly entrapped within and between collagen fibrils and fibres forming a stiff net that provide to the structure a high capacity to resist compressive and tensile forces. Proteoglycans also facilitate rapid diffusion of water soluble molecules and migration of cells. GAG distribution is different in the different sites: it is approximately 0.2% of the dry mass in tensional zones while it is up to 3.5-5.0% in the insertion areas. Within GAGs, hyaluronic acid constitutes about 6% of the total.

Glycoproteins are macromolecules that consist of a large protein fraction and a small glycidic component. Fibronectin, thrombospondins (1-5), tenascin-C, undulin and

laminin are the most common non-collagenous proteins identified in tendon tissue (Kannus, 2000). Studies on equine tendon have shown that the non-collagenous extracellular matrix is not homogeneous along the length of digital flexor tendons, reflecting the different biomechanical environments experienced in different regions of the tendon (Smith et al., 1997).

Despite proteoglycans and glycoproteins are the most abundant non-collagenous proteins of tendon, their functions have not been fully determined. Due to their conformation and presence of side-chain, it has been proposed that proteoglycans regulate fibrillogenesis and organize the matrix. In addition, the stiff net that they form between the collagen fibrils increases the resistance to tensile loading and assists in the transfer of strain forces between the fibrils (Scott, 2003; Screen et al., 2005).

The most abundant glycoprotein identified in physiologically normal tendon is thrombospondin-5, better known as Collagen Oligomeric Matrix Protein (COMP) (Smith et al., 2002; Thorpe et al., 2010).

1.3.2.Collagen Oligomeric Matrix Protein (COMP)

COMP is a 524 kDa acidic protein. It is constituted of five-armed protein joined by a central cylindrical structure which relate it to thrombospondins family (Figure 3). It has been found in many mechanically loaded tissues such as cartilage, tendon, ligament, meniscus, and intervertebral disc.

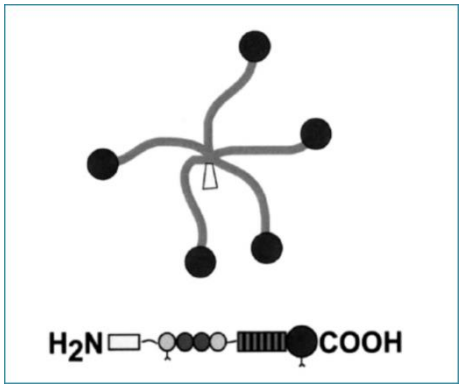

Figure 3. Simplify cartoon of the COMP protein structure (Smith et al., 2002).

The precise function is unknown, although it has been found that COMP is able to bind fibrillar collagen stabilizing the collagen fibre network. In addition, it may be involved in cell activity and interactions catalyzing fibrillogenesis and playing a key role in

assembly, organization and maintenance of the ECM (Smith and Webbon, 1996; Thorpe et al., 2010; Dakin et al., 2014; Smith et al., 2014).

In human medicine, COMP synovial fluid concentrations have prognostic value in rheumatoid arthritis and osteoarthritis. The same was demonstrated in equine medicine where COMP were proposed as useful biomarkers of different tendon disease. Moreover, COMP fragmentation was analysed in detail to develop an assay specific to injury stage for tendon disease (Dakin et al., 2014; Smith et al., 2014). Proteomic analysis of tendon tissue provided interesting data on tendon protein profile in physiological and pathological situations considering also disease stage-factor and age-factor influences. Dakin *et al.* (2014) identified a great number of proteins uniquely present in sub-acute stage disease. Within these, a novel COMP peptide was identified both in vivo and in vitro analysis and it was proposed as specific marker for injury stage. The authors speculated on the possibility to use this COMP fragment, along with the combination of other specific fragments, to develop a platform of antibodies to identify specific stage of tendon injury (Dakin et al., 2014). Peffers *et al.*(2014) compared the proteomic profiles of young and old horses demonstrating a quantitative decrease of several proteins that play a role in ECM organization in old animals. Moreover, they described an altered protein profile in injured tendon with an increase in proteins and greater degree of fragments (Peffers et al., 2014). Taken together, these last works increased the knowledge on the molecular aspects of tendon degeneration and the influence of factors such as disease and age on the functionality and healing process of the tissue. In addition, they identified specific products of protein fragmentation (peptides) that could be used as biomarkers of tendon injury.

1.3.3.Turn-over of ECM

In healthy tendon, the matrix is maintained and repaired by a small resident population of tenoblasts/tenocytes. These cells maintain a homeostatic balance between the breakdown of damaged ECM and the production of replacement proteins (Dahlgren, 2007). In healthy connective tissue, the turnover for proteoglycans seems relatively rapid and varies between 2 and 10 days (Kannus, 2000).

Tenocytes are able to remodel the matrix by synthesizing matrix molecules, including collagen and proteoglycans, and enzymes responsible for degradation, including matrix

metalloproteinases (MMPs). Specific MMPs are able to degrade different components of the matrix, but their activity is tightly regulated by a number of mechanisms. These include the presence of tissue inhibitors of metalloproteinases (TIMPs), whether the molecules are in their active form and their location within the matrix (Thorpe et al., 2010; Castagna et al., 2013).

Aging and excessive exercise, likewise stress deprivation (immobilization) affect the synthesis-degradation fine balance of ECM components. The effect of aging is primarily the decrease in cellularity which lead to a modification in cell-cell interaction and matrix production. These modifications, associating with overstimulation of the tissue, lead to cumulative microdamage within the tendon till a mechanical injury clinically apparent (Dahlgren, 2007). At the same way, lack of load input derived from physical immobilization or from damaged at the collagen network leads to overactivation of catabolic matrix proteases (MMPs) and increased apoptosis (programmed cell death) (Castagna et al., 2013).

The remodelling rate of collagen is considered negligible due to its half-life of 198 years (Thorpe et al., 2010), at the contrary the non-collagenous proteins of ECM appear to have a more rapid turn-over and therefore are likely the component more influenced by the alterations resulting from injury or aging (Smith et al., 2002; Jarvinen et al., 2003).

1.4.*Tendon injury and healing*

Typical responses of tendons to repetitive excessive load are inflammation of tendon sheaths, tissue degeneration or a combination of both. Different source of stress induces different response which should lead to a repairing mechanism in order to avoid weakening or rupture of the tendinous structure.

Hypoxia, ischaemic damage, oxidative stress (oxygen free radicals), hyperthermia, impaired apoptosis, inflammatory mediators, fluoroquinolones, and matrix metalloproteinase overactivation have been proposed as degenerative mechanisms in tendon (Goodship et al., 1994; Sharma and Maffulli, 2006).

The aetiology of tendon injury is not completely understood, although it is clear the implication of degenerative mechanisms. Tendon degeneration may lead to changes in ECM composition and collagen network, alteration of cell-cell and cell-ECM

interaction. The final result is altered biomechanics with reduced tensile strength and a consequent predisposition to rupture (Kannus, 2000). Moreover, the damaged tendinous network is unable to properly transmit mechanical load information to resident tenocytes. This lack in loading input generates a series of cell responses that lead to overactivation of MMPs and increased apoptosis (Thorpe et al., 2010).

Healing process: Tendon healing occurs in three overlapping stages: 1) acute inflammatory phase, 2) proliferation phase, 3) re-modelling phase.

The healing process in tendon is slow according to the typical characteristics of the tissue (low cellularity, low blood supply). This make critical the choice of a correct rehabilitation protocol that should be thought to accommodate the healing delayed and to match the phase of process.

1) The acute inflammatory phase begins immediately after injury and lasts 1 to 2 weeks. Heat, pain, and swelling are the characteristic clinically signs of this phase. In the first 24 hours, monocytes and macrophages massively infiltrate the tissue and help to remove the damaged ECM via phagocytosis. Furthermore, they release vasoactive and chemotactic factors that stimulate cell (tenoblasts/tenocytes) proliferation, initiate angiogenesis, and recruit other inflammatory and non-inflammatory cells for the progression of healing process. In particular tenocytes gradually migrate to the site of injury and initiated type III collagen synthesis (Sharma and Maffulli, 2006).

2) Few days after injury, the proliferation phase begins and can last for several weeks to months. Vascular and cellular elements accumulate in the endotenon conferring the characteristic hypercellular aspect of the damaged region. This cell population has progenitor cells features: they are large, plump, with round to oval nuclei suggesting an high metabolism in preparation to increase collagen and other ECM components production. Collagen type III reaches its peak of synthesis in this stage of healing process providing a first, immature fibrous network in which other ECM elements are randomly scattered. This temporary structure can support tensile strength in the early stages of the healing process. The type III collagen fibrils are progressively replaced with larger and stronger collagen type I fibrils and new ECM is synthetized in the injury site (Sharma and Maffulli, 2006).

3) The re-modelling phase of tendon healing is the critical stage to regain the biomechanical properties of a functional tendon. Re-modelling begins approximately 6 weeks after injury and can last for 6 to 12 months or longer. Tenocytes and collagen fibres become aligned in parallel fashion along lines of tension; synthesis of type I collagen increases and gradual change of fibrous tissue to scar-like tendon tissue occurs. This means that, despite the ongoing re-modelling, the healed tendon still lacks the biomechanical properties of the native tissue (Sharma and Maffulli, 2006).

Re-modelling is also involved in the physiological response of tendon to particular prolonged stress (endurance training). The tissue is shaped to adapt the mechanical repetitive loads, and prevents the tendons from incurring injuries (Sharma and Maffulli, 2006; Patruno and Martinello, 2014).

Recent research on equine tendon has demonstrated how the early stage of tendon injury (inflammatory phase) is characterized by the presence of M1 polarised macrophages which elaborate pro-inflammatory mediators and stimulate all the cell-response described above. The same study described the presence of M2 polarised macrophages during the late proliferation and re-modelling phase (>3 months after injury). M2 macrophages produce immunosuppressive cytokines and have clearly an anti-inflammatory activity. Their predominant presence during the late stages of healing process may have the function to protect this susceptible region from repeated injury by dampening pro-inflammatory activities. An interesting therapeutic outcome from these findings suggests a more targeted approach to tendon injuries with a possible modulation of the inflammation according to the disease stage (Dakin et al., 2012; Dakin et al., 2014; Patruno and Martinello, 2014).

1.5.Frequent tendon injuries in horse

All the epidemiology studies of tendon injuries in horse population have limited transferability to global scale due to national differences in horse demographics, racing and training practices, and different disciplines in which the animals are involved (Clegg, 2012).

Nevertheless, tendon injury is considered one of the most common form of musculoskeletal injuries that occur to horses competing in all disciplines. In racehorses competing in UK National Hunt and flat races, 46% of total injuries diagnosed to the musculoskeletal system involved tendons or ligaments (Williams et al., 2001). Whereas, in horses used in hurdle and steeplechase races, tendon or ligament strain accounts for 53% of musculoskeletal injuries (Pinchbeck et al., 2004).

It is well documented that some tendons are more prone to injury than others, indeed specific strain-induced injuries are associated with specific tendons (Smith et al., 2002). Forelimb tendons are the most frequently injured tendons in horses (97-99%), with the superficial digital flexor tendon (SDFT) being injured in 75-93% of cases and the remaining injuries occurring to the suspensory ligament (SL) (Kasashima et al., 2004; Smith and Wright, 2006; Lam et al., 2007), while the deep digital flexor tendon (DDFT) and common digital extensor tendon (CDET) are considered rarely affected even if they have been increasingly diagnosed thanks to the advent of magnetic resonance imaging (Mair and Kinns, 2005; Murray et al., 2006; Thorpe et al., 2010; Cillán-García et al., 2013) in cases of palmar foot pain.

As general observation, it has been reported that in training horses tendon injury accounts for 43% of injuries that can occur. Within these, 33% of injuries involve the SDFT, 31% the SL and 17% the DDFT. Jumper horses have a high risk of injury to the forelimb SDFT and DDFT, whereas dressage horses have a high risk of injury to the hind limb SL (Thorpe et al., 2010).

Moreover, the risk of tendon injury increases with increasing age (Ely et al., 2004; Kasashima et al., 2004; Perkins et al., 2005; Ely et al., 2009; Goodrich, 2011), and the healing process is slow and can be influenced by the management and training protocols applied on the horse after injury. This means that re-injury of the tendon could be a frequent result (up to 80%) of a wrong planning of the recovery and rehabilitation period (Dowling et al., 2000). In other words, micro-trauma and ageing may

synergistically predispose to severe tendon pathology in an adult horse (Beck et al., 2011; Goodrich, 2011). Recent proteomic studies provided molecular evidences to characterize all these observations (Dakin et al., 2014; Peffers et al., 2014).

1.6.*Tendon anatomical overview*

The digital flexor tendon sheath (DFTS) surrounds the superficial (SDFT) and deep digital flexor tendon (DDFT) palmar or plantar to the fetlock joint. The DFTS begins 4 to 7 cm proximal to the proximal sesamoid bones and extends distally to the middle third of the second phalanx. The DFTS is surrounded by the palmar/plantar annular ligament (PAL) and the proximal and distal digital annular ligament.

Just proximal to the proximal sesamoid bones, the SDFT encircles the DDFT. This ring is called the *manica flexoria*. The distal aspect of the MF is located underneath the PAL. Proximal to the MF the DDFT is attached to the DFTS by a medial and lateral band, called the mesotendon. On the palmar aspect of the fetlock, the SDFT is also attached sagittally with a mesotendon to the DFTS (Dik et al., 1995; Wilderjans et al., 2003).

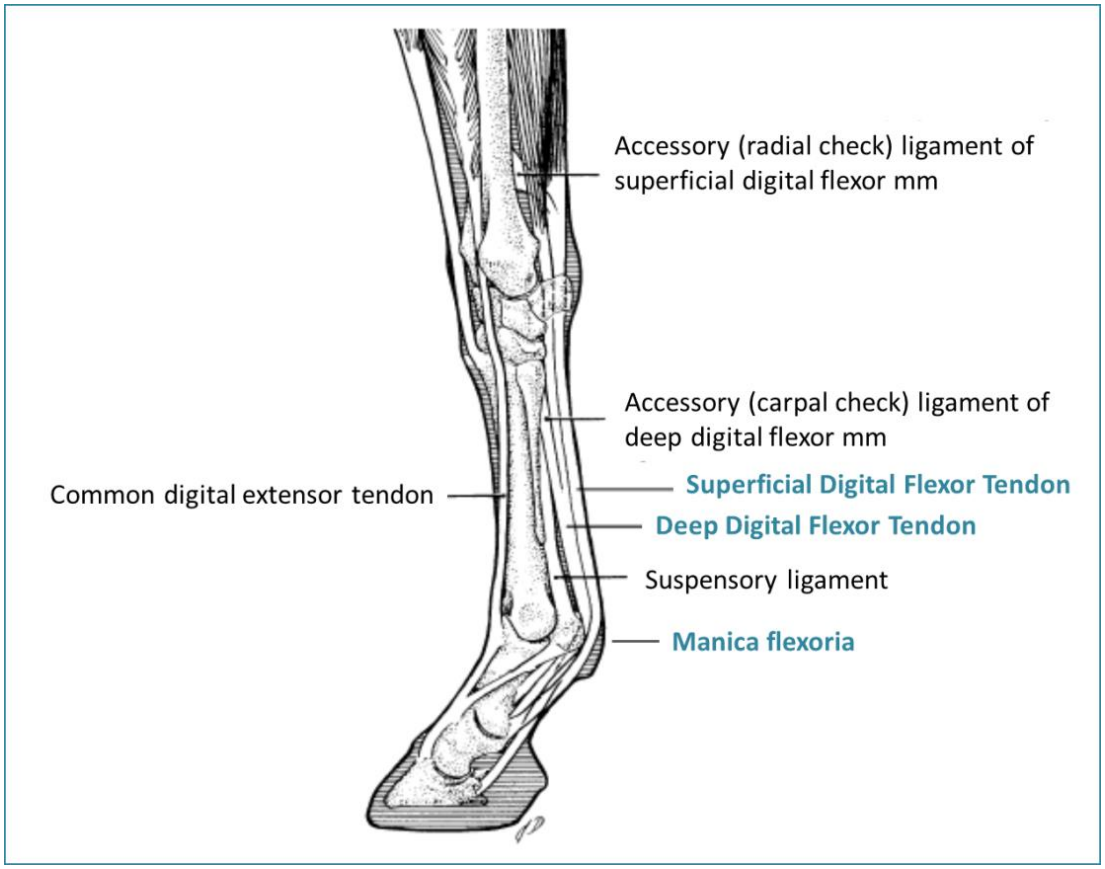

Figure 4. The normal anatomy of equine distal limb. In the image are indicated the structures mainly involved in tendinopathies (modified from Smith *et al.*, 2002).

The Superficial Digital Flexor Tendon (SDFT):

The Superficial Digital Flexor Tendon arises from its muscle at the level of the carpus where it also combines with the proximal accessory ligament. The tendon passes distally on the caudal aspect of the limb, running through the carpal canal to the metacarpus. The SDFT runs together with the DDFT in a synovial structure named carpal sheath. Just proximal to the metacarpophalangeal joint, the SDFT forms a ring-like structure called *manica flexoria* which wraps around the DDFT. From the distal metacarpus to the level of the middle phalanx, the SDFT and DDFT run together within another synovial structure named digital sheath.

At the distal end of the proximal phalanx, the SDFT divides into two branches which insert on the lateral and medial eminences of the middle phalanx. A small amount of fibres insert on the lateral aspect of the proximal phalanx (Fails and Kainer, 2011).

Lesions of SDFT range from minor partial unilateral to complete bilateral rupture. Lesions occur most frequently in the core of the mid-metacarpal (MidM) region, but can involve any site from the myotendinous junction to the branches of insertion (Patterson-Kane and Firth, 2009).

Strain maximal values have a site-specific range that is larger in metacarpal region of SDFT. In other words, different regions of the tendon have different biomechanics with different strain properties. Reported values for tendon strain at the walk range from 2.2% to 4.6%, the strain increased significantly from 2.5% to 3.2% with a rider while no significant difference was recorded in SDFT maximal strains between different shoeing. At the trot gait values for strain ranged from 4.15% to 10.1% at maximal weight bearing (Riemersma et al., 1996). At the gallop, strain values are higher and range from 11.5% to 16.6%. In vitro experiments demonstrated that 12-21% is the ultimate strain value before rupture suggesting that, at this level of exercise the SDFT works close to its physiological limits with a relatively narrow safety margin (Crevier et al., 1996; Dowling and Dart, 2005).

The Deep Digital Flexor Tendon (DDFT):

The Deep Digital Flexor Tendon arises from the three bellies of the deep flexor muscle. The main part origins from the humeral belly and it fuses with the other two parts

(ulnar and radial) to form a common tendon just proximal to the carpus on the caudal aspect of the limb. The single tendon passes distally together with the SDFT through the carpal canal. In the mid-metacarpal region the distal accessory ligament fuses with and reinforces the DDFT. At the metacarpophalangeal (MCP) joint, the DDFT passes through the *manica flexoria* becoming superficial and runs over the sesamoid groove. In the mid-region of the proximal phalanx, the DDFT runs between the branches of the SDFT and over the flexor cortex of the distal sesamoid (navicular) bone to insert on the flexor cortex of the distal phalanx. Three annular ligaments (palmar, proximal and distal) support both the superficial and deep digital flexor tendons in their distal parts (Fails and Kainer, 2011).

Injuries of the DDFT have been diagnosed alone or in conjunction with other injuries, such as lesions of the navicular bone (Dyson et al., 2003; Mair and Kinns, 2005). In a study by Dyson and Murray (2003), DDFT involvement was reported in 83% of clinical examination for foot pain, while the DDFT was considered the primary cause of lameness in 43% of pathological animals in another study (Dyson et al., 2003; Cillán-García et al., 2013). An important morphological characteristic of DDFT is its fibrocartilaginous distal dorsal layer located just proximally to the navicular bone (Blunden et al., 2006). This portion of the tendon is mostly avascular, blood supply derived from the palmar layers, the muscle and periosteal insertion and through vessels that run longitudinally in septal fascia within the digital flexor tendon sheath. These observations have suggested that vascular compromise or alteration may predispose DDFT to injury (Blunden et al., 2006; Blunden et al., 2009; Beck et al., 2011).
DDFT lesions have been classified as: core lesions, parasagittal splits, dorsal border lesions and insertional lesions. i) Core lesions are characterised by damage to the central fibres of the tendon which can measure from 5 to 135 mm in length (Blunden et al., 2006). ii) Parasagittal splits origin within the navicular bursal portion of the tendon and propagate along septal lines (Blunden et al., 2006). iii) Dorsal border lesions form in the navicular bursal portion of the tendon, often they curl up proximally in the recess of navicular bursa as strained fibres of the dorsal border of the tendon. iv) Insertional lesions are short core lesions or parasagittal splits less located close to the insertion of

the DDFT on the distal phalanx. They can occur alone or in association with other lesions in different portions of the DDFT (Blunden et al., 2009).

Tendons in the equine forelimb act mainly to position the limb correctly during locomotion. Some tendons have an additional function, acting as springs to store and release energy as they are stretched and recoiled during the stance and swing phase of each stride and so decrease the energetic cost of locomotion (Alexander, 1991). The SDFT (and SL) is the main energy storing structures in the equine forelimb, whereas DDFT do not contribute significantly to energy storage although its primary function appears to be flexion of the distal phalangeal joint during late swing (Wilson et al., 2001; Butcher et al., 2009).

An interesting observation is that during high speed locomotion, the DDFT stores little energy, but acts to stabilize the MCP joint during hyperextension. DDF muscle is more susceptible to fatigue cause of its high percentage fast twitch fibres composition, this means that, if the exercise exceeds the limit of DDF muscle resistance, the MCP joint will lose stability and consequently, the SDFT will undergo higher strain increasing the risk of fibril micro-damage (Butcher et al., 2007; C T Thorpe et al., 2010). This last observation underlines the close relation between the SDFT and DDFT that is a result of the anatomical position but also from the functional interactions.

1.7.Objectives

This side project arose from the collaboration between Professor Marco Patruno and the group of Professor Roger K. Smith and Doctor Jayesh Dudhia.
Last year of my PhD, I had the opportunity to spend three months at the Department of Clinical Sciences and Services of The Royal Veterinary College (University of London) to work with Doctor Dudhia on the extracellular matrix of tendon.
The main objective of the research was to investigate the expression and the fragmentation levels of cartilage oligomeric matrix protein (COMP) in equine tendon. The interest for this particular protein originated from recent findings that report COMP as the most abundant protein in normal ECM, second only to the collagen, that showed an increase expression in pathological situation. Moreover, specific disease stage was associated to a particular fragment of COMP. This product of COMP proteolysis was identified in vitro and in vivo by the group of Professor Smith (Dakin et al., 2014). Therefore, due to the possible implication in clinical practice, several studies has been planned to provide further information on COMP expression and cleavage products in normal and pathological tendon along with the possible influence of exercise and aging.
The research project I developed with Doctor Dudhia analysed for the first time the levels of COMP100 fragment and whole COMP expression in injury-predisposed and non-predisposed sites of normal SDFT and normal DDFT in young and old horses. Moreover, I performed the same analysis on SDFT in presence of injury (Project A).
An additional morphological study was performed on DDFT affected by naturally occurring tear lesion. I attempted to develop an analysis on three sites of the biopsy (adjacent, intermediate and remote from the injury) in order to collect data on the alterations and their grade of severity in DDFT (Project B). The main goal of this study was to deepen and reinforce the scarce information on equine injured DDFT.
The next sections will describe the two projects that were developed in collaboration with the group of London. Each section will have a short introduction followed by the detailed experimental procedures, the attained results and the preliminary considerations which were formulated. However, these projects are interesting pilot studies and, increasing the small number of analyzed samples, it will be possible to obtain important data to better understand the regeneration process of tendon.

2.PROJECT "A"

Preliminary study on COMP fragmentation level in injury-predisposed sites of Superficial Digital Flexor Tendon (SDFT) and Deep Digital Flexor Tendon (DDFT) in horse.

2.1.INTRODUCTION

The recent studies on tendon matrix composition and its alterations have shown a different proteomic profile between normal and pathological tissues and between young and old animals (Dakin et al., 2014; Peffers et al., 2014). A large number of proteins showed a variation in amount and/or in fragmentation level and cleavage site. Within these, COMP100 fragment seems to be disease-stage specific and has been proposed as useful bio-marker for possible clinical purposes (Lui et al., 2011; Dakin et al., 2014).
Therefore, the main objective of this project was to evaluate the levels of COMP fragmentation (fragment COMP100) focusing on specific regions of normal SDFT and DDFT known to be predisposed to injury.
In the following table, it is synthetized the working hypothesis for this project:

Hypothesis	
1	Injury-predisposed sites of normal SDFT and DDFT have greater levels of COMP fragmentation when compared with non-predisposed sites.
2	Tendon injury in predisposed regions of SDFT is associated with greater COMP fragmentation.
3	The difference in COMP levels between predisposed and non-predisposed sites is larger in young respect to old animals, although this difference is minor whether injured and normal SDFTs are compared.

2.2.EXPERIMENTAL PROCEDURES

2.2.1.Tendon sampling and procurement

The animals used in this study were four horses, euthanased for reasons other than tendon disease. These animals were two young Saudi horses (age: 2 and 3 years, respectively) and two old Thoroughbred horses (age: 8 and 12 years, respectively). Forelimb tendons (SDFT and DDFT) were immediately recovered post-mortem from the four animals (n=15; 7 SDFTs and 8 DDFTs, one SDFT was excluded for technical reason). Tendons which had no previous history or post-mortem evidence of tendon injury were considered normal (n=12; 4 SDFTs and 8 DDFTs). Tendons (SDFT) with previous history of diagnosed injury were included in the comparative study with the normal tendons, one was from a young animal the other two were from the two old horses[1] (n=3 SDFTs).

Superficial and deep digital flexor tendons were dissected free from cadaver limbs from the carpus to the point of insertion. The tendons were either stored entire at -80°C until further dissection procedures or divided fresh into 4 cm-thick sections. Each section has been indicated as a "level" and numbered from 1 to 7 from proximal to distal ends. Each level was subdivided in 1cm-thick slices (named a, b, c and d) that were stored at -80°C until further analysis. The sections selected for this study were the level 4, corresponding to the mid-metacarpal region (MidM, predominantly under tensional forces) and the level 7, corresponding to the metacarpo-phalangeal region (MCP, under both tensional and compressive forces). The slices "a" were chosen for the biochemical analysis performed in this project (Figure 5).

[1] The two old animals have been already used in another study performed by the group of Professor Smith in which the injured tendon were treated with bone marrow-derived mesenchymal stem cells (BM MSCs) to evaluate their effect on the healing process (Smith et al., 2013). Therefore, despite the injured tendons result in fact also treated, we considered them not-normal and thus we used them for our comparative investigation.

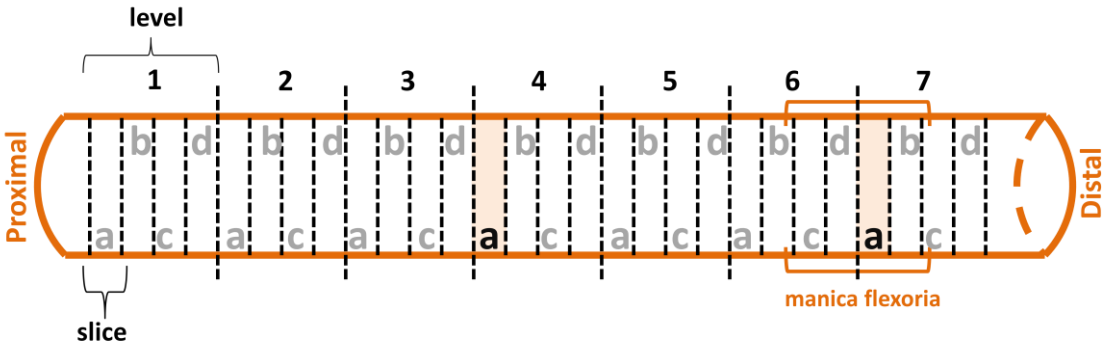

Figure 5. Schematic representation of dissection procedures of the SDFTs and DDFTs to obtain the 1 cm-thick slices used in this study (modified from original scheme gently provided by Dr. Dudhia).

For the first hypothesis (normal tendon study), level 4 (injury-predisposed) and level 7 (non-predisposed) "a" slices of normal SDFTs from three left and one right forelimbs were used to analyse and compare COMP fragmentation levels (n=4). Since the DDFTs were not injured and considered normal in all subjects, DDFT injury-predisposed and non-predisposed levels (level 7 and level 4, respectively) of both forelimbs were used to analyse and compare the COMP fragmentation levels (n=8).

For the second hypothesis (injured tendon study), level 4 (injury-predisposed) and level 7 (non-predisposed) "a" slices of SDFTs from three injured right forelimbs were used to analyse and compare COMP fragmentation levels between injured and normal (n=3).

For the third hypothesis (young VS old), predisposed and non-predisposed levels between young and old normal SDFTs (n=4) and between young and old normal DDFTs (n=8) were compared. In addition, the COMP fragmentation levels in injured SDFT of young (n=1) and old (n=2) animals comparing with the contralateral normal tendons were analysed.

Finally, a descriptive analysis on the whole COMP expression levels in the SDFT and DDFT (n=15) collected for this study was performed, reporting the observations per single subject.

2.2.2.Sample preparation and protein extraction

Each slice was grossly cut and immerged into liquid nitrogen. Afterwards, the frozen pieces were collected and rapidly powdered using a dismembrator.

For each sample, a 100 mg of powder was weighed and used for protein extraction with 4M guanidine hydrochloride. The protocol performed was as follows:

i) the sample was incubated with 1,500 µl of extraction buffer (4M Guanidine Hydrochloride, EDTA, protease inhibitors cocktail) at 4°C for 48 hours on rotating wheel;

ii) centrifuge at 13,000 rpm for 15-20 minutes at 4°C, surnatant was collected and 900 µl of precipitation buffer (cold ethanol 100%) was added, incubation at -80°C for 20 hours follows;

iii) centrifuge at 13,000 rpm for 15 minutes at 4°C, the pellet was washed and centrifuged with precipitation buffer at least 3 times;

iv) the pellet was lyophilized on a 37°C plate for 1 hour, then re-suspended in 250 µl of 0.5% SDS 50mM Tris buffer (pH 6.8).

Protein concentrations of aliquots of soluble fraction were estimated by BCA Protein assay kit (Thermo Scientific).

2.2.3.Electrophoresis and Immunoblotting

Tendon soluble extracts (10 µg) were reduced by addition of 0.1 M DTT (Dithiothreitol) and heated to 95°C for 5 minutes prior to be loaded in 8-12% Expedeon RunBlue gel (Expedeon) for one dimensional sodium dodecyl sulphate polyacrylamide gel electrophoresis (SDS-PAGE).

Electrophoresis was followed by transfer blot onto PVDF membrane (GE Healthcare, Hertfordshire, UK) for immunoblot analysis. Membranes were blocked overnight in 1X PBS 0.05% Tween20 buffer (Sigma-Aldrich) containing 10% powdered skimmed milk. After washing 5 minutes in 1X PBS 0.05% Tween20 buffer, membranes were incubated with the primary antibody diluted in the same buffer for 90 minutes. The primary antibodies used in this study were anti-COMP in rabbit (Smith, 1997) and anti-α-tubulin in mouse (Cell Signaling Tech) as house-keeping for normalization. Both primary antibodies were diluted 1:1,000 in 10X PBS 0.2% Tween20. Subsequently, membranes were washed for 2 hours changing the buffer every 15 minutes (washed 15 minutes 8

times) and incubated with secondary antibody diluted 1:50,000 in 10X PBS 0.05% Tween20 buffer for 1 hour. The secondary antibodies were HRP-linked anti-rabbit in swine (Dako) and HRP-linked anti-mouse in donkey (Cell Signaling Tech), respectively.
Antibody positive protein bands were visualized using Enhanced ChemiLuminescence (ECL) Select Western Blot Detection Reagent kit (GE Healtcare) by means through luminol-peroxide system.
The images were collected in a dark chamber (G.Box, SYNGENE) using GeneSnap software and band densities analysis was performed with AlphaEASE FC software.

The obtained density values for COMP100 fragment were divided to the values of COMP to obtain a proportion of fragmentation on the total COMP (COMP100/COMP) and acquire information on fragmentation levels in predisposed and non-predisposed sites of SDFT and DDFT. Moreover, the density values of COMP were divided to α-tubulin values to normalize the results (COMP/tubulin) and extract information on COMP expression in the analysed regions.

2.2.4.Statistical analysis

Data were expressed as ratio COMP100/COMP in the analysis of COMP fragmentation levels and as ratio COMP/tubulin in the evaluation of COMP expression.
Wilcoxon signed-rank test was performed to compare COMP fragmentation levels in L4 and L7 in normal SDFT and DDFT, and in injured SDFT; moreover, the same test was carried out to compare the levels of COMP expression between L4 and L7 in normal SDFT, in injured SDFT and in left and right DDFT.
All the statistical analyses were undertaken using STATISTICA 10 (StatSoft, USA) and Microsoft Excel 2010 (Microsoft Corporation) software. Significance level was set at 5% ($p \leq 0.05$).

2.3.RESULTS

The following section describes the results obtained from the analysis of the densitometry values. The rough optical density (OD) data of the COMP, the fragment COMP100 and the α-tubulin were organized in excel table for further elaborations.

The comparison between the L4 and L7 of SDFT and DDFT were performed using the ratio values calculated dividing the OD data of COMP100 to the OD data of COMP (COMP100/COMP) and the ratio values calculated dividing COMP data to the OD data of α-tubulin (COMP/tubulin).

Table 1 collects the ratio values (COMP100/COMP) obtained for all the samples analysed in this study for the comparison of COMP fragmentation levels. Table 2 contains the COMP100/COMP values referred to the samples obtained from injured SDFTs. Table 3 shows the ratio values (COMP/tubulin) used in the evaluation of COMP expression in the sites of interest.

		COMP100/COMP			
Animals	Age (years)	SDFT (n=4)		DDFT (n=8)	
		L4	**L7**	**L4**	**L7**
Young 1	2	0.103	0.093	0.069	0.202
Young 2	3	0.244	0.080	0.091	0.124
Old 1	8	0.218	0.260	0.091	0.111
Old 2	12	0.228	0.117	0.133	0.142
mean		0.198±0.06	0.138±0.08	0.096±0.03	0.145±0.04

Table 1. Values of COMP100/COMP ratio at L4 and L7 of normal SDFT and DDFT referred to each animal included in the study, and the mean values for the levels taken singularly.

		COMP100/COMP	
Animals	Age (years)	SDFT inj (n=3)	
		L4	**L7**
Young 1	2	0.165	0.050
Old 1	8	0.185	0.076
Old 2	12	0.064	0.103
mean		0.138±0.06	0.076±0.03

Table 2. Values of COMP100/COMP ratio at L4 and L7 of injured SDFT referred to each animal included in the comparison with the contralateral (normal) SDFT, and the mean values for the levels taken singularly.

		COMP/tubulin							
Animals	Age (years)	SDFT				DDFT			
		left		right		left		right	
		L4	**L7**	**L4**	**L7**	**L4**	**L7**	**L4**	**L7**
Young 1	2	3.769	2.434	6.005	3.796	10.80	9.832	11.97	5.560
Young 2	3	9.842	4.490	/	/	1.153	3.429	1.563	2.931
Old 1	8	5.549	10.60	5.166	8.005	10.96	9.112	3.351	11.90
Old 2	12	1.156	10.00	21.45	1.433	6.226	1.967	2.212	1.658

Table 3. Values of COMP/tubulin ratio at L4 and L7 of SDFT and DDFT referred to each animal included in the study.

2.3.1.Comparison of COMP fragmentation levels between L4 (predisposed) and L7 (non-predisposed) sites of normal SDFT

In Figure 6, the COMP fragmentation levels in L4 versus L7 of normal SDFT are graphically reported coupling the values for each single horse (histogram A).

In the histogram, young1 horse shows COMP fragmentation level in L4 barely larger than L7 whereas in young2 horse COMP fragmentation level is clearly larger in L4 versus L7. Old2 horse shows the latter pattern (L4 clearly larger than L7), while in old1 horse COMP fragmentation levels seem larger in L7 than L4.

Nevertheless, whether the mean value of COMP100/COMP ratios are taken, the new graphical representation of fragmentation levels is shown in histogram B of Figure 6. When the individual-effect is deleted, COMP fragmentation levels in L4 is larger than L7. However, statistically there was no significant difference between L4 and L7 levels in normal SDFT ($p = 0.27$).

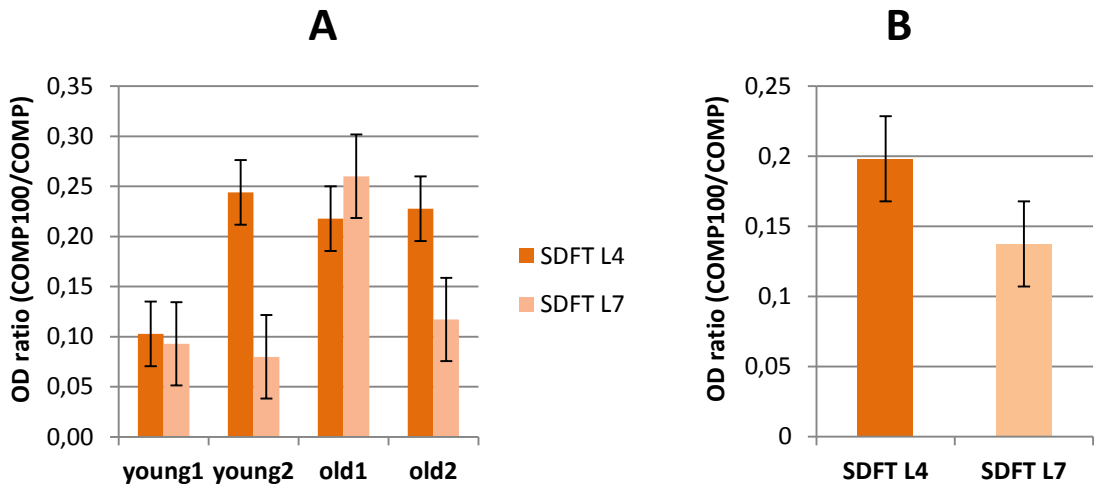

Figure 6. Graphical representation of COMP fragmentation levels in the predisposed (L4) and non-predisposed (L7) sites of normal SDFT referred to each animal included in the analysis (A) and to mean values (B).

2.3.2.Comparison of COMP fragmentation levels between L7 (predisposed) and L4 (non-predisposed) sites of normal DDFT

Figure 7 shows graphically the COMP fragmentation values for DDFT at L4 and L7 in all animals (histogram A) and the mean values of the predisposed (L7) and non-predisposed (L4) sites (histogram B).

In both graphs, the levels of L7 are larger than the levels of L4. The difference is clearer in young1 horse respecting the other horses (young2, old1 and old2). The histogram B synthetizes the general pattern with L7 higher than L4, even though there was no statistical significance (p = 0.06).

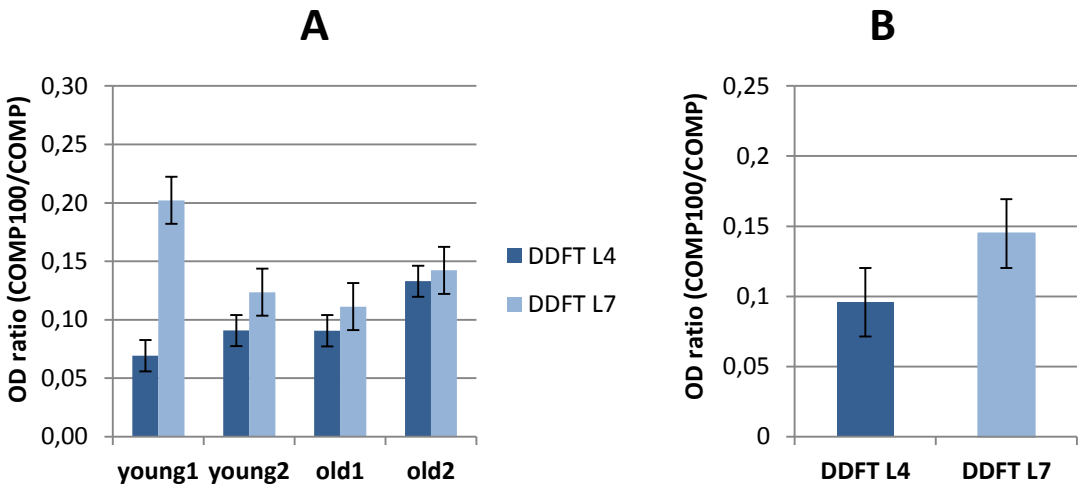

Figure 7. Graphical representation of COMP fragmentation levels in the predisposed (L7) and non-predisposed (L4) sites of normal DDFT referred to each animal included in the analysis (A) and to mean values (B).

2.3.3.Comparison of COMP fragmentation levels between L4 (predisposed) and L7 (non-predisposed) sites of injured SDFT

The COMP fragmentation levels of injured SDFT at L4 and L7 are graphically represented in the histogram A of Figure 8, whereas the corresponding normal SDFT are represented in histogram B. Although these two graphs show a variable pattern if the animal are considered singularly, the histogram with the media values (histogram C) displays L4 levels larger than L7 levels in both injured and normal samples. However, statistical analysis has found no statistically significance between L4 and L7 in injured SDFT ($p = 0.28$).

In addition, the differences of the COMP fragmentation levels between L4 and L7 of injured SDFT and normal SDFT were calculated (mean differences = 0.061592 and 0.026103, respectively). The histogram D of Figure 8 shows graphically that the difference of the injured samples was larger than the difference of normal SDFT.

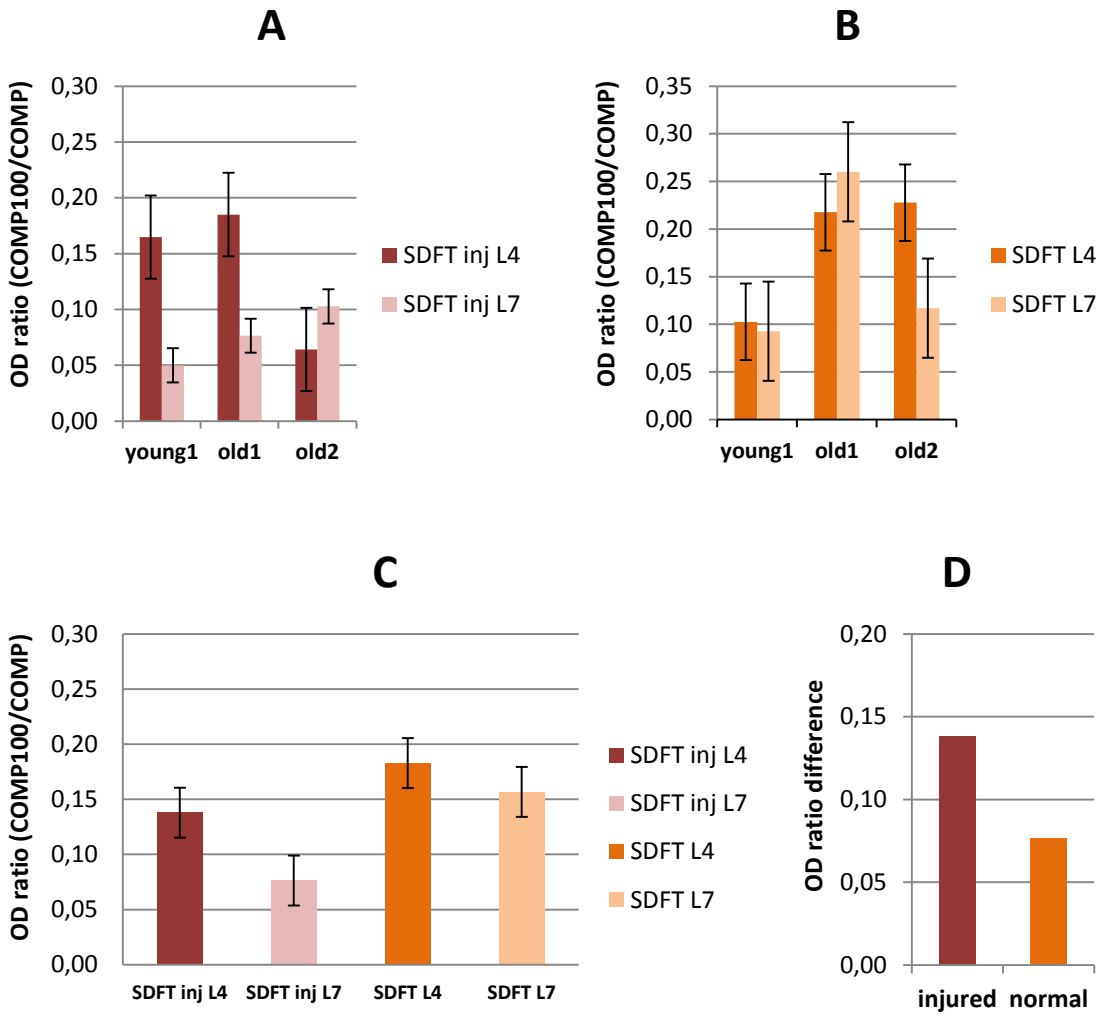

Figure 8. Graphical representation of COMP fragmentation levels in the predisposed (L4) and non-predisposed (L7) sites of injured SDFT (A) and normal SDFT (B) referred to each animal included in the analysis. (C) graphical representation of mean values of both injured and normal L4 and L7. (D) differences between L4 and L7.

2.3.4.Comparison of COMP fragmentation levels at L4 and L7 between young and old animals

Figure 9 shows the COMP fragmentation levels in L4 and L7 for young versus old horses in SDFT (histogram A) and in DDFT (histogram C), respectively. Grouping the animals in young and old revealed no differences in the pattern of COMP fragmentation levels: L4 has higher levels than L7 in SDFT and vice versa L7 has higher levels than L4 in DDFT.

The differences of the COMP fragmentation levels between L4 and L7 for all the groups were calculated. The difference obtained for young animals was compared to the difference for the old subjects (mean differences of SDFT = 0.087038 and 0.034241, respectively; mean difference of DDFT = 0.082840 and 0.014995, respectively). Histograms B and D of Figure 9 show graphically that the difference of the young samples is larger than the difference of old samples in both SDFT (B) and DDFT (D).

In addition, differences between L4 and L7 in young and old injured SDFT were calculated. Figure 10 shows graphically the results of the comparison of the differences (L4-L7) between non-injured ("normal") and injured samples. It can be noted a slightly larger difference in presence of injury in young subjects (Figure10, histogram A), whereas there is no variation in the old animals (Figure 10, histogram B).

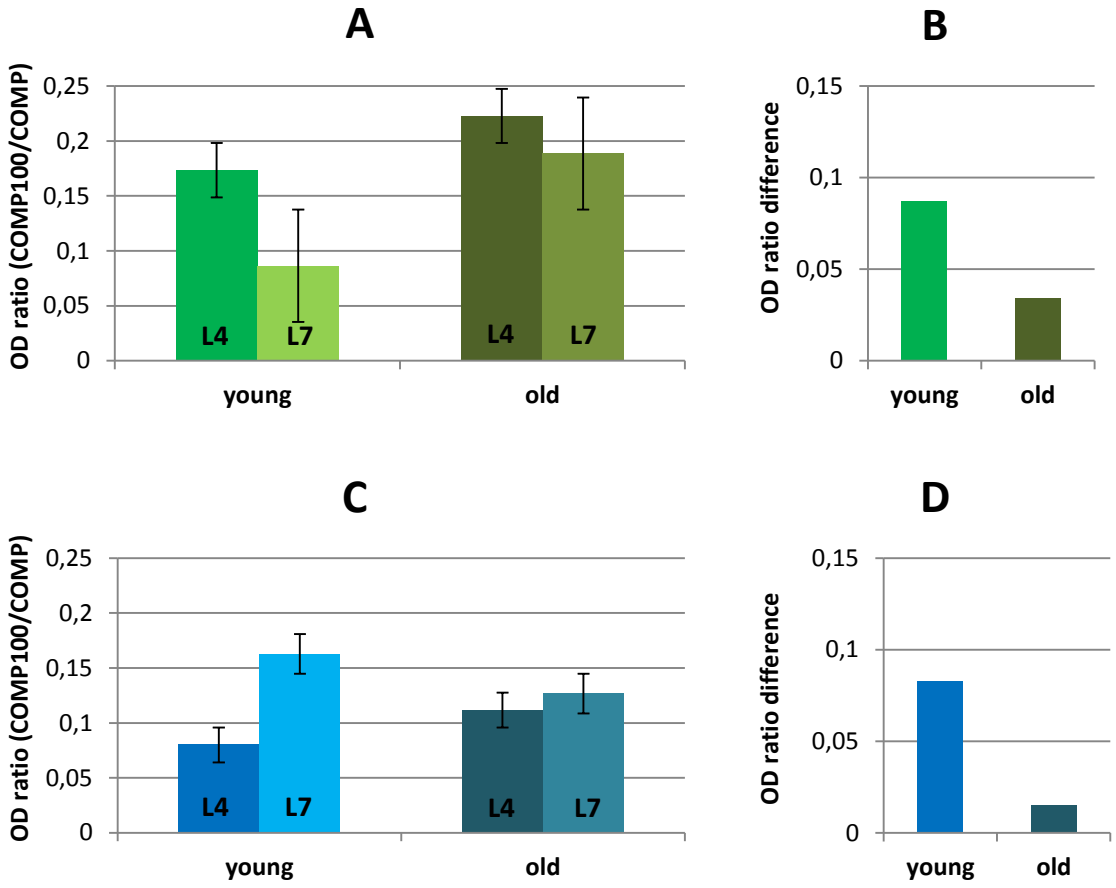

Figure 9. Graphical representation of COMP fragmentation levels in L4 and L7 sites of young versus old horses. (A) normal SDFT samples, (B) differences between L4 and L7 in young versus old SDFT samples. (C) normal DDFT samples, (D) differences between L4 and L7 in young versus old DDFT samples.

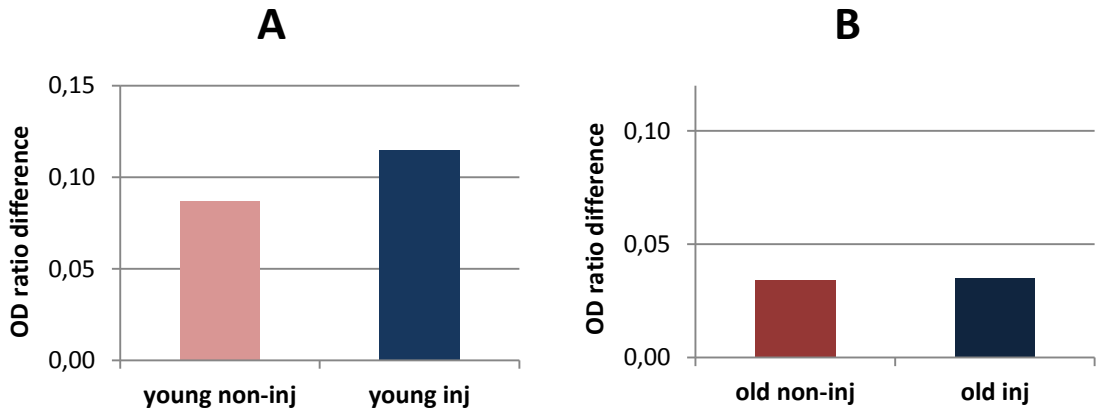

Figure 10. Graphical representation of differences between L4 and L7 in non-injured (normal) versus injured samples in young (A) and old (B) animals.

2.3.5.Evaluation of whole COMP expression in L4 and L7 sites of SDFT and DDFT

Figure 11 shows the values of whole COMP expression in L4 and L7 sites of normal SDF and DDF tendons (COMP/tubulin). Only left DDFT values were chosen for the comparison whereas the right DDFT values were used in the comparison with injured SDFT values (Figure11).

COMP expression levels were greater in SDFT L4 versus L7 in young animals while in old animals COMP was lower in SDFT L4 versus L7 (histogram A). Regarding the left DDFT, COMP expression was greater in L7 versus L4 only in young 2, while L4 has a larger level of COMP expression in the other subjects.

The histograms of Figure 12 show the values of COMP expression in L4 and L7 sites of the injured SDFTs (A) and the right DDFTs (B), thus mean tendons from the same leg.

The COMP expression levels were greater in SDFT L4 versus L7 in young1 and old2 whereas in old1, L7 was greater than L4 in association with the presence of an injury in the site (histogram A). Regarding the right DDFTs, COMP expression was greater in L7 versus L4 only in old1, while L4 had a larger level of COMP expression in the other two subjects, more clear in young1.

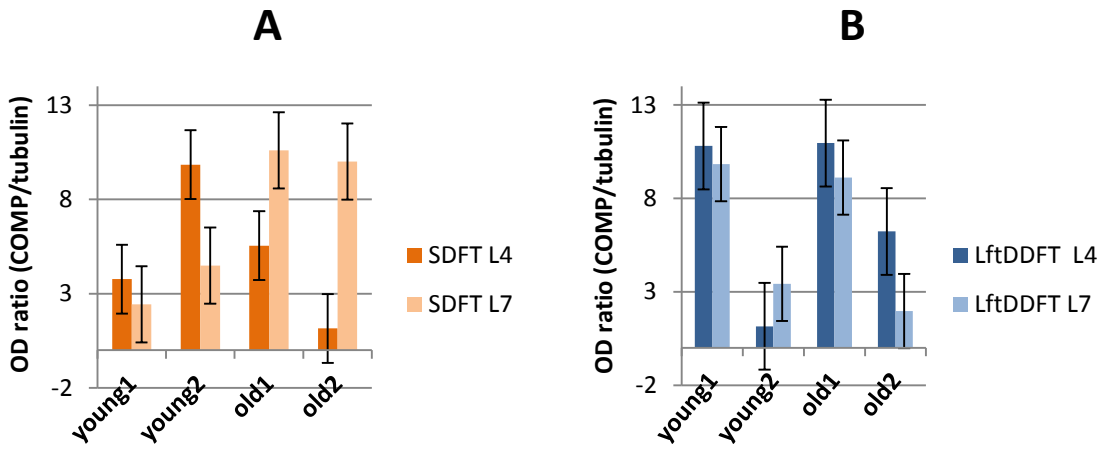

Figure 11. COMP expression in L4 and L7 sites of normal SDFT (A) and left DDFT (B). The COMP values were expressed as ratio to the α-tubulin values to normalize the results.

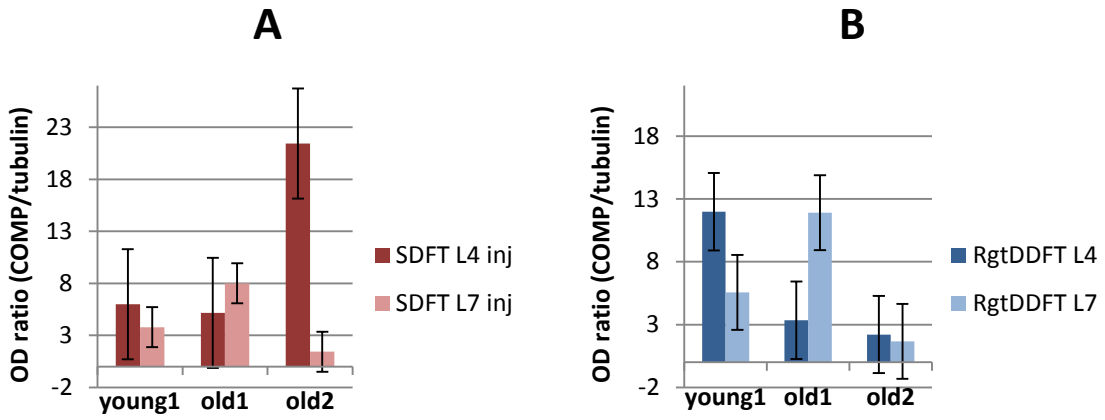

Figure 12. COMP expression in L4 and L7 sites of injured SDFT (A) and right DDFT (B). The COMP values were expressed as ratio to the α-tubulin values to normalize the results.

2.4.DISCUSSION

This project was focused on particular tendon regions well-known to be injury-predisposed. Recent proteomic studies provide a wider protein profile considering the whole SDF tendon (Dakin et al., 2014; Peffers et al., 2014). The work presented here was a further preliminary novel investigation on COMP expression and fragmentation in predisposed sites of the SDFT and DDFT.

In the normal tendons examined in this study, higher trends of COMP fragmentation in predisposed sites of SDFT and DDFT (L4 and L7, respectively) were observed. This supported and proved the first hypothesis showing that injury-predisposed site has greater levels of COMP fragmentation when compared with non-predisposed site.
Level peaks were observed in L4 of young2 and L7 of old1 in normal SDFTs, while a peak was noted in L7 of young1 in DDFT. Probably, these observations were a consequence of an injury that was not diagnosed during the clinical evaluation or a macroscopic alteration not evident before the tissue collection.
In the analysed injured SDFT, the observed trend was similar to the normal situation with larger level of fragmentation in predisposed sites. Interestingly, the gap between the predisposed (L4) and non-predisposed (L7) sites seemed larger in presence of lesion in the predisposed site. This proved the second hypothesis that supposed an association between presence of an injury and greater COMP fragmentation.
In order to evaluate the possibility of an age influence on the observed trends of COMP fragmentation levels, a descriptive analysis was attempted on young animals separately from old animals. The most interesting observations were that young animals showed larger gap between the COMP levels of L4 and L7 in both normal SDFT and DDFT suggesting a greater fragmentation and consequently an higher re-modelling activity in young tissue in predisposed sites. In presence of injury, young or old did not show larger differences when compare to the corresponding non-injured tendon. However, young animals showed again a larger gap between L4 and L7 in comparison with the old animals. This observation disproved the third hypothesis in which a smaller gap

between the two sites was expected in young animals where the COMP fragmentation levels have been reported physiologically higher.

The observations reported on the whole COMP expression level revealed a particular trend in which young animals showed more COMP at L4 and old animals at L7 in normal SDFT. In the homolateral DDFTs (left), COMP seemed to be more express in L4 in all samples except for young2. Therefore, COMP was more expressed in young animals in injury-predisposed site of SDFT suggesting a possible important role of this protein in the functionality of the tendon. Indeed, in the old animals COMP was relatively less expressed in L4. This may lead to a major risk of lesion in this site in accordance with the studies that reported a greater probability of injury in old animals and with the findings on the proteomic profile alterations with age (Clayton and Court-Brown, 2008; Peffers et al., 2014).

Interestingly, the peaks of COMP expression observed in injured SDFT showed a perfect match with the presence of lesion at the site with high levels. Therefore, young1 with lesion at L4 had a peak of COMP expression at L4 site whereas old1 subject had the peak at L7 corresponding to the site of diagnosed injury and old 2 showed an extreme peak at L4 site where a severe lesion were diagnosed. An intriguing correspondence was found between the high COMP expression levels of SDFT and the high levels of DDFT.

Taken all together, the last descriptive observations may suggest that the presence of a lesion stimulate an increase in COMP production and it is well established that non-collagenous proteins content in the ECM shows a general augmentation. Moreover, the corresponding high levels of COMP in the same levels of injured SDFTs and normal DDFTs may be explained proposing a possible effect of the lesion not only on the tendon physically affected but also on the homolateral non-affected tendon. It will be interesting to deepen these observations with the aim of investigating the effect of altered biomechanisms and the compensatory response of the tendon tissue non directly affected by an injury.

The small size sample was certainly a limit of this research, although the observations of this study were in agreement with the mentioned recent proteomic findings in which

a larger number of samples was used (Dakin et al., 2014; Peffers et al., 2014). In particular, this research provided the first evidence that COMP fragmentation is physiologically greater in predisposed sites of tendon both in SDFT and in DDFT (L4 and L7, respectively) when compared with a non-injured site. This fact may indicate a more reactive tissue in sites that are more subjected to mechanical stress. Consequently, the tissue results to have higher adaptive characteristics maintaining a certain grade of re-modelling activity.

The greater fragmentation levels in SDFT predisposed sites seemed further increased when a lesion was present in the site supporting that pathological situation causes a major activation of proteolytic enzymes (Dickinson et al., 2003; Hosaka et al., 2010) and a consequent increase of COMP fragments. Furthermore, the whole COMP expression was greater in predisposed sites with injury whereas in physiological situation showed an age-dependent trend. The considerations on the age effect on COMP fragmentation are limited cause of the small size sample although it is interesting to note the general lower differences in old animals that suggest less reactive tissue.

2.5.CONCLUSIONS and FUTURE PERSPECTIVES

Despite the fact that the small size sample of this study did not provide a statistical significance, the evidences reported on COMP fragmentation resulted interesting as platform for further and larger size investigations.

This project was the first that focussed on specific injury-predisposed sites of SDFT and DDFT. The preliminary results obtained herein need to be reinforced and integrated increasing the size of the sample. However, these observations seem to be in accordance with the recent investigations and might be a starting point and an inspiration for future steps of research. Indeed, the data collected provided an intriguing view of COMP100 fragment levels supporting the studies that suggesting COMP100 as bio-marker for tendinopathies. In addition, the evaluation of whole COMP expression and COMP fragmentation in SDFT and, for the first time, also in DDFT provided preliminary results that open new interesting possible physiological implication of COMP and clinical applications of the evaluation of COMP fragmentation level.

3.PROJECT "B"

Morphological comparison between maximum injured site and remote site of DDFT naturally affected by tear-type injury. A pilot study.

3.1.INTRODUCTION

Magnetic resonance imaging (MRI) and Computer tomography (CT) diagnostic technologies facilitated the investigation of equine DDFT. Since the introduction of this procedures in the clinical practice, the interest in DDFT and in its alterations notably increased. The main motivation of this interest is correlated to the implication that DDFT lesions have on foot pain and SDFT injuries (Blunden et al., 2006; Butcher et al., 2007). Moreover, equine DDFT shows structure and biomechanics similar to human rotator cuff, therefore it might be an interesting comparative model to study (Lui et al., 2011). Several studies investigated the histopathological features of different type lesions in DDFT. However, the actual state of art is non-homogeneous and there are scarce information on the effects of tear-type injury within the equine DDFT.

Therefore, the objective of this study was to further characterize the morphology of DDFT in presence of naturally occurring tear-type injury through the histopathological evaluation of the tendon tissue surrounding and far from the lesion.

The following table synthetizes the working hypothesis of the project:

Hypothesis	
1	The tendon tissue near the lesion site is characterized by alteration of the cellularity, the matrix composition and vascularization. These alterations influence also the tissue far or remote from the tear site.

3.2.EXPERIMENTAL PROCEDURES

3.2.1.Samples and preparation of the serial slides

Two bioptic samples from two different DDFTs were used in this study and named CASE1 and CASE2. Both the biopsies contain the region of tear-type injury and tendon tissue without macroscopic evidences of alteration. Figure 13 shows the macroscopic sections of the original biopsies and indicates the two parts compared in this study: one containing the tissue surrounding the lesion (maximum injured site -In-) and the other containing the tissue distant from the injury site (remote site -Rm-).

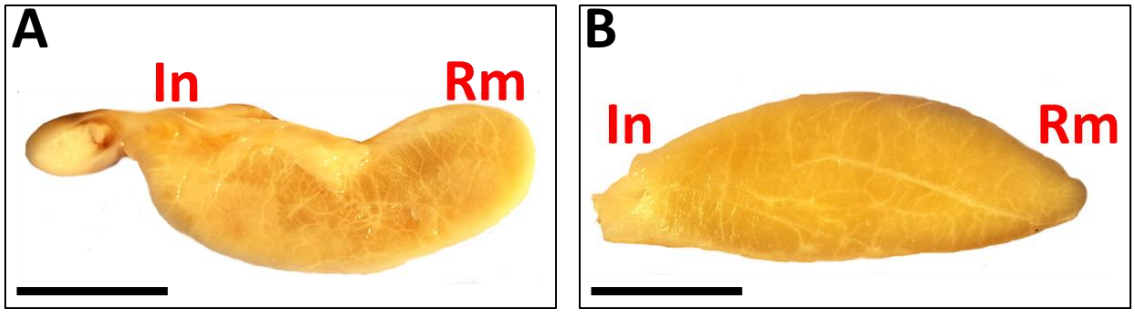

Figure 13. Transverse view of the whole biopsies of CASE1 (A) and CASE2 (B). "In" indicates the maximum injured site which contains the tear. "Rm" is the site distant from the injury or remote site and shows no macroscopic alterations. Scale bar = 1cm.

Smaller pieces including In or Rm site were obtained from the whole biopsies. These small tissue samples went under softening process which consisted in placing the tissue in a solution made of 2 parts of 4% phenol (Sigma-Aldrich) and 1 part glycerol (VWR) for two weeks. The sample had been rinsed gently in running tap water and placed back into formalin before going under long dehydration process. Finally, the samples were embedded in wax in the desired orientation. Serial 7µm-thick sections were cut at the microtome, mounted on microscope slides and used for histological and immunohistochemical studies.

3.2.2.Histology and immunohistochemistry

Morphological analysis has been displayed using histological techniques such as hematoxylin-eosin (H&E) staining and Masson trichrome staining. Moreover, immunohistochemical protocols were performed using antibodies against cartilage oligomeric matrix protein (COMP), collagene type I (Coll1) and collagene type III (Coll3).

Table 4 reports the staining protocols used in this study. HIC protocol included always a negative control and it was the same for all three antibodies. The dilution is indicated in brackets in the first column.

The sections series obtained for both cases were divided in three level groups according to their proximity to the injury. The "a" level contained the sections more adjacent to the lesion and corresponding to the maximum injured site. The slides with sections collected further in the "In" site were considered "b" level group and slides from the remote site corresponded to "c" level.

Consequently, four slides per staining have been prepared for the following sample: i.Case1 maximum injured site (a); ii.Case1 intermediate site (b); iii.Case1 remote site (c); iv.Case2 maximum injured site; v.Case2 intermediate site (b); vi.Case2 remote site (c).

Stained sections were imaged at the same magnification (20x) using D-Sight slide scanner and software (A.Menarini diagnostic, Firenze, Italy) to obtain from four to eight images. Each image was evaluated for cellularity, vascularity and extracellular matrix organization based on the system described in Table 4 [Movin, 1997; Smith, 2013]. Scores referring to each image were combined for each variable to give a general panel for each sample.

In addition, stained sections were imaged at 0.5x, 10x and 20x magnification to analyse the general histopathological appearance and to evaluate the expression of matrix components. To obtain semi-quantitative data, stain intensity comparison between HIC sections (CASE1In versus CASE1Rm and CASE2In versus CASE2Rm) was displayed using ImageJ 1.47v software (Wayne Rasband, NIH, USA).

Staining	Protocol
H&E	1.Dewax in xylene (3x5min); 2.Rehydrate in alcohol 2x100%>1x95%> 1x70% (5min each), rinse in deionized water; 3.Stain 1x12min in haematoxylin, rinse 1x3min in deionized water, rinse 1x5min in running tap water, dip few seconds in HCl-ethanol (1/70), rinse 1x3min in deionized water; 4.Stain 1x40 seconds Eosin, de- hydrate in alcohol 2x95%>2x100% (3min each), 3x5min in xylene; 5.Mount slides and dry ON in the hood.
Masson trichrome [HT15; Sigma, Milan Italia]	1.Dewax in xylene (3x5min); 2.Rehydrate in alcohol 2x100%>1x95%> 1x70% (5min each), rinse in deionized water; 3.Stain 1x15min in Bouin's Solution at 56°C, cool slides in tap water and wash 1x5min in running tap water; 4.Stain 1x10min in haematoxylin, wash 1x5min in running tap water, rinse in deionized water; 5.Stain 1x5min in Biebrich Scarlet-Acid Fucshin, rinse in deionized water; 6.Place slides 1x5min in Phosphotungstic/phosphomolybdic Acid Solution, 1x5min in Aniline Blue Solution, 1x2min in 1% Acetic Acid; 7.Rinse in deionized water, de- hydrate in alcohol 2x95%>2x100% (3min each), 3x5min in xylene, mount slides and dry ON in the hood.
HIC anti-COMP [ab74524; Abcam, polyclonal in rabbit, 1:100]	1.Dewax in xylene (3x5min); 2.Rehydrate in alcohol 2x100%>1x95%> 1x70% (5min each), rinse in deionized water and in PBS; 3.Block 1x45min in 3%BSA-PBS; 4.Incubate primary antibody ON; 5.Wash 3x5min in PBS; 6.Incubate 60min with secondary antibody conjugated with biotin (diluted 1:200); 7.Wash 3x5min in PBS; 8.Incubate 60min with ABCkit (Avidin-Biotin Complex, Vector); 9. Wash 1x5min in PBS; 10.Stain with DAB (3, 3'diaminobenzidine, Vector) from 45seconds till 1min and 45seconds depending on the signal; 11.Rinse in deionized water, dehydrate in alcohol 2x95%>2x100% (3min each), 3x5min in xylene, mount slides and dry ON in the hood.
HIC anti-Coll1 [C2456; Sigma, monoclonal in mouse, 1:500]	
HIC anti-Coll3 [C7805; Sigma, monoclonal in mouse, 1:500]	

Table 4. Synthetic explanation of staining protocols used in Project B.
[HIC = immunohistochemistry; ON = over-night; PBS = phosphate buffered saline; BSA = bovine serum albumin].

Score type	Appearance	Description
Cellularity		
0	**normal**	Presence of flattened cells in linear pattern between fibres
1	**slightly abnormal**	Some rounded cells present, slight increase in cellularity
2	**abnormal**	Many rounded cells present, obvious increase in cellularity
3	**markedly abnormal**	Mostly rounded cells present, much higher numbers
Vascularity		
0	**normal**	Presence of some vascular bundles parallel to collagen fibres
1	**slightly abnormal**	Slight increase in number of vascular bundles
2	**abnormal**	Increased number of vascular bundles
3	**markedly abnormal**	Large increase in number of vascular bundles
Organization		
0	**normal**	Parallel collagen fibres of similar widths
1	**slightly abnormal**	Some loss of fibre organization, some loss of linearity
2	**abnormal**	Moderate loss of fibre organization, few linear regions
3	**markedly abnormal**	Total loss of organization, no linear fibres
Crimp		
0	**normal**	Regular crimp angle and parallel spacing of fibres
1	**reduced**	Irregular crimp angle and spacing
2	**absent**	Poorly defined crimp angle or absent

Table 5. Scoring system utilized in the assessment of cellularity, matrix organization and vascularity in the histological sections (modified from Smith *et al.*, 2013).

3.3.RESULTS

3.3.1.Morphological analysis with scoring table

Figure 14 summarizes graphically the results obtained from the scoring assessment performed on CASE1. The maximum injured site had highest scores at "a" level for all the parameters considered (cellularity, vascularity, organization and crimp) indicating severe situation in the tendon tissue immediately adjacent to the tear-type lesion. The "b" level of the injured site had lower organisational and crimp scores although high scores for cellularity and vascularity were observed when compared with the "a" level suggesting a tendon tissue still reactive but with a structural pattern closer to normal tissue. The remote site ("c" level) showed the lowest scores indicating normal situation. Figure 15 shows CASE1 representative micro-sections of the three levels which the scoring analysis was performed on.

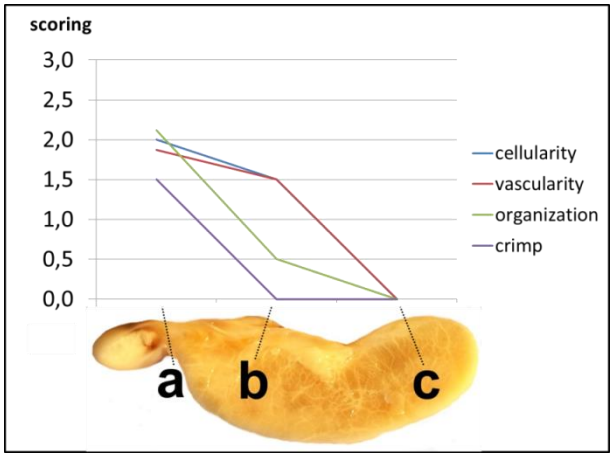

Figure 14. Scoring results for CASE1 collected at three levels: (a) maximum injured site, (b) intermediate site and (c) remote site. Scoring values referred to Table 5.

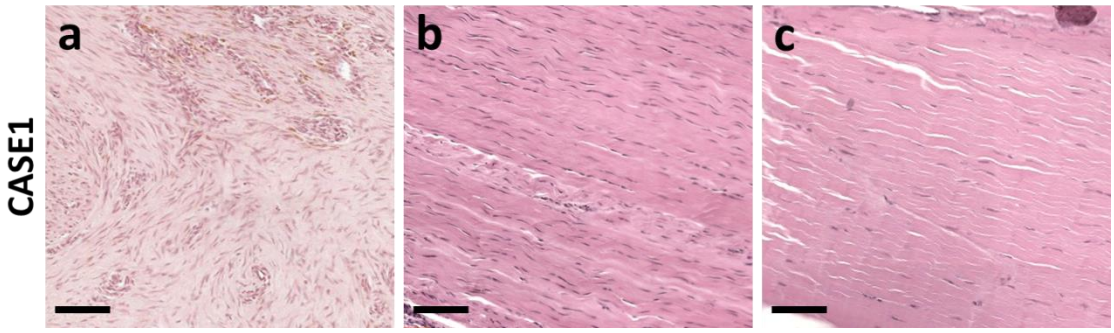

Figure 15. Representative micro-sections of CASE1 analysed in the scoring assessment: (a) maximum injured site, (b) intermediate site and (c) remote site. Scale bar = 100µm.

The scoring analysis performed on CASE2 showed an extremely high organisational score and high values for cellularity and crimp at level "a" (maximum injured site). On the contrary, level "b" had score 0 for all the parameters considered indicating a normal situation in a region not far from the injury site but closer to the core of the tendon. The remote site had a slightly higher cellularity, organization and crimp scores compared to the intermediate site. Vascularity parameter maintained low scores in all levels indicating a poorly vessels presence throughout the whole tendon cross-section (Figure 16).

Examples of the histological appearance of the three levels are given in Figure 17.

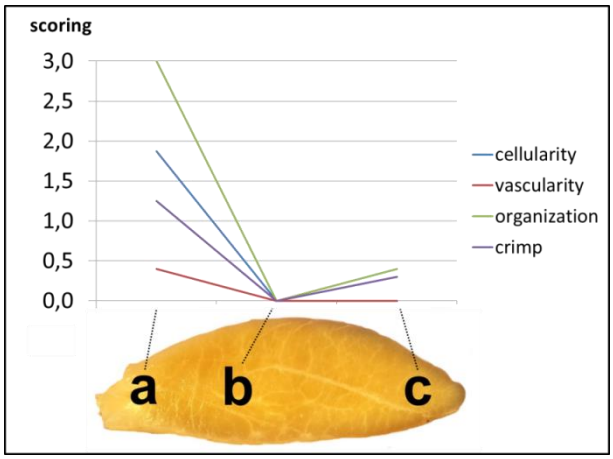

Figure 16. Scoring results for CASE2 collected at levels (a) maximum injured site, (b) intermediate site and (c) remote site. Scoring values referred to Table 5.

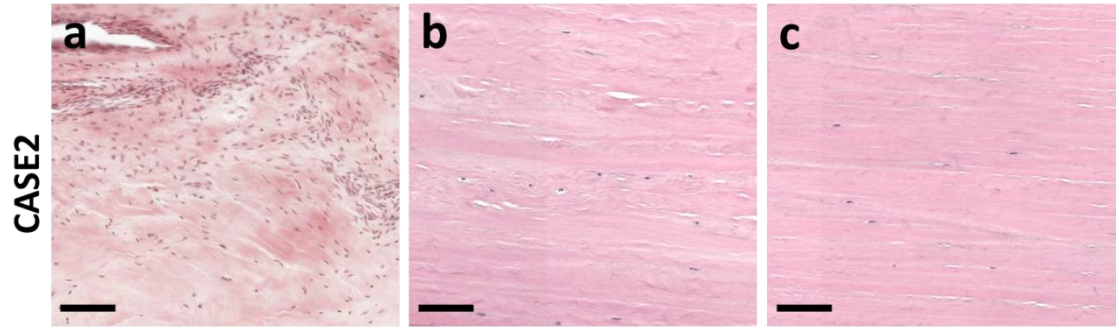

Figure 17. Representative micro-sections of CASE2 analysed in the scoring assessment: (a) maximum injured site, (b) intermediate site and (c) remote site. Scale bar = 100µm.

3.3.2.Histopathological findings

The images collected from the maximum injured site sections in both cases showed the typical features of pathologic tendon. H&E and Masson trichrome revealed increased vascular density, increased thickness of synovial lining with blood vessels infiltration and increased number of fibroblast-like cells with plump nuclei. Moreover, high level of disorganization in the extracellular matrix (ECM) with collagen fibrils fragmented and irregularly aligned, presence of fibrocartilagineous metaplasia and oedema within the ECM were observed (Figure 18). Interestingly, CASE1 showed dramatic hypervascularisation whereas CASE2 was characterized by poor vessels presence. At the same way, CASE2 showed extreme levels of matrix disorganization and degeneration whereas CASE1 had no degeneration areas and the matrix disorganization was consequent to higher vascular density.

The Masson trichrome staining made an intriguing distinction between the maximum injured sites uniformly stained in blue and the remote sites that assumed also the red coloration (Figure 19). The Rm sections of CASE1 showed an irregular spotted red coloration probably due to artefacts. At the contrary, the Rm of CASE2 had a more homogeneous red stain, especially in the lower part of the section. The upper part stained in blue and showed microscopically damaged tissue.

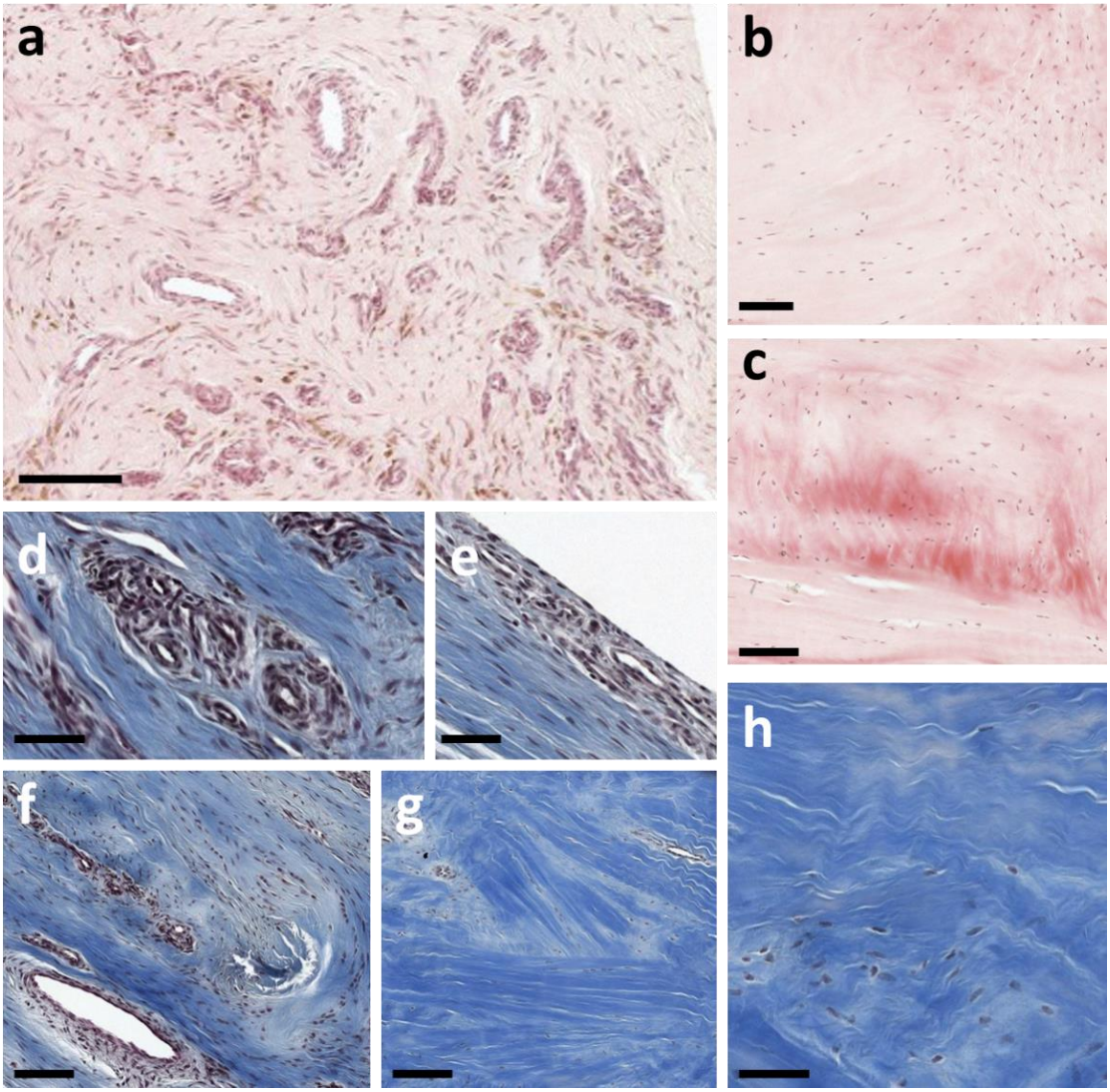

Figure 18. Representative microscopic images from maximum injured site of the two cases. H&E: (a) hypervascularization; (b) and (c) cells with plump nuclei, ECM metaplasia and oedema. Masson trichrome: (d) cluster of vessels; (e) increased thickness and vessel infiltration in the synovial lining; (f) degenerated area, hypervascularization and increased cell number; (g) and (h) high level of matrix disorganization, crimp pattern is usually regular but the orientation of fibrils is irregular. Scale bar = 100μm (a,b,c,f,g), 50μm (d,e,h).

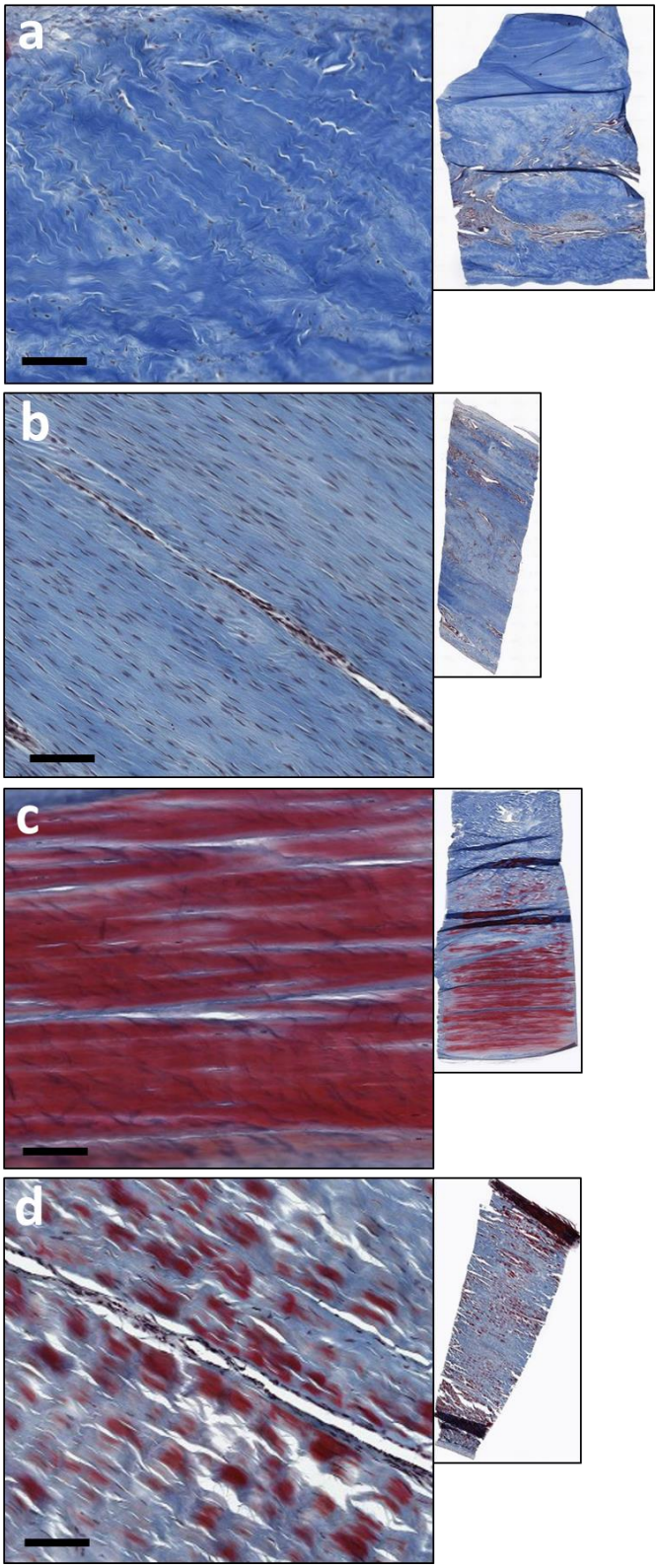

Figure 19. Masson trichrome staining of CASE1 (left) and CASE2 (right). (a) and (b), maximum injured site sections appear completely blue; (c) and (d), the remote site sections stain with red colour, the areas that remain blue area associated to tissue damage or artefacts. Scale bar = 100µm. The images of whole sections are 0.5X magnification.

3.3.3.COMP and Collagens expression

The subjective evaluation of IHC stain intensity was supported by the use of an imaging software with the aim of obtaining semi-quantitative measurements for a comparison.

In CASE1, the immunostaining for all three antibodies used in this study showed a relative higher intensity in the maximum injured site sections than the corresponding remote site sections. In particular, COMP antibody seemed to localize diffusely in the matrix in both sites although in injured site the higher intensity suggested a possible increase in quantity. Type I and III collagens antibodies showed a labelling clearly diffuse in the matrix and in the nuclei in the "In" sections, whereas the labelling was primarily limited to the nuclei in the Rm sites. Only for type I collagen, there was a diffuse light staining in the matrix of this site.

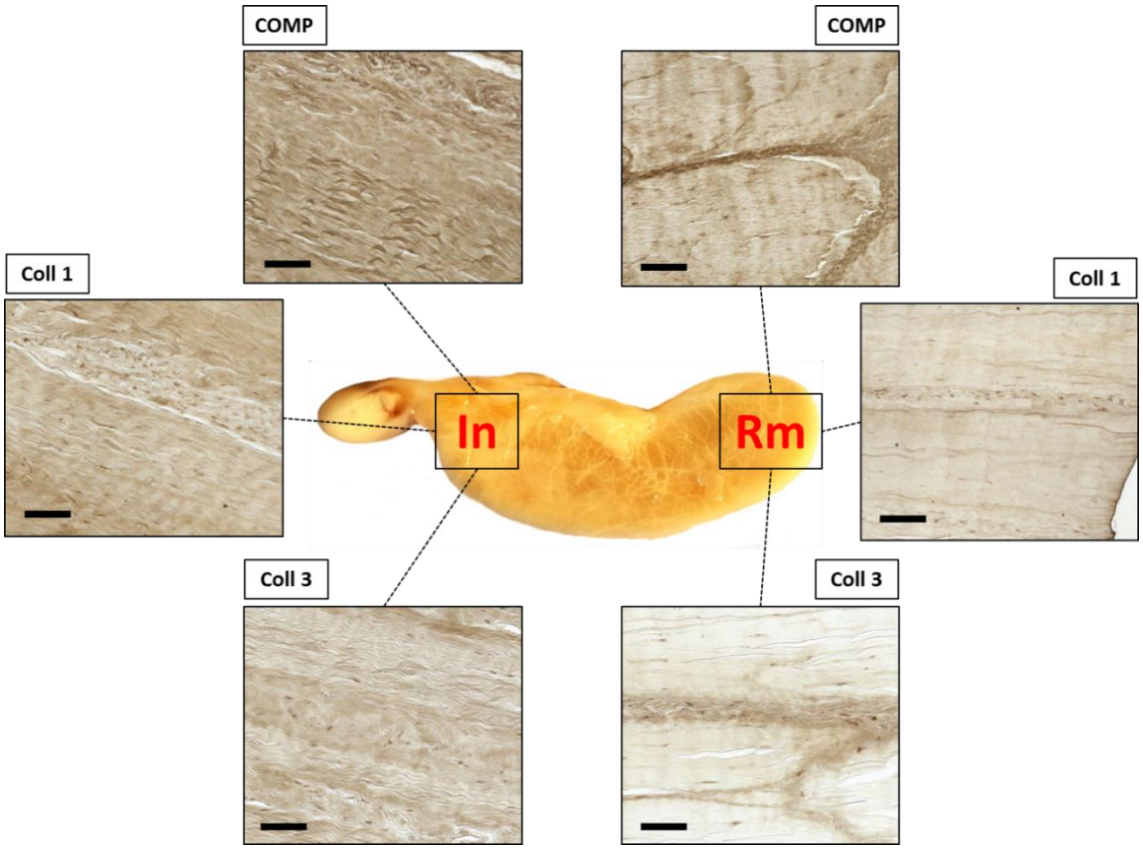

Figure 20. Representative IHC staining for Cartilage Oligomeric Matrix Protein (COMP), Collagen I (Coll1) and Collagen III (Coll3) in CASE1. The three images on the left were taken in the maximum injured site (In), the three on the right were sections from the remote site (Rm). The injured sections show a relative higher intensity of the labelling when compared to the corresponding remote sections. Scale bar = 50µm.

In CASE2, COMP antibody seemed to have a similar intensity between the two sites although the imaging software gave higher values for "In" site. Type I collagen antibody showed a light labelling diffuse in the matrix of "In" site whereas it localized primarily in the nuclei in the Rm sections. Type III collagen immunostaining showed a low intensity in both sites, nevertheless, it seemed to have a matrix diffusion in the injured section and a nuclear localization in the other sections.

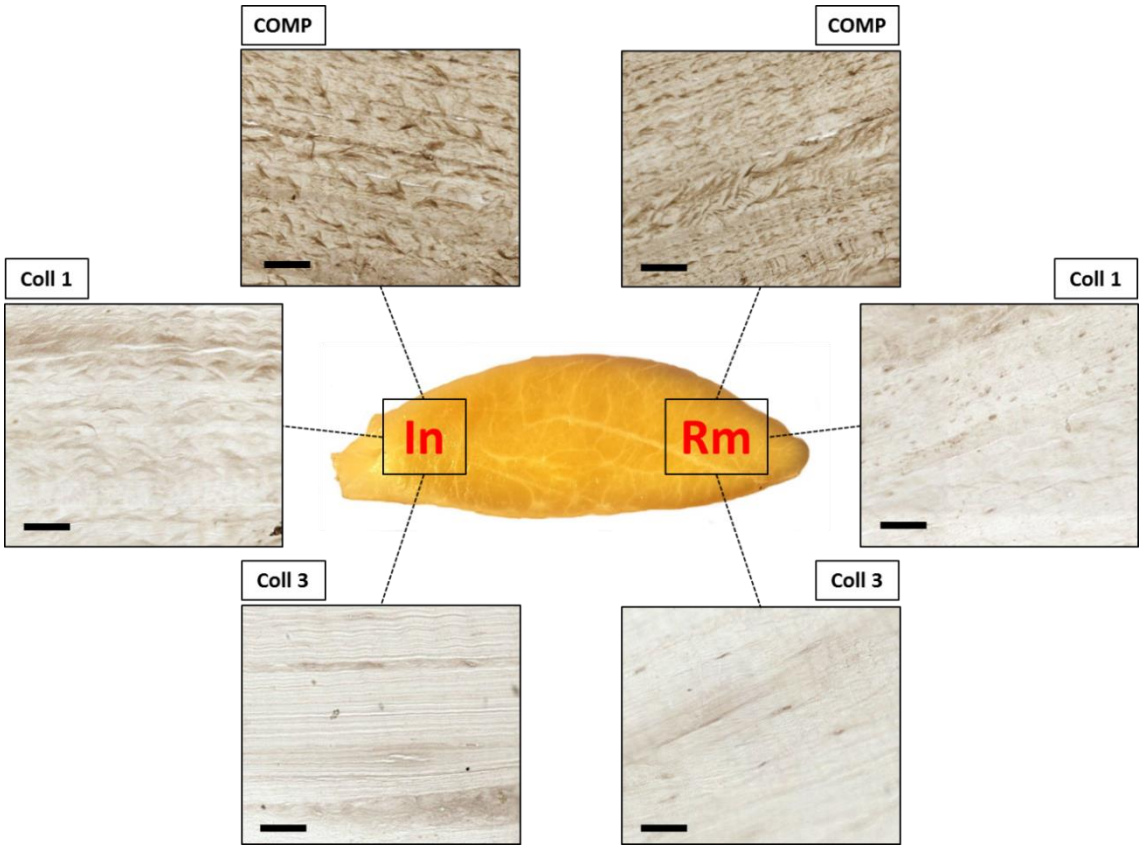

Figure 21. Representative IHC staining for Cartilage Oligomeric Matrix Protein (COMP), Collagen I (Coll1) and Collagen III (Coll3) in CASE2. The three images on the left were taken in the maximum injured site (In), the three on the right were sections from the remote site (Rm). Scale bar = 50µm.

3.4.DISCUSSION

This project provided interesting observations that enlightened the tendon tissue response to a tear-type injury. In accordance with the working hypothesis, the tissue near the lesion site (maximum injured site) showed alterations of cellularity, matrix composition and vascularization; also the region far or remote from the lesion site revealed some minor alterations suggesting a possible influence of the tear it-self. Moreover, a difference in severity of the alterations between the cases, and between the different regions of the same tendon was reported.

CASE1 showed a clear grading from severe (in maximum injured site) to normal (in remote site), especially if cellularity and vascularization were considered. Matrix organization and crimp pattern were severely altered in the region near the lesion whereas they turn to normal appearance in the other regions suggesting that the tear influences dramatically the tissue adjacent to the lesion it-self. In addition, intermediate site showed increased cellularity and vascularity indicating that the tissue is still healing although characterized by a well-organized matrix.

At the same way, in CASE2 the tissue was extremely altered in the maximum injured site although it obtained low scores (suggesting condition similar to normal) in the intermediate and remote sites of the biopsy. Curiously, some areas of the remote sites showed alterations in cellularity, matrix organization and crimps. These observations can be explained suggesting an accumulation of micro-damages that might precede a macroscopic lesion. The remote site in CASE2 may represent a site predisposed to evolve a further lesion.

The histological observations collected the typical alterations were reported in other studies on DDFT (Józsa and Kannus, 1997; Blunden et al., 2006; Murray et al., 2006; Blunden et al., 2009; Crişan et al., 2013). Interestingly, CASE1 showed a greater level of vascularization in the injured site, on the contrary CASE2 had less vascular infiltration although it was characterize by a dramatic matrix disorganization. These different responses might be due to a different grade of lesion severity or they might be

a different stage of the same response influenced by the variable composition of DDFT. Some studies reported the influence of tear dimension in the tissue response (Matthews et al., 2006) and the variation in cellularity, vascularization and fibrotic tissue content in the different parts of DDFT (Blunden et al., 2006). These studies supported my interpretations of the morphological findings in this evaluation.

Intriguing findings were observed with Masson trichrome stain. The injured tissue was completely blue whereas the tissue far from the lesion showed a red coloration. Recently, Martinello *et al.* (submitted for publication) proposed that Masson staining might be considered a precise and quick tool in discerning between healthy and injured tendons. Indeed, during healing process the tendon ECM is constantly under rearrangement and therefore the collagen and non-collagenous proteins turnover might influence the penetration of the stains used in the Masson trichrome procedure. My observation reinforced this study providing evidence of this theory applied on naturally occurring injury in equine tendon.

The IHC analysis demonstrated an increased presence of COMP in CASE1 supporting the previous studies on SDFT and the proteomic analysis (Smith et al., 1997; Dakin et al., 2014). In CASE2, the difference between injured site and remote site was not evident, therefore, according to histological findings, my interpretation was that the remote site showed micro alteration preceding the injury.

The collagens had a clear greater expression in the injured than the remote site of CASE1 suggesting a reactive tissue under re-modelling. On the contrary, in CASE2 only collagen type I seemed more expressed. This observation might be interpreted as a tissue in a chronic stage of the disease.

Taken all together, the data collected in this project have highlighted many aspects of the morphological alteration caused by a tear lesion within DDFT. It has been demonstrated a strict correlation between the proximity to the lesion site and the severity of alteration. In addition, it was noticed that cellularity and vascularity were higher than normal also in a location far (but not remote) from the lesion suggesting a reactive tissue area larger than the sole injured site. Possible pre-injury alterations were also noticed in a remote site in CASE2 giving histological evidences of the well establish theory of tendinopathy aetiopathogenesis. On the author's knowledge, it was

the first time that COMP and collagens expression was evaluate in DDFT affected by tear lesion. It was interesting to report a pattern of expression in accordance with the healing process theory in which collagen III is produced in early stages of disease and later substituted by collagen I. Moreover, the helping role of COMP in ECM re-organization was highlighted once again reporting an increase expression in reactive tissue.

A limit of this study was that no detailed anamnestic information were available on the two analysed cases. However, the sectional shape of the biopsy might suggest the tendon region was involved by the tear. Thus, we supposed that CASE1 sample was a biopsy from metacarpo-phalangeal (MCP) region whereas CASE2 biopsy was probably from midmetacarpal (MidM) region. Both regions are known to be frequently involved in tendon injury, in particular the MCP region is indicated as an injury-predisposed site in DDFT. It is interesting to note that CASE1 showed, already macroscopically, a severe reaction to the lesion with a tissue reaction that microscopically displayed increased cellularity and vascularization, matrix disorganization and degeneration. Due to the particular stresses that the MCP region is subjected to (tensional and compressive forces), all the described alterations might be site-related pathological changes. MidM region is under predominantly tensional forces and in DDFT is not considered a predisposed site to injury. It is probable that the microscopic evidences of alterations in CASE2 were a consequence of the particular features of the site in terms of forces along with tissue constitution.

It will be interesting to investigate and deepen the site-influence on the injury resolving process by tendon tissue.

3.5.CONCLUSIONS and FUTURE PERSPECTIVES

In conclusion, this project reported interesting observations on DDFT affected by tear type lesion. Even though the small number of samples did not permit to generalize the results obtained, they might be considered a well-structured platform for further investigations.

The present data could be integrated by increasing the number of cases and adding other histological and immunohistochemical analysis. Antibodies against matrix metallo proteinases (MMP) and macrophages (esterase, CD172a) could be used to describe the degradation and inflammatory processes and antibodies against activated-Caspase 3 or Asp175 could be used to obtain some information about the apoptotic processes. Moreover, to assess the alteration in the vascularization of the injured areas, IHC using an antibody against Factor VII (Willebrands factor) could be performed.

The observations reported on the different response of the tendon to the presence of injury suggest an important role played by vascularization in the process of healing. Therefore, an evaluation of re-modelling process in tendon tissue with more or less vascular support might be an interesting investigation to evaluate the importance of the tenogenic precursors contribution from the vascular system.

4.BIBLIOGRAPHY

Alexander, R. M. 1991. Energy-saving mechanisms in walking and running. J. Exp. Biol. 160:55–69.

Beck, S., T. Blunden, S. Dyson, and R. Murray. 2011. Are matrix and vascular changes involved in the pathogenesis of deep digital flexor tendon injury in the horse? Vet. J. 189:289–295.

Blunden, a., R. Murray, and S. Dyson. 2009. Lesions of the deep digital flexor tendon in the digit: A correlative MRI and post mortem study in control and lame horses. Equine Vet. J. 41:25–33.

Blunden, A., S. Dyson, R. Murray, and M. Schramme. 2006. Histopathology in horses with chronic palmar foot pain and age-matched controls. Part 2: The deep digital flexor tendon. Equine Vet. J. 38:23–27.

Butcher, M. T., J. W. Hermanson, N. G. Ducharme, L. M. Mitchell, L. V Soderholm, and J. E. a Bertram. 2009. Contractile behavior of the forelimb digital flexors during steady-state locomotion in horses (Equus caballus): an initial test of muscle architectural hypotheses about in vivo function. Comp. Biochem. Physiol. Part A 152:100–114.

Butcher, M. T., J. W. Hermanson, N. G. Ducharme, L. M. Mitchell, L. V Soderholm, and J. E. A. Bertram. 2007. Superficial digital flexor tendon lesions in racehorses as a sequela to muscle fatigue: a preliminary study. Equine Vet. J. 39:540–5.

Castagna, A., E. Cesari, R. Garofalo, A. Gigante, M. Conti, N. Markopoulos, and N. Maffulli. 2013. Matrix metalloproteases and their inhibitors are altered in torn rotator cuff tendons, but also in the macroscopically and histologically intact portion of those tendons. Muscles. Ligaments Tendons J. 3:132–138.

Cillán-García, E., P. I. Milner, A. Talbot, R. Tucker, F. Hendey, J. Boswell, R. J. M. Reardon, and S. E. Taylor. 2013. Deep digital flexor tendon injury within the hoof capsule; does lesion type or location predict prognosis? Vet. Rec. 173.

Clayton, R. A. E., and C. M. Court-Brown. 2008. The epidemiology of musculoskeletal tendinous and ligamentous injuries. Injury 39:1338–44.

Clegg, P. D. 2012. Musculoskeletal disease and injury, now and in the future. Part 2: Tendon and ligament injuries. Equine Vet. J. 44:371–375.

Crevier, N., P. Pourcelot, J. M. Denoix, D. Geiger, C. Bortolussi, X. Ribot, and M. Sanaa. 1996. Segmental variations of in vitro mechanical properties in equine superficial digital flexor tendons. Am. J. Vet. Res. 57:1111–1117.

Crişan, M. I., A. Damian, A. Gal, V. Miclăuş, C. L. Cernea, and J.-M. Denoix. 2013. Vascular abnormalities of the distal deep digital flexor tendon in 8 draught horses identified on histological examination. Res. Vet. Sci. 95:23–26.

Dahlgren, L. A. 2007. Pathobiology of tendon and ligament injuries. Clin. Tech. Equine Pract. 6:168–173.

Dakin, S. G., R. K. W. Smith, D. Heinegård, P. Önnerfjord, A. Khabut, and J. Dudhia. 2014. Proteomic analysis of tendon extracellular matrix reveals disease stage-specific fragmentation and differential cleavage of COMP (cartilage oligomeric matrix protein). J. Biol. Chem. 289:4919–4927.

Dakin, S. G., D. Werling, A. Hibbert, D. R. E. Abayasekara, N. J. Young, R. K. W. Smith, and J. Dudhia. 2012. Macrophage sub-populations and the lipoxin A4 receptor implicate active inflammation during equine tendon repair. PLoS One 7.

Dickinson, S. C., M. N. Vankemmelbeke, D. J. Buttle, K. Rosenberg, D. Heinegård, and A. P. Hollander. 2003. Cleavage of cartilage oligomeric matrix protein (thrombospondin-5) by matrix metalloproteinases and a disintegrin and metalloproteinase with thrombospondin motifs. Matrix Biol. 22:267–278.

Dik, K. J., S. J. Dyson, and T. B. Vail. 1995. Aseptic tenosynovitis of the digital flexor tendon sheath, fetlock and pastern annular ligament constriction. Vet. Clin. North Am. Equine Pract. 11:151–162.

Dowling, B. A., A. J. Dart, D. R. Hodgson, and R. K. W. Smith. 2000. Review Article Superficial digital flexor tendonitis in the horse. Equine Vet. J. 32:369–378.

Dowling, B., and A. Dart. 2005. Mechanical and functional properties of the equine superficial digital flexor tendon. Vet. J. 170:184–192.

Dyson, S., R. Murray, M. Schramme, and M. Branch. 2003. Lameness in 46 horses associated with deep digital flexor tendonitis in the digit: diagnosis confirmed with magnetic resonance imaging. Equine Vet. J. 35:681–690.

Ely, E. R., C. S. Avella, J. S. Price, R. K. W. Smith, J. L. N. Wood, and K. L. P. Verheyen. 2009. Descriptive epidemiology of fracture, tendon and suspensory ligament injuries in National Hunt racehorses in training. Equine Vet. J. 41:372–378.

Ely, E. R., K. L. P. Verheyen, and J. L. N. Wood. 2004. Fractures and tendon injuries in National Hunt horses in training in the UK: a pilot study. Equine Vet. J. 36:365–367.

Fails, A. D., and R. A. Kainer. 2011. Functional Anatomy of the Equine Musculoskeletal System. In: G. M. Baxter, editor. Manual of Equine Lameness. Wiley-Blackwell. p. 3–63.

Goodrich, L. R. 2011. Tendon and ligament injuries and disease. In: G. M. Baxter, editor. Adams and Stashak's Lameness in Horses -sixth edition-. Wiley-Blackwell. p. 927–938.

Goodship, A. E., H. L. Birch, and A. M. Wilson. 1994. The pathobiology and repair of tendon and ligament injury. Vet. Clin. North Am. Equine Pract. 10:323–49.

Hosaka, Y. Z., T. Uratsuji, H. Ueda, M. Uehara, and K. Takehana. 2010. Comparative study of the properties of tendinocytes derived from three different sites in the equine superficial digital flexor tendon. Biomed. Res. 31:35–44.

Jarvinen, T. A. H., L. Jozsa, P. Kannus, T. L. N. Jarvinen, T. Hurme, M. Kvist, M. Pelto-Huikko, H. Kalimo, and M. Jarvinen. 2003. Mechanical loading regulates the expression of tenascin-C in the myotendinous junction and tendon but does not induce de novo synthesis in the skeletal muscle. J. Cell Sci. 116:857–866.

Jozsa, L., P. Kannus, J. B. Balint, and A. Reffy. 1991. Three-dimensional ultrastructure of human tendons. Acta Anat. (Basel). 142:306–312.

Józsa, L., and P. Kannus. 1997. Histopathological findings in spontaneous tendon ruptures. Scand. J. Med. Sci. Sports 7:113–118.

Józsa, L., A. Réffy, and J. B. Bálint. 1984. The pathogenesis of tendolipomatosis; an electron microscopical study. Int. Orthop. 7:251–255.

Kannus, P. 2000. Structure of the tendon connective tissue. Scand. J. Med. Sci. Sports 10:312–320.

Kasashima, Y., T. Takahashi, R. K. W. Smith, A. E. Goodship, A. Kuwano, T. Ueno, and S. Hirano. 2004. Prevalence of superficial digital flexor tendonitis and suspensory desmitis in Japanese Thoroughbred flat racehorses in 1999. Equine Vet. J. 36:346–350.

Kastelic, J., A. Galeski, and E. Baer. 1978. The multicomposite structure of tendon. Connect. Tissue Res. 6:11–23.

Lam, K. H., T. D. H. Parkin, C. M. Riggs, and K. L. Morgan. 2007. Descriptive analysis of retirement of Thoroughbred racehorses due to tendon injuries at the Hong Kong Jockey Club (1992-2004). Equine Vet. J. 39:143–148.

Lui, P. P. Y., N. Maffulli, C. Rolf, and R. K. W. Smith. 2011. What are the validated animal models for tendinopathy? Scand. J. Med. Sci. Sports 21:3–17.

Maganaris, C. N., N. D. Reeves, J. Rittweger, A. J. Sargeant, D. a Jones, K. Gerrits, and A. De Haan. 2006. Adaptive response of human tendon to paralysis. Muscle Nerve 33:85–92.

Mair, T. S., and J. Kinns. 2005. Deep Digital Flexor tendonitis in the equine foot diagnosed by low-field Magnetic Resonance Imaging in the standing patient: 18 cases. Vet. Radiol. Ultrasound 46:458–466.

Martinello, T., F. Pascoli, G. Caporale, A. Perazzi, I. Iacopetti, and M. Patruno. 2014. Might the Masson Trichrome stain considered a useful method for categorizing experimental tendon lesions? (submitted for publication).

Matthews, T. J. W., G. C. Hand, J. L. Rees, N. a Athanasou, and a J. Carr. 2006. Pathology of the torn rotator cuff tendon. Reduction in potential for repair as tear size increases. J. Bone Joint Surg. Br. 88:489–495.

Murray, R. C., T. S. Blunden, M. C. Schramme, and S. J. Dyson. 2006. How does magnetic resonance imaging represent histologic findings in the equine digit? Vet. Radiol. Ultrasound 47:17–31.

Patruno, M., and T. Martinello. 2014. Treatments of the injured tendon in Veterinary Medicine: from scaffolds to adult stem cells. Histol. Histopathol. 29:417–22.

Patterson-Kane, J. C., and E. C. Firth. 2009. The pathobiology of exercise-induced superficial digital flexor tendon injury in Thoroughbred racehorses. Vet. J. 181:79–89.

Peffers, M. J., C. T. Thorpe, J. a Collins, R. Eong, T. K. J. Wei, H. R. C. Screen, and P. D. Clegg. 2014. Proteomic analysis reveals age-related changes in tendon matrix composition, with age-and 1 injury-specific matrix fragmentation. J. Biol. Chem. 289:25867–25878.

Perkins, N. R., S. W. J. Reid, and R. S. Morris. 2005. Risk factors for injury to the superficial digital flexor tendon and suspensory apparatus in Thoroughbred racehorses in New Zealand. N. Z. Vet. J. 53:184–192.

Pinchbeck, G. L., P. D. Clegg, C. J. Proudman, A. Stirk, K. L. Morgan, and N. P. French. 2004. Horse injuries and racing practices in National Hunt racehorses in the UK: the results of a prospective cohort study. Vet. J. 167:45–52.

Riemersma, D. J., A. J. van den Bogert, M. O. Jansen, and H. C. Schamhardt. 1996. Tendon strain in the forelimbs as a function of gait and ground characteristics and in vitro limb loading in ponies. Equine Vet. J. 28:133–138.

Rowe, R. W. 1985. The structure of rat tail tendon fascicles. Connect. Tissue Res. 14:21–30.

Scott, J. E. 2003. Elasticity in extracellular matrix “shape modules” of tendon, cartilage, etc. A sliding proteoglycan-filament model. J. Physiol. 553:335–343.

Screen, H. R. C., J. C. Shelton, V. H. Chhaya, M. V Kayser, D. L. Bader, and D. A. Lee. 2005. The influence of noncollagenous matrix components on the micromechanical environment of tendon fascicles. Ann. Biomed. Eng. 33:1090–1099.

Sharma, P., and N. Maffulli. 2006. Biology of tendon injury: healing, modeling and remodeling. J. Musculoskelet. Neuronal Interact. 6:181–190.

Smith, M. R. W., and I. M. Wright. 2006. Noninfected tenosynovitis of the digital flexor tendon sheath: a retrospective analysis of 76 cases. Equine Vet. J. 38:134–141.

Smith, R. K. W., H. L. Birch, S. Goodman, D. Heinegård, and a E. Goodship. 2002. The influence of ageing and exercise on tendon growth and degeneration-hypotheses for the initiation and prevention of strain-induced tendinopathies. Comp. Biochem. Physiol. A. Mol. Integr. Physiol. 133:1039–1050.

Smith, R. K. W., and P. M. Webbon. 1996. The Physiology of Normal Tendon and Ligament. In: M. R. Rantanen and M. L. Hauser, editors. Dubai International Equine Symposium: the equine athlete : tendon, ligament and soft tissue injuries : March 27-30. Matthew R. Rantanen Design. p. 55–82.

Smith, R. K. W., N. J. Werling, S. G. Dakin, R. Alam, A. E. Goodship, and J. Dudhia. 2013. Beneficial effects of autologous bone marrow-derived mesenchymal stem cells in naturally occurring tendinopathy. PLoS One 8:e75697.

Smith, R. K., L. Zunino, P. M. Webbon, and D. Heinegård. 1997. The distribution of cartilage oligomeric matrix protein (COMP) in tendon and its variation with tendon site, age and load. Matrix Biol. 16:255–271.

Smith, R., W. McIlwraith, R. Schweitzer, K. Kadler, J. Cook, B. Caterson, S. Dakin, D. Heinegård, H. Screen, S. Stover, N. Crevier-Denoix, P. Clegg, M. Collins, C. Little, D. Frisbie, M. Kjaer, R. van Weeren, N. Werpy, J.-M. Denoix, A. Carr, A. Goldberg, L. Bramlage, M. Smith, and A. Nixon. 2014. Advances in the understanding of tendinopathies: a report on the Second Havemeyer Workshop on equine tendon disease. Equine Vet. J. 46:4–9.

Thorpe, C. T., P. D. Clegg, and H. L. Birch. 2010. A review of tendon injury: why is the equine superficial digital flexor tendon most at risk? Equine Vet. J. 42:174–180.

Thorpe, C. T., I. Streeter, G. L. Pinchbeck, A. E. Goodship, P. D. Clegg, and H. L. Birch. 2010. Aspartic acid racemization and collagen degradation markers reveal an accumulation of damage in tendon collagen that is enhanced with aging. J. Biol. Chem. 285:15674–15681.

Wilderjans, H., B. Boussauw, K. Madder, and O. Simon. 2003. Tenosynovitis of the digital flexor tendon sheath and annular ligament constriction syndrome caused by longitudinal tears in the deep digital flexor tendon: a clinical and surgical report of 17 cases in warmblood horses. Equine Vet. J. 35:270–275.

Williams, R. B., L. S. Harkins, C. J. Hammond, and J. L. Wood. 2001. Racehorse injuries, clinical problems and fatalities recorded on British racecourses from flat racing and National Hunt racing during 1996, 1997 and 1998. Equine Vet. J. 33:478–486.

Wilson, A. M., M. P. McGuigan, A. Su, and A. J. van Den Bogert. 2001. Horses damp the spring in their step. Nature 414:895–899.